THE KRKONOŠE-JIZERA COMPOSITE MASSIF

NEVER ENDING GRANITE STORIES

JOSEF KLOMÍNSKÝ

Czech Geological Survey

THE KRKONOŠE-JIZERA COMPOSITE MASSIF

NEVER ENDING GRANITE STORIES

Biotite schlieren and two microgranular mafic enclaves showing interaction of their different rigidities in the Liberec Granite – Bedřichov water supply tunnel section B (1/4 of natural size). Photo J. Klomínský.

THE KRKONOŠE-JIZERA COMPOSITE MASSIF

NEVER ENDING GRANITE STORIES

JOSEF KLOMÍNSKÝ

With contributions and assistance from
F. Fediuk – P. Schovánek – T. Jarchovský

Published by the Czech Geological Survey
Prague 2018

Photo on the book jacket:
Dominant granite cliff in upper part of the Labe river valley next to the Pančava water falls in central part of the Krkonoše Mountains. Photo Vl. Žáček 2005.

ISBN 978-80-7075-929-5

Content

1. Introduction

1.1 Purpose

This book is not a geological monograph but only summary of the geological investigations conducted by a group of geologists from the Czech Geological Survey (CGS) in a broad area of the Czech part of the Krkonoše-Jizera Composite Massif (KJCM, Fig. 1.1.1.) within the last two decades. The first object of our observations was the interiors of the Bedřichov and Souš water supply tunnels in the Jizerské hory Mts. The second object of our observations was detailed geological mapping at the scale of 1 : 25 000 within a broad area between Liberec, Hejnice, Tanvald and Jablonec nad Nisou. Our geological investigation were accelerated by mineralogical and fluid inclusions analysis, isotopic rock dating, multivariate statistical analysis, remote sensing, hydrogeological and seismic monitoring, image analysis of rock alteration and 3D fracture modelling. All these methods were used to describe processes within the granite massif, and to demonstrate the results of its geological activity up to recent times in terms of newly formed minerals and responses to natural and induced seismicity from near and distant epicentres.

The results of our work were mainly published in Czech or archived as internal Czech Geological Survey reports. In this book our aim is to deliver new information from geology, petrology, mineralogy, geochemistry, hydrogeology and geophysics in internationally accepted English. Each theme contains a short summary supported by diagrams, maps and photographs from original publications. This book is intended to acquaint interested international colleagues in Poland, Germany and elsewhere with our geological investigations of the Krkonoše-Jizera Composite Massif and its broad environs.

The KJCM is a geological body shared by two countries: 60 % of it lies in Poland, 40 % in the Czech Republic. It covers over 1000 km^2 and is about 60 km long in the W-E direction (Fig. 1.1.2.). The largest portion of the Czech part occupies the western half of the Massif in the Jizerské hory Mts. Even though the KJCM forms a uniform Polish/Czech geological body, the Czech part has some special features unknown in the Polish sector. The Czech part includes the two-mica garnet-bearing Tanvald Granite, the Fojtka Hybrid Granitoids and the topaz rich greisen at Růžek. Further differences in comparison with the Polish part are represented by Variscan as well as Kenozoic (especially melilitic) polzenite dykes penetrating the KJCM, and by specialized Ba-F-U-W-Mo-Sn mineralization. Contact-metamorphic rocks, used some 5000 years ago by a neolithic population for the production of stone tools exported to a broad Central European area, have been found here. One special advantage for CGS research is the coherent profiles of water-supply tunnels many kilometres long that cut through the KJCM, enabling a detailed and sophisticated insight into the granite body. The influence of the granite basement and of its tectonics on the dense and

Figure 1.1.1. Geographic position of the Krkonoše--Jizera Composite Massif (red) in the Bohemian Massif. Klomínský and Woller (2010). Other granitic massifs and orthogneisses are shown in grey.

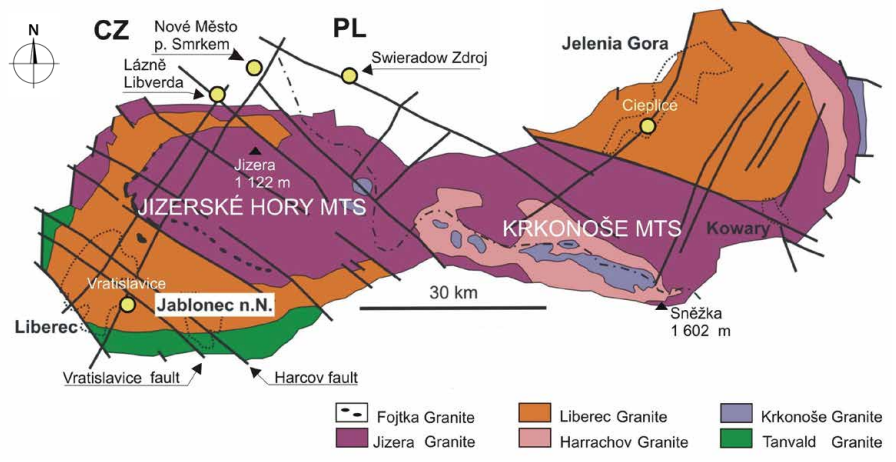

Figure 1.1.2. The main lithologic rock types, geological faults, and geomorphologic structures of the Krkonoše-Jizera Composite Massif (Jizerské hory Mts. and Krkonoše Mountains). Klomínský and Woller (2010). State border is marked by dashed line.

almost continuous Liberec – Jablonec nad Nisou – Tanvald settlement agglomeration is discussed. Relevant papers and reports are mostly cited at the end of each chapter.

The porphyritic Jizera and Liberec Granites are rather unique in preserving a wide spectrum of the magmatic structures first investigated by Cloos (1925) who documented various geometries of mafic schlieren, mapped their patterns in the eastern part of the Krkonoše-Jizera Composite Massif, and inferred the schlieren as being parallel to the flow plane of flowing magma. He also noted that the mafic schlieren define a dome-like structure in the eastern half of the Krkonoše-Jizera Composite Massif. A similar structural study was performed by Klomínský (1969) who detected

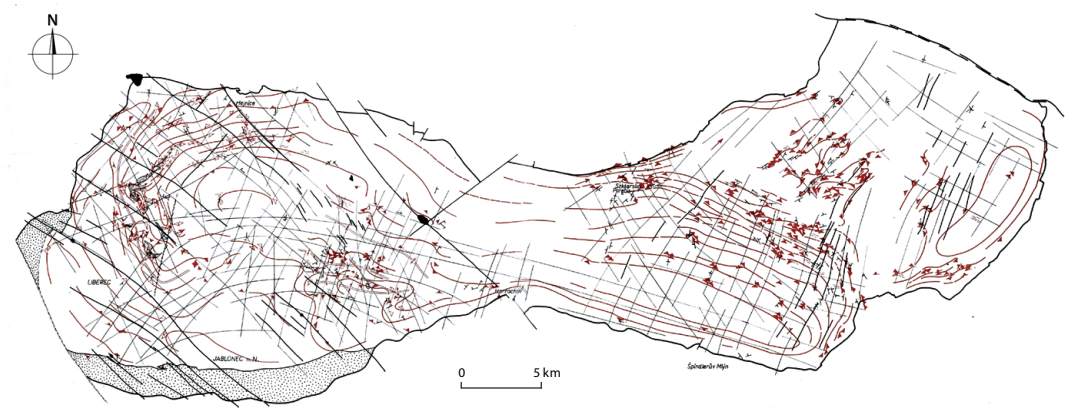

Figure 1.1.3. Granittectonic map of the Krkonoše-Jizera Composite Massif after Cloos (1925) and Klomínský (1969). Red lines are magmatic foliation and/or lineation in granites,thin black lines are a major granite joint network, thick black lines are geological faults and/or rock dykes, large black spots are major Tertiary basaltoids bodies and the hatched area is the Tanvald Massif.

similar geometries of mafic schlieren, enclaves and join networks also in the dome-like western part of the KJCM (Fig. 1.1.3.).

The culmination zone of the eastern elongated dome is located near the southern contact of the massif. The extensive western dome has an oval shape with culmination in the most elevated part of the Jizerské hory Mts.

Several antiformal closures with amplitude up to thirty metres were studied in detail in the Bedřichov water-supply tunnel (Klomínský and Woller, 2010). The orientation of the long axes of these structures shows WNW-ESE trend in the Bedřichov water-supply tunnel (Žák and Klomínský, 2007, Žák et al. 2009).

1.2 Geophysical maps

Gravimetric maps

The gravity survey of the western part of the KJCM has been provided at the scale of 1 : 25 000 in 2002 to 2003 (Sedlák et al. 2003, 2007). Gravity measurements executed in the KJCM in past and in recent times (Watznauer, 1935, Sedlák, et. al. 2007) are interpreted as the manifestation of the ethmolith thickness and asymmetric position of the root (Figs. 1.2.1. and 1.2.2.). The Tanvald Massif participates in the distinct abrupt negative gravity gradient along the southern margin of the western segment of the KJCM.

Airborne aeromagnetic and radiometric maps

In 2004–2005 a low level gamma spectrometric and magnetometric survey was conducted over a large area of the Liberec region (Dědáček et al. 2005). Radiometric maps (potassium, uranium, thorium and caesium) and also the map of the magnetic

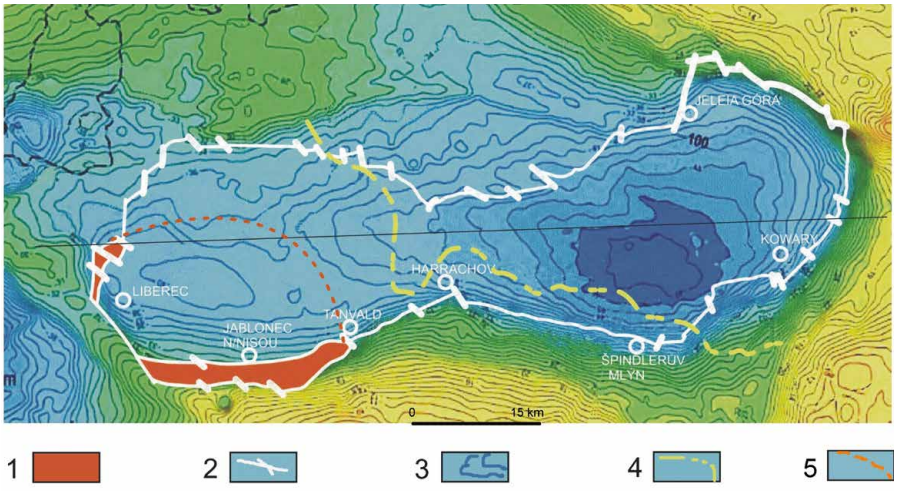

Figure 1.2.1. Gravity map of the Krkonoše-Jizera Composite Massif (Sedlák et al. 2007).

1 – Tanvald Massif, 2 – geological faults, 3 – Boguer gravity isolines and negative anomalies (deep blue), 4 – state border.

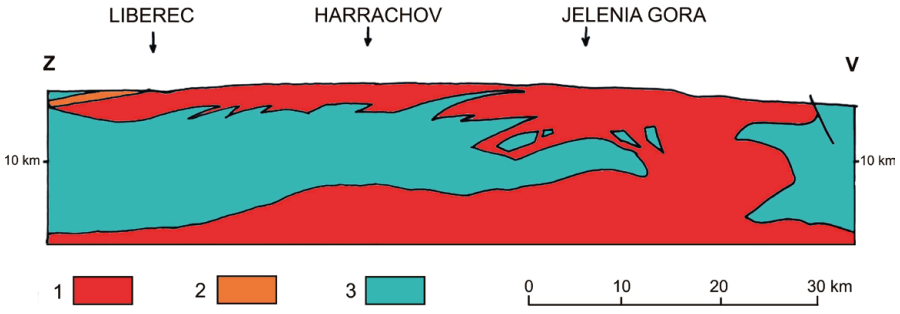

Figure 1.2.2. Model of the asymmetric ethmolith for the Krkonoše-Jizera Composite Massif – KJCM (adapted after Watzenauer 1935). Profile line is marked in Fig. 1.2.1.

1. – granites of the KJCM. 2 – Tanvald Massif, 3 – Krkonoše-Jizera Crystalline rocks.

field at a scale of 1 : 50 000 demonstrate the distinct zoned structure of the western part of the KJCM (Fig. 1.2.3.). Higher magnetic susceptibility and uranium content corresponds to Liberec Granite outcrops making the base for the Jizera Granite (Fig.1.2.4.).

Satellite fracture network maps of granitic intrusions – a new tool for geological mapping

Correlation of the results of distant field analysis of the western part of the Krkonoše-Jizera Composite Massif with the results of geological and geophysical mapping permits the definition of linear swarms of brittle deformation of the granite massif. Such analysis is complemented significantly by the construction of fractal maps of the massif's tectonic network based on a statistical analysis of the density and trend orientation of morphotectonic linear elements reflecting the structure and level of

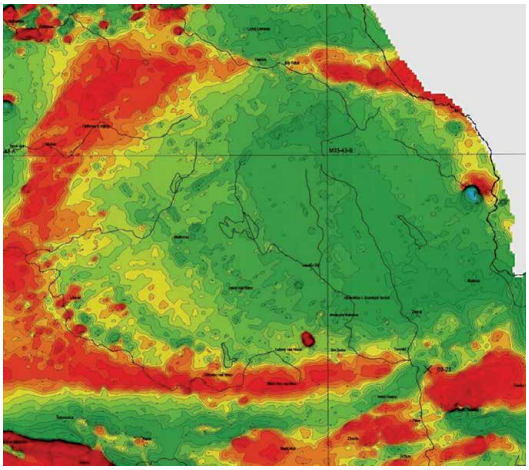

Figure 1.2.3. Airborne map of the magnetic anomalies in the western segment of the Krkonoše-Jizera Composite Massif (Dědáček et al. 2005). Higher magnetic susceptibility (red and yellow) corresponds to Liberec Granite outcrops.*

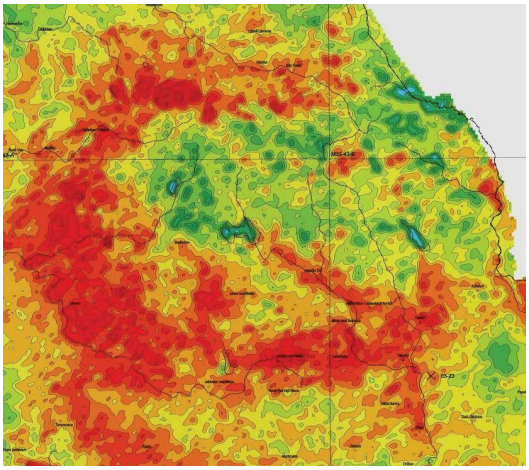

Figure 1.2.4. Airborne map of the total gamma activity anomalies in the western segment of the Krkonoše-Jizera Composite Massif (Dědáček et al. 2005). Positive total gamma activity anomalies (red) correspond to the Liberec Granite and negative total gamma activity anomalies (green) belong to the Jizera Granite.*

disturbance of the massif (Fig. 1.2.5.). Fractal maps of the joint network enable the classification of faults, their lateral extension and probable depth range. The construction of fractal maps of the joint network at the surface of granite bodies can be used in the search for solitary blocks with a widely-spaced fracture network within a granite massif (Kopačková in Klomínský et al. 2008).

Production of the fracture network maps from the satellite images is an example of their utilization in geological survey of the granitic plutons. They offer a regional model of the tectonic network density and vector orientation. Areas marked in red represent high density of linear morphostructures which could correspond to a high degree of granite alteration and fracture density.

1.3 New basic geological maps 1 : 25 000 of the Czech Republic

CGS initiated a new geological mapping of the western part of the KJCM including the Jizera Mts. protected landscape area in the 1990s (Fig. 1.3.1.). The first maps were finished in 2000. Most of these basic geologic maps of the Czech Republic (map sheet Jablonec nad Nisou, Liberec and Tanvald) and their explanatory notes are available in the CGS bookshop or on the CGS website www.geology.cz. In preparation are map sheets for Rokytnice nad Jizerou, Raspenava, Hejnice, Harrachov and Jizerka.

* Detailed legend see Dědáček et al. 2005.

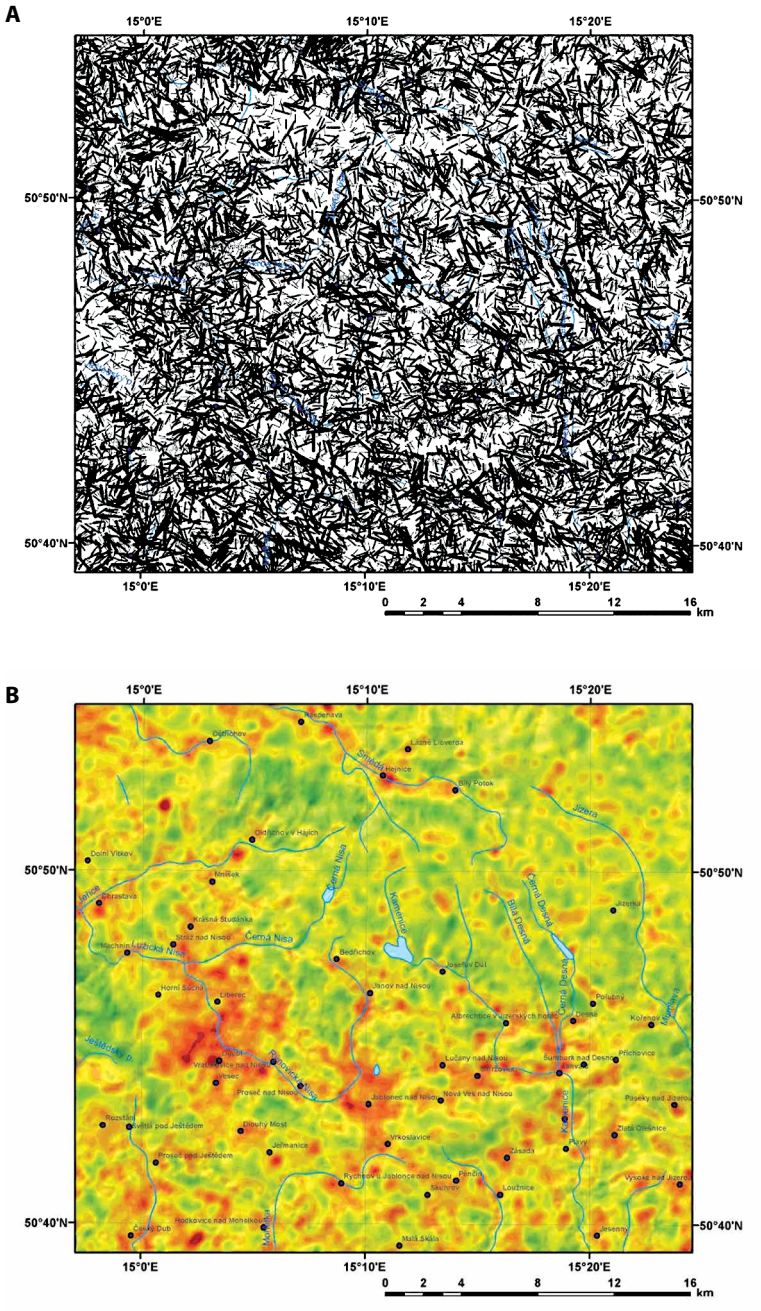

Figure 1.2.5. 2-D fractal maps of the frequency and orientation of linear morphological structures (fractures) are derived from a satellite image of the western part of the Krkonoše-Jizera Composite Massif and its surroundings. Klomínský et al. (2008).
A – Map of fractal lineation network. B –map of the fractal lineation density (red – high density of lineation, green – low density of lineation).

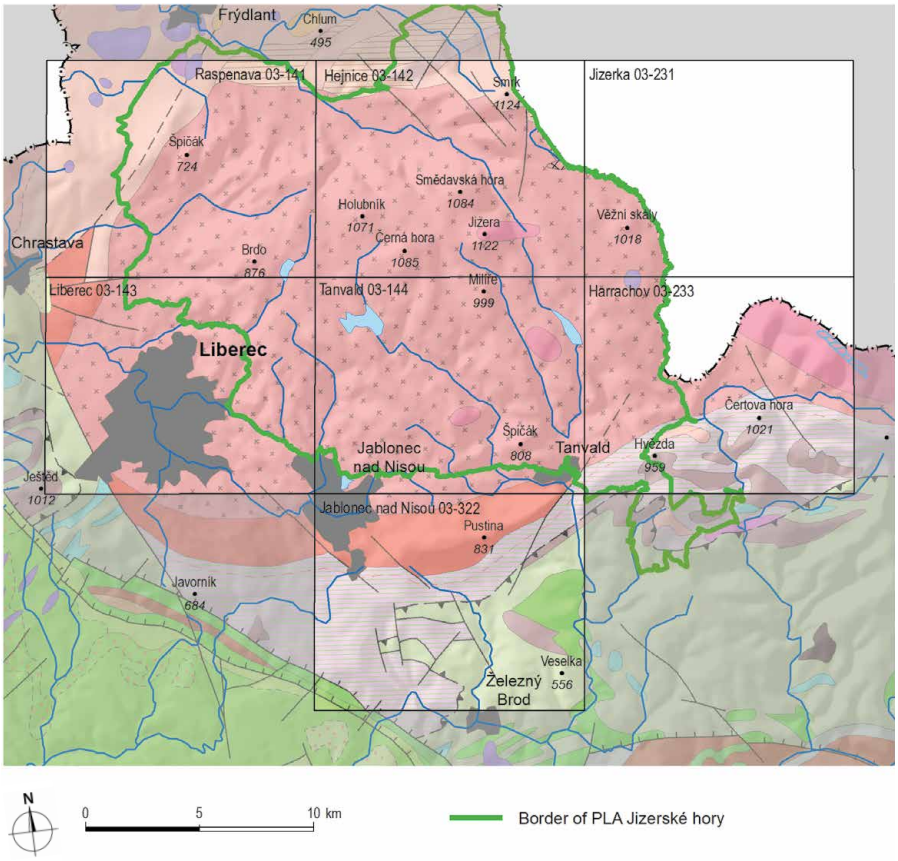

Figure 1.3.1. Seven new basic geological maps of the Jizerské hory Mts. at a scale of 1 : 25 000.

REFERENCES

Bernard, J. H. (1991): Empirical types of ore mineralizations in the Bohemian Massif. – Czech Geological Survey, 181 p. Prague.

Borkowska, M. (1966): Petrografia granitu Karkonoszy. – Geologia Sudetica 2, 7–119. (in Polish (French summary).

Cloos, H. (1925): Einführung in die tektonische Behandlung magmatischer Erscheinungen (Granittektonik). 1. Das Riesengebirge in Schlesien. Borntraeger, Berlin, pp 1–194

Danišík, M. – Migoń, P. – Kuhlemann. J. – Evans, N. J. – Dunkl, I. – Frisch, W. (2010): Thermochronological constraints on the long-term erosional history of the Karkonosze Mts., Central Europe – Geomorphology 117 (2010) 78–89.

Dědáček, K. – Gnojek, I. – Sedlák, J. – Zabadal, S. (2005): Letecké geofyzikální mapování radioaktivních zátěží Liberecka. – MS ČGS Praha.

Dobeš, P. – Klomínský, J. – Jačková, I, – Veselovský, F. (2017): Puklinové kalcity jako indikátory paleohydrologie v granitech krkonošsko-jizerského plutonu (Česká republika). Zprávy o geol výzk. Vol. 50, 2016. 195–201.

Model scenario of tectonothermal history of the Krkonoše-Jizera Composite Massif.

Intrusion and emplacement of granites of the Krkonoše-Jizera Composite Massif (U/Pb zircon age, Žák et al. (2013).	~ 320 Ma
Emplacement of the Krkonosze Granite (CA-ID-TIMS zircon data, Kryza et al. 2014).	ca. 312 Ma
Solidification and cooling of granites down to < 300 ºC (K/Ar biotite, Šmejkal 1964).	304–293 Ma
Intrusion of basaltandesite and trachyandesite (melaphyre) dyke swarm (K/Ar whole rock, Pecskay 2008).	296–280 Ma
Temperatureof the Krkonoše-Jizera granites below 190º C (Danišík et al. 2010).	290–250 Ma
Brittle destruction of basalt-andesite dykes, hydrothermal alteration of granite and melaphyre dykes, silicification and origin of the hematite mineralization. Harrachov barite-fluorite mineralozation (U/Pb in galenite, Bernard 1991).	280 – 170 Ma
Exhumation and erosion history of the Krkonoše-Jizera Composite Massif onto the Earth surface (82 ± 5 to 90 ± 8 Ma and from 77 ± 5 to 91 ± 6 Ma (U–Th)/He (ZHe), apatite fission track (AFT) and apatite (U–Th–[Sm])/He (AHe) thermochronology (Danišík et al. 2010, Dobeš et al. 2013).	ca. 91 – 77 Ma
Drop of temperature of the Jizera Granite below 120°C (AFTA, Dobeš et al. 2017).	ca. 70 Ma
Intrusion of polzenite dykes along NE-SW trending structures (K/Ar whole rock, Peczkay 2008).	61.9 ± 3.0 Ma
Dykes and pipes of alkali basalts (K/Ar whole rock, Pecskay 2008).	30 ± 1 Ma
Formation of the calcites in granite fractures (radiocarbon dating, Dobeš et al. 2017).	> 50 000 y BP
Formation of clay minerals and Fe oxi-hydroxides along faults trending NE-SW, in mylonitized and cataclastic Jizera Granite (Klomínský et al. 2008).	subrecent
Precipitation of newly formed uranium and carbonate minerals (schröckingerite) in the Bedřichov water supply tunnel A (Klomínský et al. 2008).	recent

Dobeš, P. – Veselovský, F. – Klomínský, J. (2013): Geochemické studium karbonátových a křemen – karbonátových žil v granitech bedřichovského tunelu. MS ČGS Praha.

Duthou, J.L. – Couturie, J.P. – Mierzejewski, M.P. – Pin, C. (1991): Next dating of granite sample from the Karkonosze Mountains using Rb–Sr total rock isochrone method. – Przegląd Geologiczny 36, 75–79. (in Polish, English summary).

Klomínský, J. (1969): Krkonošsko-jizerský granitoidní masiv. – Sbor. geol. Věd, Geol., 15, 7–133.

Klomínský, J. – Adamová, M. – Bělohradský, V. —Burda, J. – Kachlík, V. – Lochmann, Z. – Manová, M. – Nekovařík,Č. – Nývlt, D. – Šalanský, K. (2004): Vysvětlivky k základní geologické mapě České republiky 1 : 25 000 03-143 Liberec. 68 s. – ČGS. Praha. ISBN 80-7075-623-3.

Klomínský J. – Adamová, M. – Burda, J. – Jarchovský, T. – Kachlík, V. – Kořán, V. – Kříbek, B. – Manová, M. – Nekovařík, Č. – Šalanský, K. (2006): Základní geologická mapa České republiky 1 : 25000 s Vysvětlivkami, 03 – 323 Jablonec n. N. – 62 s. ČGS. Praha.

Klomínský, J. – Schovánek, P. – Jarchovský, T. – Sulovský, P. – Toužimský, M. (2007): Kontakt tanvalského a libereckého granite u Jablonce nad Nisou. – Zprávy Geol. Výzk. v r. 2006, 24-29.

Klomínský, J. ed. (2008): Studium dynamiky puklinové sítě granitoidů ve vodárenském tunelu Bedřichov v Jizerských horách. Etapa 2006–2008. – MS ČGS. Praha.

Klomínský, J. – Woller, F. eds (2010): Geological studies in the Bedřichov water supply tunnel. Technical report 02/2010. SÚRAO, ČGS Prague. 104 pp.

Kröner, A. – Hegner, E. – Hammer, J. – Haase, G. – Bielicki, K-H. – Krauss, M. – Eidam, J. (1994): Geochronology and Nd–Sm systematics of Lusatian granitoids: significance for the evolution of the Variscan orogen in east-central Europe. – Geologische Rundschau 83, 357–376.

Kryza, R. – Pin, C. – Oberc-Dziedzic, T. – Crowley, Q. G. – Larionov, A. (2014): Decifering the geochronology of a large granitoid pluton Krkonosze Granite, SW Poland): An assessment of U-Pb zircon SIMS and Rb-Sr whole-rock dates relative to U-Pb zircon CA-ID-TIMS. – Int. Geol. Rev. 56, 6, 786–782.

Kusiak, M.A. – Dunkley, D.J. – Slaby, E. – Budzyń, B. – Martin, H. (2008): U–Pb chronology of zircon from granites of the Karkonosze Pluton, NE Bohemian Massif. – 4th SHRIMP workshop. Saint Petersburg, Russia, Abstract Volume, 70–80.

Machowiak, K. – Armstrong, R.(2007): SHRIMP U–Pb zircon age from the Karkonosze granite. Mineralogia Polonica. – Special Papers 31, 193–196.

Marheine, D. – Kachlik, V. – Maluski, H. – Patocka, F. – Żelaźniewicz, A. (2002): New 40Ar/39Ar ages in the West Sudetes (Bohemian Massif): constraints on the Variscan polyphase tectonothermal development. In: Winchester, J.A., Paharaoh, T.C., Verniers, J. (Eds.), Palaeozoic Amalgamation of Central Europe. – Geological Society Special Publication 201, 133–155.

Mrázová, Š. – Adamová, M. – Burda, J. – Knésl, I. – Klomínský, J. – Lochman, Z. – Manová, M. – Nekovařík, Č. – Nývlt, D. – Šalanský, K. (2006): Základní geologická mapa České republiky 1 : 25 000 s Vysvětlivkami, list 03-144 Tanvald. – 33 str. ČGS, Praha.

Pécskay, Z. (2008): K/Ar age determination on intrusive magmatic rocks of SURAO project 2008 – Institute of Nuclear Research of the Hungarian Academy of Sciences (ATOMKI), Debrecen, Hungary. Research report.

Sedlák, J. – Gnojek, I. – Zabadal, S. – Farbisz, J. – Cwojdzinski, S. – Scheibe, R. (2007): Geological interpretation of a gravity low in the central part of the Lugian Unit (Czech Republic, Germany and Poland). – Journ.Geosci. 52 (2007), p. 181–197, Praha.

Sedlák, J. – Hanák, J. – Mrlina, J. – Krejčí, Z. – Mrázová, Š. (2003): Gravimetrické mapování 1 : 25 000 v oblasti krkonošsko-jizerského krystalinika. – Zpráva za roční výseč prací 2003. – MS CGS Praha.

Šmejkal, V. (1964): Absolutní stáří některých vyvřelých a metamorfovaných hornin Českého masivu stanovené kalium-argonovou metodou (II. část). – Sbor. Geol. Věd. G 4, 121–136. Praha.

Šrámek, J. – Sedlák J. – Mrlina J. – Hanák, J. – Ondra, P. – Mrázová, Š. – Krejčí, Z. (2002): Gravimetrické mapování 1 : 25 000 v oblasti krkonošsko-jizerského krystalinika. – MS Archive CGS Brno.

V**erner, K. – Mrázová, Š. – Břízová, E. – Buriánek, D. – Holub, F. – Klomínský, J. – Malík, J. – Martínek, K. – Pecina, V. – Rambousek, P. – Rukavičková, L. – Skácelová, D. – Skácelová, Z. – Štor, T. – Vrána, S. – Žáčková, E. (2013b):** Vysvětlivky k Základní geologické mapě České republiky 1 : 25.000, list 03-142 Hejnice a 03-231 Jizerka. 143 s. MS Archiv CGS Praha.

Vondrovic, L. – Klomínský, J. eds (2015): Základní geologická mapa České republiky 1 : 25 000 03 – 322 Raspenava. Geologické mapy 1 : 25 000 s textovými vysvětlivkami. 57 s. – MS Archive CGS, 202 s. Praha.

Watznauer, A. (1935): Die Geologie des Bezirkes Gablonz. Heimattkunde des Bezirkes Gablonz. Neue Augabe, 118 p.

Žák, J. – Klomínský, J. (2007): Magmatic structures in the Krkonoše-Jizera Composite Massif Complex, Bohemian Massif: evidence for localized multiphase flow and small-scale thermal-mechanical instabilities in a granitic magma chamber. – Journal of Volcanology and Geothermal Research 164, 4, 254–267.

Žák, J. – Verner, K. – Klomínský, J. – Chlupáčová, M. (2009): Granite tectonics revisited: insights from comparison of K-feldspar shape-fabric, anisotropy of magnetic susceptibility (AMS), and brittle fractures in the Jizera Granite, Bohemian Massif. – International Journal of Earth Sciences 98, 5, 949–967.

Žák, J. – Verner, K. – Sláma, J. – Kachlík, V. – Chlupáčová M. (2013): Multistage magma emplacement and progressive strain accumulation in the shallow-level Krkonoše-Jizera plutonic complex, Bohemian Massif. – Tectonics, 32, 1493–1512.

2. Basic parameters of the Krkonoše-Jizera Composite Massif

Basic parametres sof the Krkonoše-Jizera Composite Massif (adopted according to Klominsky et al. 2010b).

Regional position: The Krkonoše-Jizera Composite Massif intrudes into the Krkonoše-Jizera Crystalline Complex (Proterozoic-Lower Palaeozoic metasediments, metavolcanics and orthogneisses) in the Lugicum, one of the principal tectonostratigraphic units of the Bohemian Massif.

Rock types

Suite A:

1. *Jizera Granite* – porphyritic medium-grained biotite granite to granodiorite (G1).
2. *Liberec Granite* – porphyritic coarse-grained biotite granite (G2).
3. *Harrachov Granite* – medium-grained biotite granite (G3).
4. *Krkonoše Granite* – fine-grained biotite granite (G4).

Suite B:

1. *Fojtka Hybrid Granitoids* – porphyritic medium to fine-grained hornblende-biotite granodiorites to quartz diorite (F).

Suite C:

1. *Tanvald Granite* – medium-grained two-mica alkali-feldspar granite (D).

In the Polish part of the KJCM four main granite facies predominate (Borkowska 1966, in Klomínský et al. 2010 b): Porphyritic coarse-grained granite, medium-grained granite, fine-to medium, equigranular granite, granophyric granite.

Size and shape (on erosion level)

The KJCM has a long elliptical shape covering over 1000 km^2 (70 × 10–20 km). An inclined (from N to S) wedge-like (asymmetric) ethmolith (4 to 10 km thick) has been

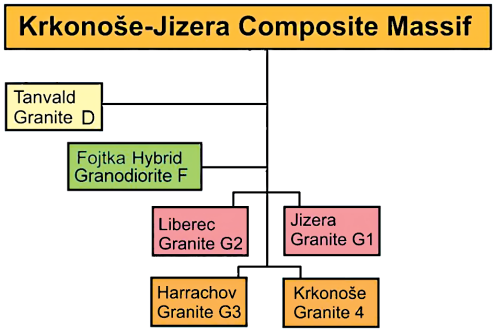

Figure 2.1. Krkonoše-Jizera Composite Massif hierarchical relationship of the rock types (the granite age sequence is shown down in diagram)**.**

interpreted from the gravity data. The depth of magma solidification is about 5–7 km (Dudek et al. 1991 in Klomínský et al. 2010a).The shape of the Tanvald Granite can be modelled as a steeply inclined slab of around 25 km in length with an approximate thickness of some 2–3 km (based on gravity data).

Age and isotopic data (References see p. 13)

The ages obtained for the Krkonoše-Jizera Granites so far are scattered between c. 304 and 328Ma, even for the same granite type. **Šmejkal (1964):** *Jizera and Liberec Granite* 304–293 Ma (K-Ar W rock). **Borkowska (1966):** Krkonoše Granite 292 Ma (Rb-Sr W rock). **Duthou et al. (1991):** Central porphyritic granite (328 ± 12 Ma Rb-Sr W rock). **Kröner et al. (1994):** *porphyritic granite* 304 ± 14 Ma **(**U–Pb multigrain zircon). **Marheine et al. (2002):** *Liberec Granite* (320 ± 2 Ma $^{40}Ar^{39}Ar$ biotite). **Machowiak and Armstrong, (2007):** porphyritic granite 314 ± 3 Ma and 318 ± 4 Ma (U–Pb SHRIMP zircon). **Klomínský et al. (2007):** *Tanvald Granite* is intruded by the Liberec Granite, 321± 14 Ma (U-Th-Pb monazite). **Kusiak et al. (2008):** *m-g porphyritic granite* 313.0 ± 6.0 Ma (U-Pb SHRIMP zircon), *c-g porphyritic granite* 308.7 ± 4.7 Ma (U-Pb SHRIMP zircon), f-*g granite* 303.7 ± 6.6 Ma (U-Pb SHRIMP zircon,). **Žák et al. (2013):** *Liberec Granite* 319.5 ± 2.3, *Jizera Granite* 319.3 ± 3.7, 320.1 ± 3.0 Ma, *Tanvald Granite* 317 ± 2.1 Ma, *Fojtka Granodiorite* 318.4 ± 2.3 Ma, *Harrachov Granite* 315.0 ± 2.7 Ma (U-Pb zircon). **Kryza et al. (2014):** *porphyritic granite* 311 ± 3 Ma (Rb-Sr W rock), 318 ± 4 Ma (Pb-U SHRIMP zircon).

Zoning

Well defined subhorizontal compositional and structural reverse zoning (layering) – Jizera Granite (upper layer) Liberec Granite (lower layer). Younger (G3 and G4) phases are asymmetrically located along southern and eastern margins. N-S stratification and distinct asymmetric zoning of the Tanvald Granite. Transition of the porphyritic muscovite -biotite granite at the northern endocontact with the Liberec Granite into highly evolved (high Rb and F content) biotite – muscovite granite in the southern part of the Tanvald intrusion.

Contact aureole: pronounced up to 1.5 km wide zone – biotite (hornblende) hornfelses, spotted schists with cordierite and andalusite in contact with the Tanvald Granite and Proterozoic-Lower Palaeozoic metasediments. Almost sharp (intrusive) sub-vertical southern contact plane of the Liberec Granite with the Tanvald Granite.

Geological environment

Neoproterozoic two-mica schists and amphibolites, Cambrian-Ordovician Jizera orthogneiss and Ordovician-Silurian to Lower Devonian phyllites.

Mineralization

W-Sn, Ba-F, U, Co, Cu, Ag.

Heat production (μWm^{-3})

Tanvald Granite 5.53, 2.81 (μWm^{-3}), *Liberec Granite* 3.95 (μWm^{-3}), *Jizera Granite* 4.18 (μWm^{-3}).

2.1. Chemical classification and composition* (Klomínský et al. 2010b)

Krkonoše-Jizera Granites (G1–G4)

Quartz-rich to quartz-normal, sodic to potassic, weakly peraluminous, mesocratic, S-type, I- and M-series granite

n = 42	Median	Min	Max	QU1	QU3
SiO_2	71.61	68.91	77.11	70.21	72.86
TiO_2	0.39	0.05	0.62	0.24	0.50
Al_2O_3	13.77	12.03	15.20	13.23	14.28
Fe_2O_3	0.59	0.00	1.39	0.49	0.95
FeO	1.72	0.32	2.55	1.18	1.87
MnO	0.06	0.01	0.08	0.04	0.06
MgO	0.69	0.00	1.20	0.47	0.85
CaO	0.75	0.59	2.58	1.29	1.98
Na_2O	3.34	2.95	3.82	3.23	3.47
K_2O	4.54	3.26	5.22	4.29	4.75
P_2O_5	0.11	0.00	0.66	0.08	0.14
Mg/(Mg+Fe)	0.35	0.00	0.48	0.28	0.38
K/(K+Na)	0.47	0.37	0.53	0.45	0.49
Nor.Or	28.05	20.18	31.88	26.22	29.07
Nor.Ab	31.03	27.37	35.35	30.34	32.37
Nor.An	8.13	–0.19	12.45	5.92	9.48
Nor.Q	29.05	22.30	37.06	26.00	31.44
Na+K	204.82	184.82	218.77	200.76	207.01
*Si	176.58	140.71	215.74	158.68	187.75
K-(Na+Ca)	–41.32	–78.98	–4.23	–54.62	–27.91
Fe+Mg+Ti	53.12	12.60	79.51	40.14	62.65
Al-(Na+K+2Ca)	6.39	–11.94	33.75	-1.04	13.83
(Na+K)/Ca	6.49	4.66	20.12	5.86	8.92
A/CNK	1.03	0.97	1.24	1.00	1.06

Trace elements (mean values in ppm): *Krkonoše-Jizera Granite* – **Ba** 11, **Ce** 30, **Cr** 44, **Cu** 45, **La** 14, **Nb** 20, **Ni** 5, **Pb** 58, **Rb** 336, **Sr** 9, **Ta** 8, **Th** 38, **U** 7, **Y** 23, **Zn** 15, **Zr** 59 (Lorenc et al. 1998 in Klomínský et al. 2010 b).

* Water content is omitted.

Jizera Granite (G_1) – **Pb** 50**, Ga** 18, **Ni** <10, **V** 33, **Co** <10, **W** 51, **Sn** 12, **Zr** 146, **Rb** 219, **Sr** 170, **Nb** 12, **U** 4.0 (Klomínský 1969).
Liberec Granite (G_2) – **Pb** 26, **Ga** 14, **Ni** <10, **V** 16, **Co** <10, **W** 22, **Sn** 15, **Zr** 125, **Rb** 239, **Sr** 112, **Nb** 11, **U** 5.1 (Klomínský 1969).
Harrachov Granite (G_3) – **Pb** 12**, Ga** 14, **Ni** <10, **Co** <10, **W** 15, **Sn** 14, **Zr** 100, **Rb** 246, **Sr** 186, **Nb** 12, **U** 3.8 (Klomínský 1969).
Krkonoše Granite (G_4) – **Pb** 23, **Ga** 15, **Ni** <10, **Co** <10, **W** 17, **Sn** 35, **Zr** 25, **Rb** 277, **Sr** 50 (Klomínský 1969).

Tanvald Granite

Quartz-rich, sodic, peraluminous, leucocratic, S-type, I and M series, granite

n = 10	Median	Min	Max	QU1	QU3
SiO_2	74.43	73.77	75.15	74.18	74.65
TiO_2	0.05	0.01	0.15	0.04	0.07
Al_2O_3	14.28	13.61	14.63	14.26	14.41
Fe_2O_3	0.31	0.01	0.49	0.21	0.32
FeO	0.68	0.43	0.97	0.60	0.73
MnO	0.07	0.04	0.09	0.05	0.08
MgO	0.07	0.02	0.20	0.05	0.07
CaO	0.27	0.19	0.88	0.21	0.46
Na_2O	4.00	3.53	4.41	3.89	4.12
K_2O	4.19	4.07	4.86	4.17	4.29
P_2O_5	0.12	0.07	0.15	0.10	0.13
Mg/(Mg+Fe)	0.11	0.04	0.23	0.09	0.12
K/(K+Na)	0.41	0.38	0.46	0.40	0.42
Nor.Or	25.33	24.56	29.14	25.14	25.94
Nor.Ab	36.81	32.42	40.45	35.75	37.78
Nor.An	0.51	0.09	3.97	0.31	1.52
Nor.Q	31.15	29.58	33.70	30.35	32.65
Na+K	217.62	211.38	237.43	213.34	224.95
*Si	183.94	174.12	199.81	178.69	193.16
K-(Na+Ca)	–43.86	–59.99	–30.66	–49.77	–43.16
Fe+Mg+Ti	15.65	10.01	23.26	13.77	18.22
Al-(Na+K+2Ca)	46.22	23.03	59.21	41.22	50.38
(Na+K)/Ca	32.51	13.56	70.08	24.73	55.77
A/CNK	1.21	1.10	1.28	1.18	1.23

Trace elements (mean values in ppm): *Tanvald Granite* – **B** 18, **Ba** 9**, Be** 4.5, **Co** 13**, Cr** 15, **Cs** 14.5**,Cu** 7, **Ga** 22, **Hf** 6.1**, Ni** 7, **Nb** 22, **Pb** 16, **Rb** 474**, Sc** 7, **Sn** 15, **Sr** 7, **Y** 16, **Zn** 43, **Zr** 18, **Pb** <10, **Ga** 22, **Ni** <10, **Co** <10, **W** 5, **V** 15, **Sn** 28, **Zr** 8, **Rb** 362, **Sr** 90**, Nb** 25, **U** 4.2 (Klomínský 1969).

Fojtka Hybrid Granitoids

Quartz-poor, sodic, metaluminous, melano-mesocratic, I-type, I-series, granodiorite

	471FOJ	472FOJ	473FOJ	474FOJ
SiO_2	67.63	60.36	69.02	62.26
TiO_2	0.72	1.30	0.57	0.98
Al_2O_3	13.88	14.97	14.22	15.78
Fe_2O_3	0.77	1.09	0.54	1.13
FeO	3.00	5.30	2.69	4.31
MnO	0.07	0.11	0.07	0.12
MgO	1.60	3.14	1.00	1.76
CaO	2.63	5.39	2.51	4.02
Li_2O	n.d.	n.d.	n.d.	n.d.
Na_2O	3.38	3.41	3.29	3.67
K_2O	4.29	3.03	4.40	3.51
P_2O_5	0.18	0.30	0.15	0.41
Mg/(Mg+Fe)	0.43	0.47	0.35	0.37
K/(K+Na)	0.46	0.37	0.47	0.39
Nor.Or	27.10	19.78	27.50	22.42
Nor.Ab	32.46	33.83	31.25	35.62
Nor.An	12.69	27.36	12.13	18.64
Nor.Q	22.09	10.66	24.42	14.88
Na+K	200.16	174.37	199.59	192.95
*Si	143.77	96.42	153.48	104.66
K-(Na+Ca)	–64.88	–141.82	–57.50	–115.59
Fe+Mg+Ti	100.15	181.66	76.18	130.13
Al-(Na+K+2Ca)	–21.38	–72.62	–9.85	–26.44
(Na+K)/Ca	4.27	1.81	4.46	2.69
A/CNK	0.94	0.82	0.98	0.95

Trace elements (mean values in ppm): *Fojtka Hybrid Granitoids* – **Pb** <10, **Ga** 11, **Ni** 17, **Co** 14, **W** <10, **V** 59, **Sn** 17, **Zr** 90, **Rb** 180, **Sr** 210, **Nb** 6 (Klomínský 1969).

REFERENCES

Klomínský, J. – Jarchovský, – Rajpoot, G. (2016): Atlas of plutonic rocks and orthogneisses in the Bohemian Massif – Data Supplement. CGS Prague.

Klomínský, J. – Jarchovský, – Rajpoot, G. (2010 a): Atlas of plutonic rocks and orthogneisses in the Bohemian Massif — Introduction 95 p., CGS Prague.

Klomínský, J. – Jarchovský, – Rajpoot, G. (2010 b): Atlas of plutonic rocks and orthogneisses in the Bohemian Massif –Lugicum 78 p. CGS Prague.

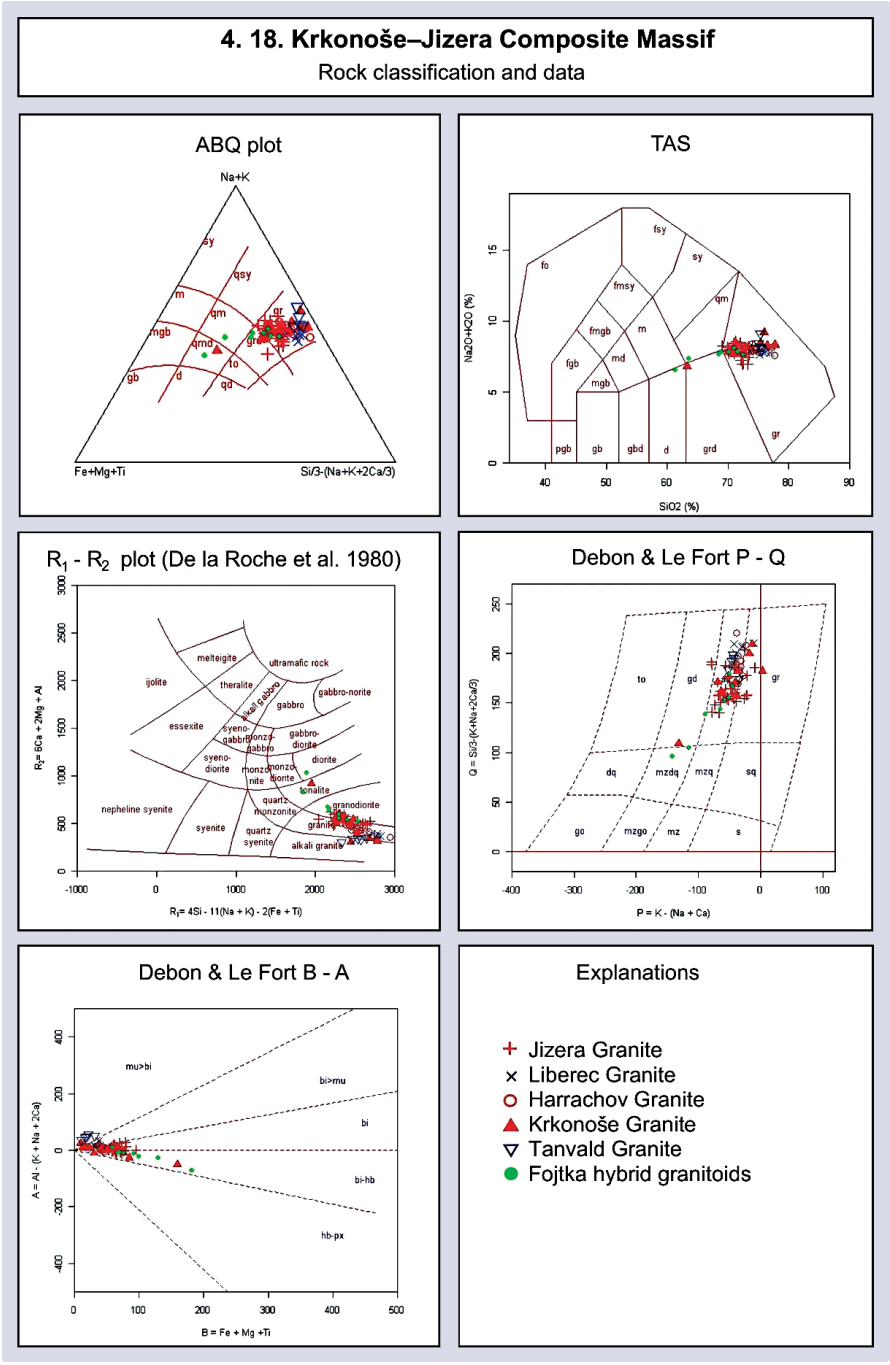

Figure 2.2. Krkonoše-Jizera Composite Massif rock classification diagrams (Klomínský et al. 2016).

3. Architecture of the western segment of the Krkonoše-Jizera Composite Massif

3.1 Granite typology and petrology

The western segment of the **Krkonoše-Jizera Composite Massif** consists of the three separate magmatic intrusions: **Tanvald Massif, Krkonoše-Jizera Massif** and **Fojtka Hybrid Bodies** (Klomínský 2009)**.**

Nine granite types were distinguished in the western part of the KJCM in the 1 : 25 000 map sheets 03-143 Liberec (Klomínský et al. 2004), 03-144 Tanvald (Mrázová et al. 2006) Jablonec nad Nisou, (Klomínský et al. 2006), Hejnice and Jizerka (Verner and Mrázová et al. 2013), and Raspenava (Vondrovic and Klomínský 2015).

Granite typology

TANVALD MASSIF

Tanvald Granite – medium grained two-mica alkali-feldspar granite (main rock type),
– weakly porphyritic biotite granite (marginal facies) (Fig. 3.1.1.).

KRKONOŠE-JIZERA MASSIF

Jizera Granite – distinctly porphyritic medium grained biotite granite (Figs. 3.1.2.A. and 3.1.3.).

Marginal Granite – porphyritic light pink medium grained biotite granite.

Liberec Granite – porphyritic coarse-grained biotite granite (Fig. 3.1.2.B.).

Bída Granite – fine grained leucocratic biotite granite (Fig. 3.1.4.).

Mšeno Granite – porphyritic small grained biotite granite (Fig. 3.1.5.).

FOJTKA HYBRID BODIES

Fojtka Granodiorite – weakly porphyritic small to fine grained biotite-hornblende granodiorite to quartz monzodiorite (Figs. 3.1.6. and 3.1.7.).

Žulový Vrch Granodiorite – markedly porphyritic small grained biotite to biotite-hornblende granodiorite (Fig. 3.1.8.).

Novina Granite – distinctly porphyritic medium grained biotite granite (Fig. 3.1.9.).

Granite petrology

Tanvald Granite is medium grained two-mica alkali-feldspar granite with marginal facies of the weakly porphyritic biotite granite. Two-mica granite contains about 22% plagioclase ($An_{1–5}$), 30 % quartz, 40 % potash feldspar, 2.5 % biotite and 3.5 % muscovite. Accessory minerals are represented by garnet up to 0.3 % and furthermore monazite, magnetite, andalusite and sporadic zircon. Tanvald Granite is peraluminous S-type with a relatively high content of Rb, Sn, Nb and F (Klomínský et al. 2009).

Figure 3.1.1. Tanvald Granite from the Černá Studnice granite quarry (real size). Photo J. Klomínský.

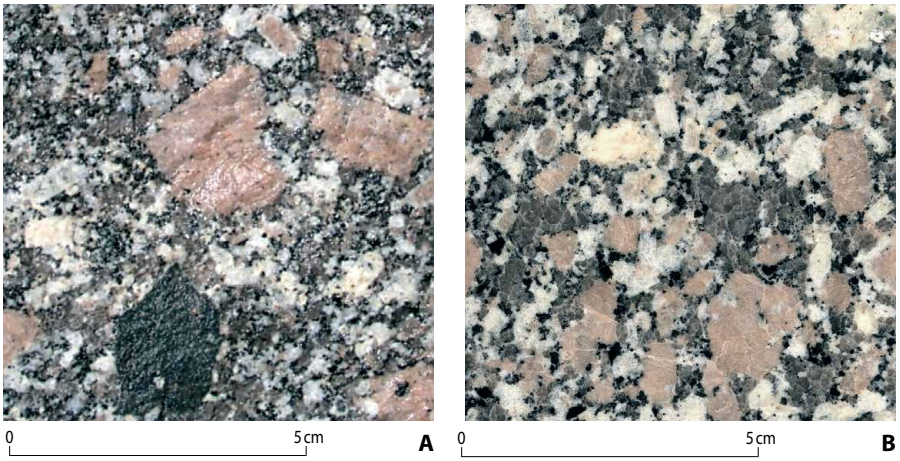

Figure 3.1.2. Jizera Granite (A), Liberec Granite (B). Photo J. Klomínský. Dominant granite types in the western part of the Krkonoše-Jizera Composite Massif.

Jizera Granite is light pink distinctly porphyritic up to megacrystic monzogranite with medium to coarse-grained groundmass. The main components comprise K-feldspar (mainly as phenocrysts of several generations), plagioclase and quartz present in nearly equal proportions, followed by abundant biotite and frequently by minor amphibole. Apatite, zircon and allanite present in mostly idiomorphic corroded and zoned crystals are the main accessory minerals; xenotime presence is suspected. Opaque minerals may be represented by traces of magnetite, but they are often completely absent. Chlorite, sericite, epidote, titanite and rare calcite are secondary minerals. According to the IUGS classification the Jizera Granite corresponds on average to nearly an ideal monzogranite.

Marginal Granite is light pink distinctly porphyritic medium grained biotite monzogranite comprising 1 to 2 km wide zone along the KJCM contact with Krkonoše-Jizera Crystalline Complex in the Hejnice and Jizerka (Verner and Mrázová 2013) and Raspenava (Vondrovic and Klomínský 2015) map sheets. This granite has gradational contact with the Liberec Granite with increasing contrast between the matrix grain

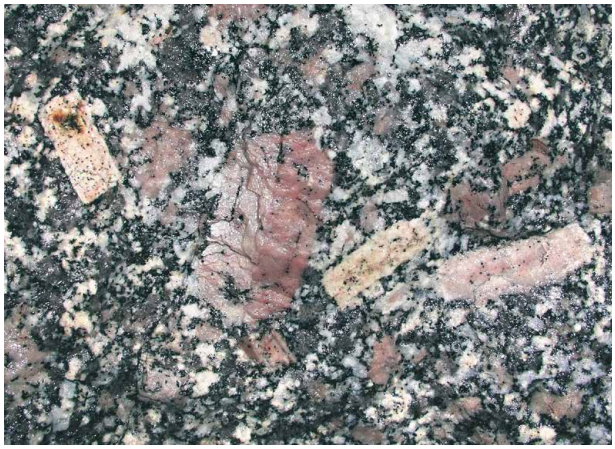

Figure 3.1.3. Different generations of K-feldspar phenocrysts in the Jizera Granite in the Souš water-supply tunnel. Size of the pink phenocryst is 5 cm. Photo J. Klomínský.

size and size of the K-feldspar phenocrysts towards the boundary with country rocks. Marginal Granite becomes texturally similar to the Jizera Granite but its high magnetic susceptibility (20 times higher than the Jizera Granite) is closer to the Liberec Granite.

Liberec Granite is pink porphyritic coarse grained biotite monzogranite with biotite frequently affected by chloritization. Intensity of this alteration varies considerably. In its mineralogical composition and structural-textural properties the granite seems to be uniform across the entire large area of the Liberec lowland. Specific features include sporadic amphibole and muscovite, occurrence of allanite.

Figure 3.1.4. Bída Granite from the abandoned quarry in the Bída locality in Liberec Centrum. (real size). Photo J. Klomínský.

Bída Granite is pale grey small to fine grained biotite syenogranite with distinctive orbicular biotite aggregates edged by pink quartz-feldspar seams. The unusual rock is exposed in the abandoned quarry near the Liberec Centrum. This granite forms a small dyke-like body in the older Liberec Granite. Bída Granite has been intensively quarried for cobblestones in the past.

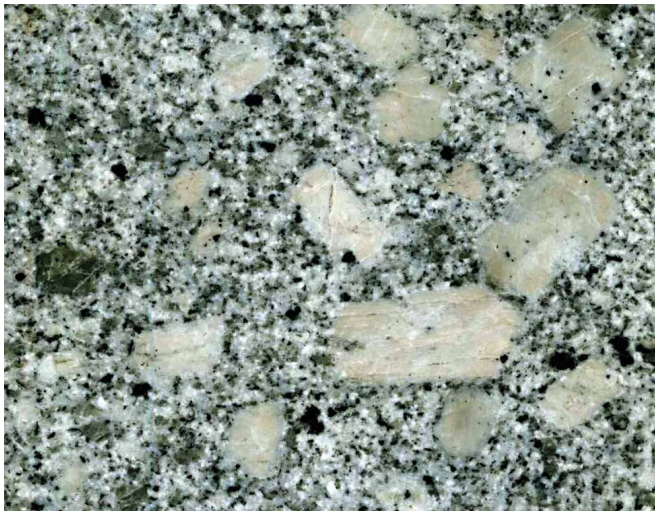

Figure 3.1.5. Mšeno Granite (real size). Photo J. Klomínský.

Mšeno Granite is grey to pink porphyritic small grained biotite syenogranite. Drop-like quartz phenocrysts up to 1 cm in size are a distinctive feature of this rock which forms relatively subhorizontal or pitched thin sheets inclining to the south up to several tens of meters thick mainly within the Liberec Granite.The unusually low magnetic susceptibility of the Liberec Granite (0.114 . 10^{-3} SI) is developed next to endocontact of the younger Mšeno Granite.

Fojtka Hybrid Bodies

Fojtka Granodiorite is dark greenish small to medium grained biotite-hornblende hybrid quartz monzodiorite to granodiorite (Fojtka type, Figs. 3.1.6., 3.1.7.).

Žulový Vrch Granodiorite is grey distinctly porphyritic small to medium grained hybrid hornblende-biotite granodiorite (Žulový vrch type, Fig. 3.1.8.).

Novina Granite is pale grey porphyritic medium grained biotite hybrid monzogranite (Novina type, Fig. 3.1.9.).

A distinctive feature of all these rocks is frequent small oval microgranular melanocratic diorite and globular aggregates of smoky quartz up to 2 cm in size imported from surrounding granites with thin amphibole and biotite rims. In porphyritic types pink or white idiomorphic K-feldspar phenocrysts with thin white rims of albite rich up to 4 cm in length (Fig. 3.1.9.).

REFERENCES

Klomínský J. (2009): Architecture of Krkonoše-Jizera Composite Massif granites and recent activity of their tectonic network in the Bedřichov water-supply tunnel in Jizerské hory Mts. – Zpr. Geol. Výzk. 2008, 154–157.

Klomínský, J. – Adamová, M. – Bělohradský, V. – Burda, J. – Kachlík, V. – Lochmann, Z. – Manová, M. – Nekovařík, Č. – Nývlt, D. – Šalanský, K. (2004): Vysvětlivky k základní

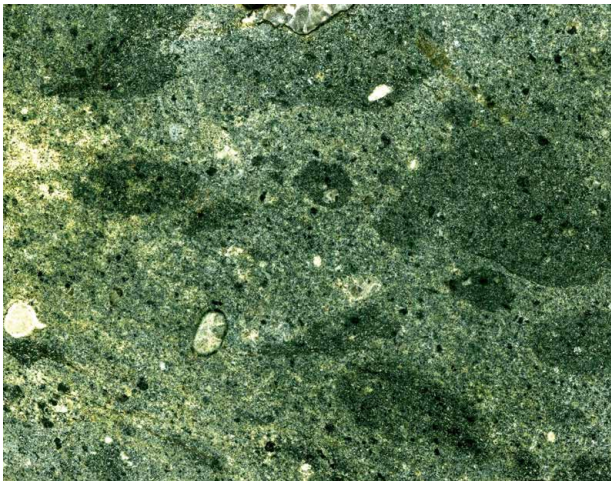

Figure 3.1.6. Fojtka type hybrid quartz monzodiorite in magmatic melange of the microgranular mafic enclaves from the abandoned quarry in Fojtka (real size). Photo J. Klomínský.

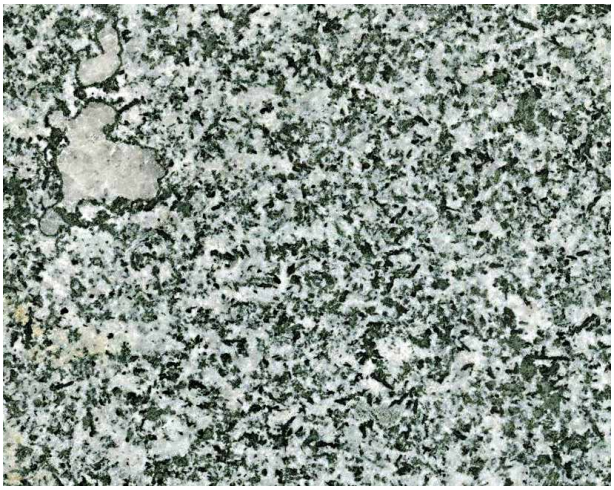

Figure 3.1.7. Fojtka type quartz monzodiorite from the abandoned quarry in Fojtka (real size). Photo J. Klomínský.

Figure 3.1.8. Žulový Vrch type hybrid granodiorite from the abandoned quarry in Rudolfov (1/2 size). Photo J. Klomínský.

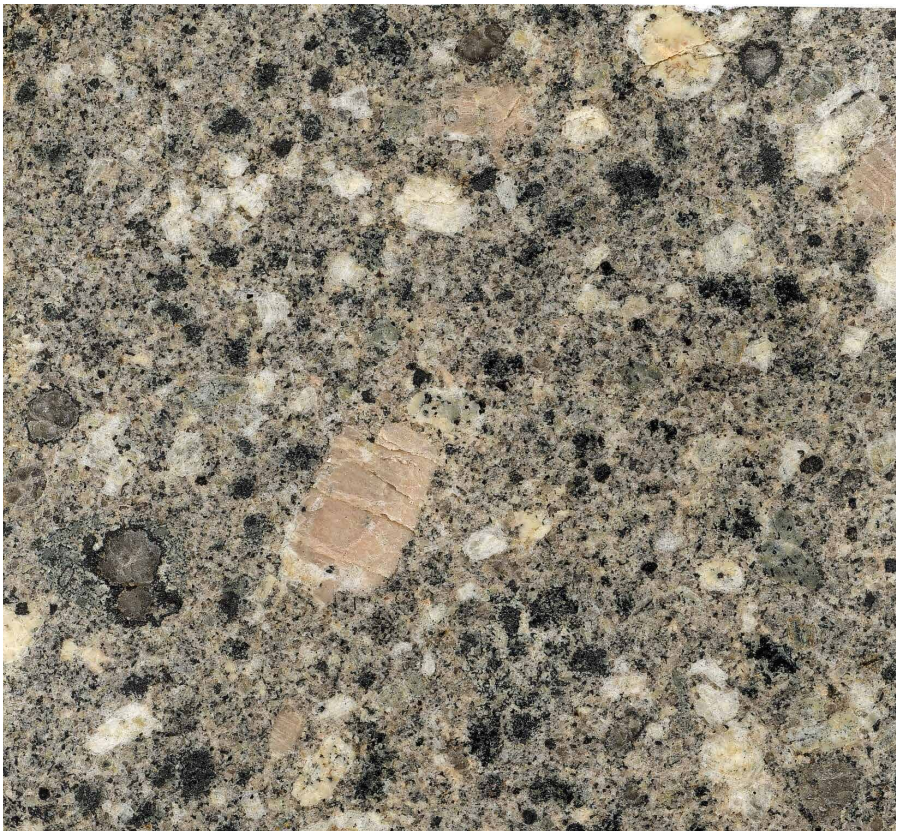

Figure 3.1.9. Novina type hybrid granite from outcrops near Novina village (real size). Photo J. Klomínský.

geologické mapě České republiky 1 : 25 000 03-143 Liberec. 68 s. – ČGS. Praha. ISBN 80-7075-623-3.

Klomínský J. – Adamová, M. – Burda, J. – Jarchovský, T. – Kachlík, V. – Kořán, V. – Kříbek, B. – Manová, M. – Nekovařík, Č. – Šalanský, K. (2006): Základní geologická mapa České republiky 1 : 25000 s Vysvětlivkami, 03 – 323 Jablonec n. N. – 62 s. ČGS. Praha.

Mrázová, Š. – Adamová, M. – Burda, J. – Knésl, I. – Klomínský, J. – Lochman, Z. – Manová, M. – Nekovařík, Č. – Nývlt, D. – Šalanský, K. (2006): Základní geologická mapa České republiky 1 : 25 000 s Vysvětlivkami, list 03-144 Tanvald. – 33 str. ČGS, Praha.

Verner, K. – Mrázová, Š. – Břízová, E. – Buriánek, D. – Holub, F. – Klomínský, J. – Malík, J. – Martínek, K. – Pecina, V. – Rambousek, P. – Rukavičková, L. – Skácelová, D. – Skácelová, Z. – Štor, T. – Vrána, S. – Žáčková, E. (2013): Vysvětlivky k Základní geologické mapě České republiky 1 : 25 000, list 03-142 Hejnice a 03-231 Jizerka. 143 s. MS Archive CGS Praha.

Vondrovic, L. – Klomínský, J. et al. (2015): Základní geologická mapa České republiky 1 : 25 000 03 – 322 Raspenava. Geologické mapy 1 : 25 000 s textovými vysvětlivkami. – MS Archive CGS, 189 s. Praha.

Žák, J. – Verner, K. – Sláma, J. – Kachlík, V. – Chlupáčová M. (2013): Multistage magma emplacement and progressive strain accumulation in the shallow-level Krkonoše-Jizera Granite complex, Bohemian Massif. – Tectonics, 32, 1493–1512, 34 p.

3.2 Geochemical discrimination of the Liberec and Jizera Granites

The Liberec and Jizera Granites are most dominant rock types in the western part of the Krkonoše-Jizera Composite Massif. Visual discrimination of these two very similar granites has until now been rather subjective, bringing complications and uncertainty during field mapping. The main problem is definite recognition of the individual rock types in the vicinity of their demarcation line because of their gradational nature.

All field parameters in Tab. 3.3.1. are not always sufficient for classification of both rocks within their domains. An approach to this problem is proposed on geochemical parameters (Jarchovský 2010). Specific geochemical characteristics of the Liberec and Jizera granites can demarcate their boundaries. MgO and TiO_2 contents are useful in characterising the two granites, while SiO_2, CaO, P_2O_5, Ba and Sr are good but less reliable indicators, and Th, As and some REE elements also appear useful. On the contrary, MnO, Na_2O, CO_2, Ga, Zr, Y, Ni, Co, Cu and Zn seem to be practically without any discriminating significance. The most powerful discriminator is MgO with a 0.70 % limit between Liberec Granite (< 0.70 %) and Jizera Granite (> 0.70 %). Likewise unequivocal is TiO_2, which in Liberec Granite is less than 0.40 %, and always higher in Jizera Granite (Fig. 3.2.1.). Fig. 3.2.2. shows a map of the geochemical discrimination scores for the Liberec and Jizera granites (Tab. 3.2.1.).

Based on more precise geochemical discrimination between these two granites it is possible to state that the Liberec Granite is overlain by the Jizera type and that the Liberec Granite represents a more advanced differentiation state in the magmatic evolution in the western segment of the Krkonoše-Jizera Composite Massif.

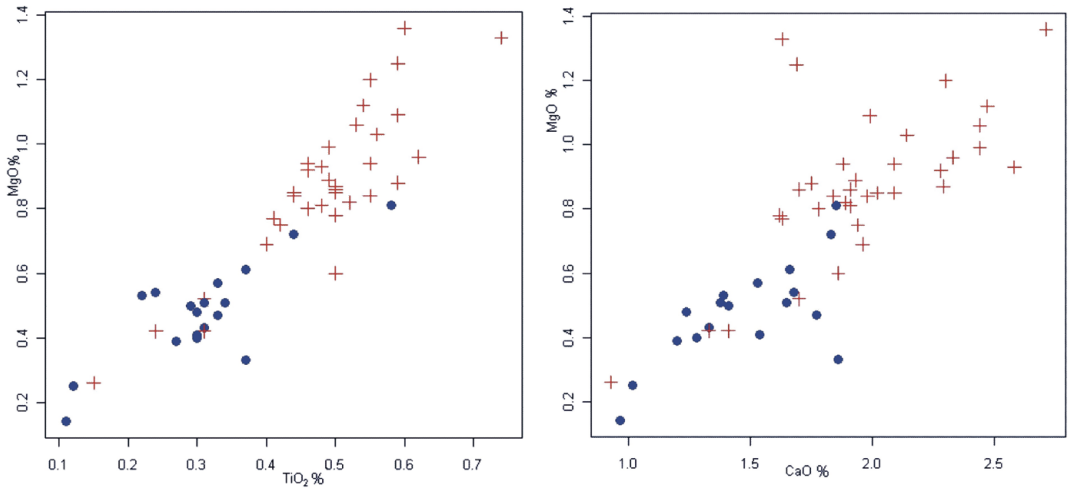

Figure 3.2.1. Binary diagrams: a) MgO-TiO_2, b) MgO-CaO of the Liberec (●) and Jizera Granite (+). Jarchovský et al. (2010).

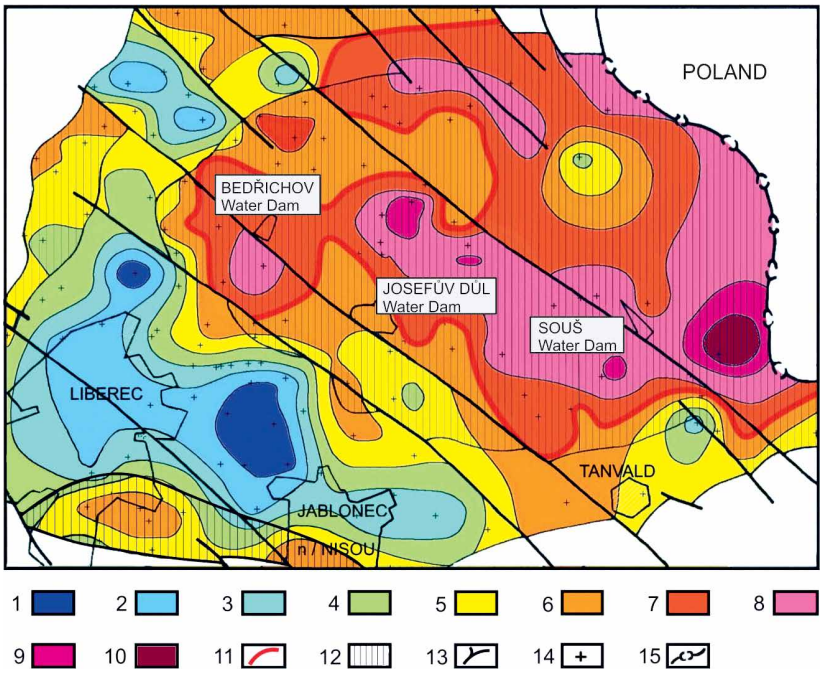

Figure 3.2.2. Map of the discriminant score for Jizera and Liberec Granite. Jarchovský et al. (2010).

Discriminant score : 1 – <10, 2 – 10–12, 3 – 12–14, 4 – 14–16, 5 – 16–18, 6 – 18–20, 7 – 18–20, 8 – 20–22, 8 – 22–24, 9 – 24-26, 10 – >26. 11- isoline of the geochemical discriminant index R_0, 12 – field of the Jizera Granite in the geological map, 13 – geological faults, 14 – rock sample locality, 15 – state border.

Table 3.2.1. Evaluation of the discrimination efficiency. Jarchovský et al. (2010).

	Total a priori probability	Classified as Liberec Granite	Classified as Jizera Granite
Liberec Granite	29 (0.263)	27 (0.245)	2 (0.018)
Jizera Granite	81 (0.737)	6 (0.055)	75 (0.682)
Total	110 (1.000)	33 (0.300)	77 (0.700)

Well classified 102 samples (92.7%)
Incorrectly classified 8 samples (7.2%)

REFERENCES

Jarchovský, T. – Fediuk, F. – Klomínský, J. – Schovánek, P. (2010): Geochemická diskriminace libereckého a jizerského granitu v západní části krkonošsko-jizerském kompozitního masivu. – Zprávy o geologických výzkumech v roce 2009, 219–222.

3.3 Petrophysical discrimination of the Liberec and Jizera Granites

Magnetic susceptibility (MS) is one of the quantitative parameters for field recognition of the Jizera and Liberec Granites in the KJCM (Vondrovic and Klomínský et al. 2015). This petrophysical parameter reflects the amount and proportion of the paramagnetic biotite and ferromagnetic minerals, mostly magnetite. For detection of the gradual contact of the granites MS values > 0.5 . 10^{-3} SI are characteristic for the Liberec Granite, where MS values < 0.5 . 10^{-3} SI are typical for the Jizera Granite (Tab. 3.3.1.). The magnetic susceptibility has been gauged on 1241 localities of the Liberec and Jizera Granites in the western segment of the Krkonoše-Jizera Massif (Fig. 3.3.1.) Žitný (2017). MS was measured by portable kappameter SM-20.

Table 3.3.1. Main field parameters used for the Liberec and Jizera Granite geochemical discrimination.

Rock	Size of K-feldspars	Size of matrix	Magnetic susceptibility
Liberec Granite	~ 2 cm	coarse	> 0.5 . 10^{-3} SI
Jizera Granite	~5 cm	medium	< 0.5 . 10^{-3} SI).

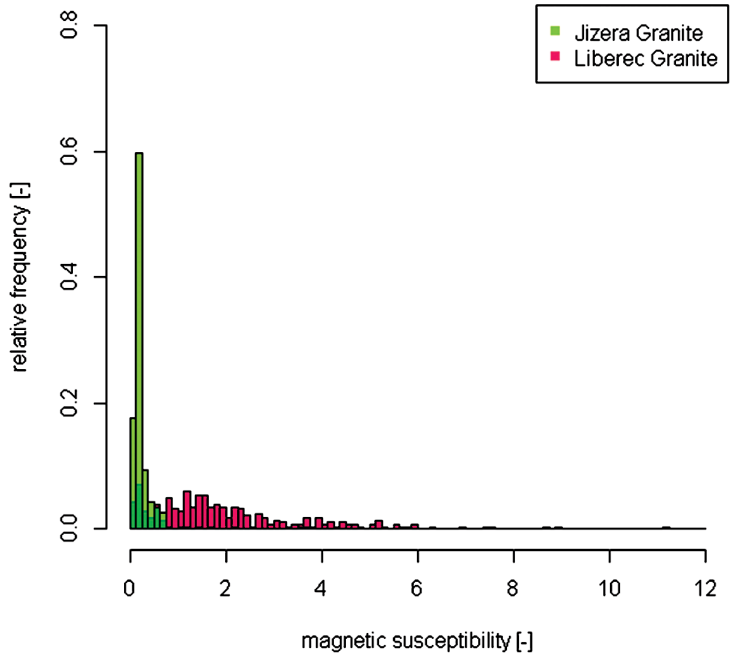

Figure 3.3.1. Frequency of the Jizera (green) and Liberec Granite (red) magnetic susceptibility field measurement in the western segment of the KCM (1241 localities). Žitný (2017). Pale-green colour marks the overlap of the Jizera and Liberec magnetic susceptibility.

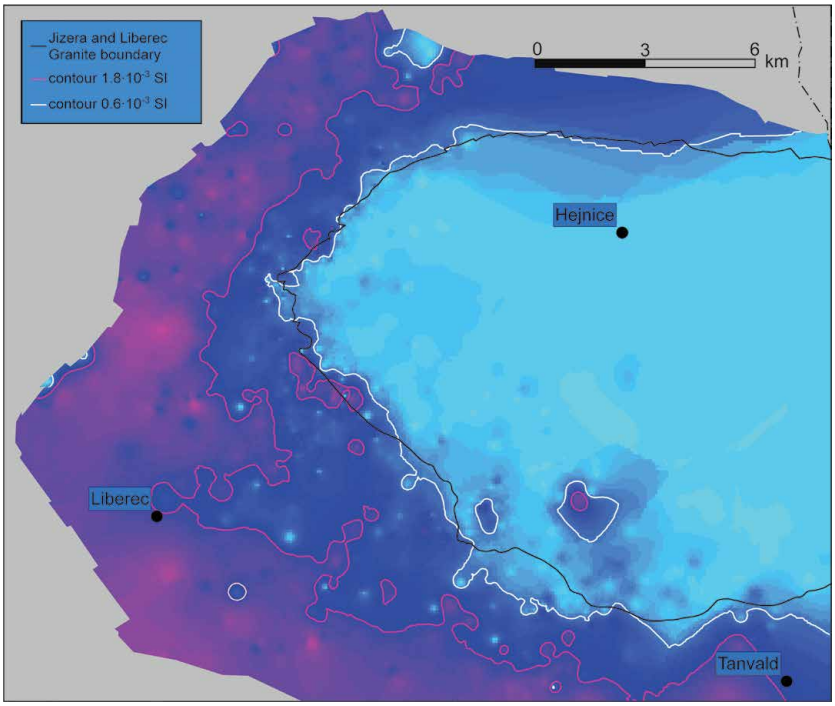

Figure 3.3.2. Map of the magnetic susceptibility field measurements in the western segment of the KJCM. Žitný (2017). Magnetic susceptibility contours represents boundary between the Jizera and Liberec Granites according to petrophysical field discrimination. 0.6 . 10^{-3} SI contour outlines the field of the Jizera Granite. The area between contours 1.8 . 10^{-3} and 0.6 . 10^{-3} SI is occupied by Transitional Granite (marginal facies of the Liberec Granite). Red area (>1.8 . 10^{-3} SI) represents outcrops of the Liberec Granite. Black line represents the Jizera and Liberec Granite boundary according to the field geological mapping.

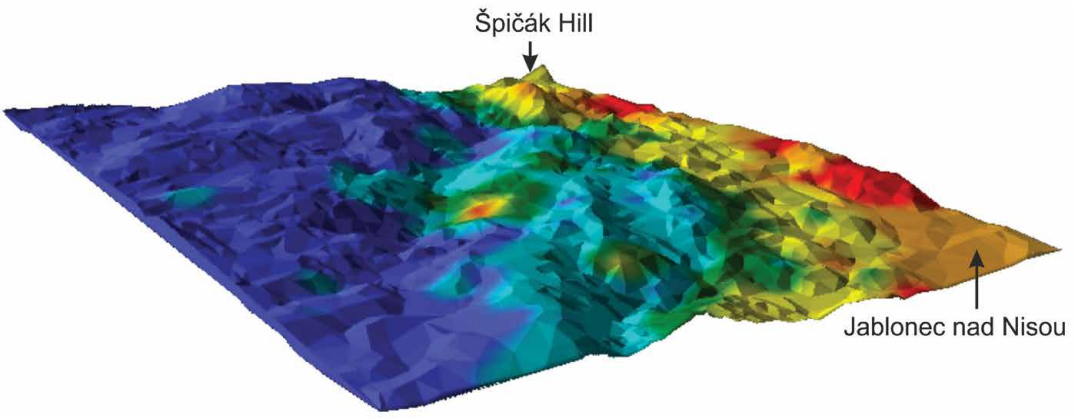

Figure 3.3.3. 3D model of the magnetic susceptibility distribution in the Jizera and Liberec Granites on the Tanvald geomorphologic map sheet 1 : 25 000 (view from NW to SE). K. Martínek personal communication. The lowland on the right side is occupied by the Liberec Granite with high magnetic susceptibility (red and yellow) and the highland on the left side is formed by the Jizera Granite with low magnetic susceptibility (blue and green). The highest point is Špičák Hill near Tanvald.

The map of the magnetic susceptibility field measurements in the western segment of the KJCM (Fig.3.3.2.) represents the petrophysical discrimination between the spaces occupied by Jizera and Liberec Granites. Magnetic susceptibility contour 1.8 . 10^{-3} SI forms the boundary of the optimal Liberec Granite area and magnetic susceptibility contour 0.6 .10^{-3} SI defines the area of the optimal Jizera Granite. Blue space belongs to the buffer zone between the Jizera and Liberec Granites (see Chapter 5 and Fig. 5.2.8.).

A 3D model of the magnetic susceptibility distribution in the Jizera and Liberec Granites on the Tanvald geomorphologic map sheet 1 : 25 000 (view from NW to SE) is shown in Fig. 3.3.3. Higher magnetic susceptibility corresponds to Liberec Granite outcrops in the lowland making the base for the Jizera Granite in upland.

REFERENCES

Vondrovic, L. – Klomínský, J. et al. (2015): Základní geologická mapa České republiky 1 : 25 000 03 – 322 Raspenava. Geologické mapy 1 : 25 000 s textovými vysvětlivkami. – MS Archive CGS, 189 s. Praha.

Žitný, T. (2017): Vyhodnocení měření magnetické susceptibility hornin v mapových listech 03-141 Raspenava, 03-143 Liberec a 03-144Tanvald 03-144. – Semestrální projekt ke kurzu GIS a DPZ v geologii. 7 p. MS report ČGS.

3.4 Fojtka Hybrid Granitoids – structural and lithological markers

The western segment of the Krkonoše-Jizera Composite Massif contains Fojtka Hybrid Granitoids (FHG) in the form of the sheet like bodies tens to several hundred metres long of multiple ellipsoidal microgranular enclaves and also large angular rafts enclosed in the Liberec Granite and in the Jizera Granite (Figs. 3.4.3.A and 3.4.3.B). These enclaves constitute a discontinuous nearly linear swarm about 30 km long, running between Fojtka village (Fig. 3.4.1.) in the north-west and Tanvald town in the east. The position of the Fojtka Hybrid Granitoids near the gradational Liberec and Jizera boundary emphasizes their role as structural and lithologic markers in the KJCM interior. The Hrabětice-Novina belt occupies the highest stratigraphic position while the Žulový Vrch belt is situated in the deeper level of the KJCM. This dominant enclave "horizon" trending NW-SE is moderately dipping (up to 45º) to NE, beneath the Jizera Granite. Several abandoned quarries north of Fojtka village show examples of all varieties of Fojtka Hybrid Granitoids (Fig. 3.4.1.). They exhibit sharp contacts with the Liberec Granite and locally a magmatic breccia with angular fragments of the Fojtka Hybrid Granitoids in the Liberec Granite occurs (Klomínský 1969). All the Fojtka Hybrid Granitoids have a low magnetic susceptibility (0.2 . 10^{-3} SI) contrasting with susceptibility values for the Liberec Granite (2–3 . 10^{-3} SI). The Fojtka Hybrid Granitoids represent products of magma mixing, resulting from mixing and hybridization of mainly basic rocks with granite magma. The resulting rock series includes fine-grained amphibole-biotite quartzdiorite, quartzmonzodiorite, porphyritic amphibole-biotite granodiorite up to biotite granites (monzogranites), Fig. 3.4.2.

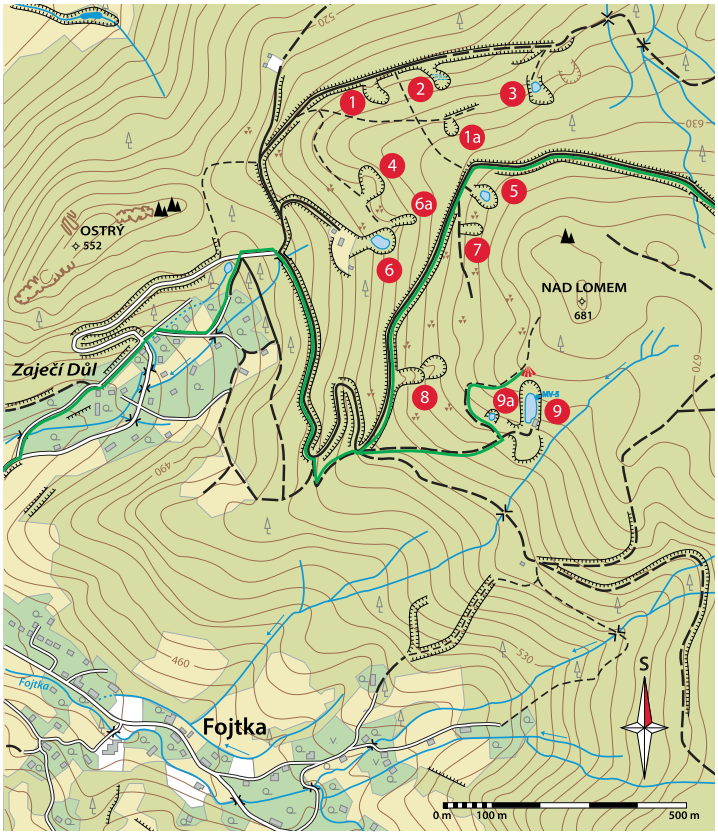

Figure 3.4.1. A cluster of abandoned quarries for Fojtka hybrid granitoids near Fojtka village. Šrek (2012).

Complex enclaves indicating successive batches of melts document a time sequence in production of hybrid melts. The general scheme is one of relatively more basic enclaves in more felsic granite. Introduction of potassium from granite magma is documented by the increasing size and number of K-feldspar phenocrysts. Enclaves typically contain equate quartz grains rimmed by common hornblende and biotite.

According to early geological studies, the hybrid rocks of the Fojtka type are older magmatic rocks suspended in younger granite melt, or they derived from country rocks (amphibolites) and were affected by granitization of variable intensity (Klomínský 1969). The planar pattern and large lateral extent of the Fojtka Hybrid Granitoid enclaves possibly indicate a former presence of mafic magma, either in the floor of the granite magma chamber or in the form of syn-plutonic dykes (Slabý and Martin 2008).

The mafic magma crystallized at higher temperatures and was involved in mixing with the surrounding granite magma during production of mafic and hybrid layers, lenses and enclave clusters, mainly near the floor of the Jizera Granite. The sequence of layers of the Fojtka Hybrid Granitoids and surroundings granites in structurally overlying and underlying parts can be seen as a "stratigraphic" section, representing a record of crystallization, melt filling and mixing in the magmatic chamber in a similar way as observed in some layered mafic intrusions. The location of the Fojtka Hybrid Granitoids in the vicinity of the Liberec and Jizera Granite gradational boundary

supports their function as ribbons structurally dividing the KJCM into definite subhorizontal layers (Klomínský 2014).

FHG represent residues of the former synmagmatic basic bodies or lamproid dykes (Slaby a Martin 2008), which intruded into the Jizera and Liberec Granites at the stage of their solidification. FHG bodies represent basic dykes of mantle origin which suffered the turbulent process of magmatic mixing and mingling with surrounding granites and solidified faster than surrounding granites (Slaby and Martin 2008). This is indicated by synchronous FHG zircon ages (318.4 ± 2.3 Ma) compared with the Krkonoše-Jizera Granites (319.5 ± 2.3 and 320, 1 ± 3.0 Ma) according to Žák et al. (2013).

Former shapes of the basic dykes were extensively modified into numerous multiple enclaves and synmagmatic breccias which are now arranged into three subhorizontal intermittent layers predominantly within the Jizera Granite (Figs. 3.4.3.A and 3.4.3.B). Older microgranular enclaves are enclosed by younger rocks with more acid composition. FHG voluminous expansion is documented by an increase in amount and size of K-feldspar phenocrysts in the surrounding granites. (Fig. 3.4.4.).

REFERENCES

Klomínský, J. (1969): Krkonošsko-jizerský granitoidní masiv. – Sbor. geol. Věd, Geol., 15, 7–133.

Klomínský, J. (2014): Fojtské hybridní granitoidy-strukturní a litologické markery v krkonošsko-jizerském masivu. – Zprávy o geologických výzkumech v roce 2013, 120–125.

Šrek, J. (2012): Žulové lomy nad Fojtkou. – Ročenka Jizersko-ještědského horského spolku 11. R. 75–96 str.

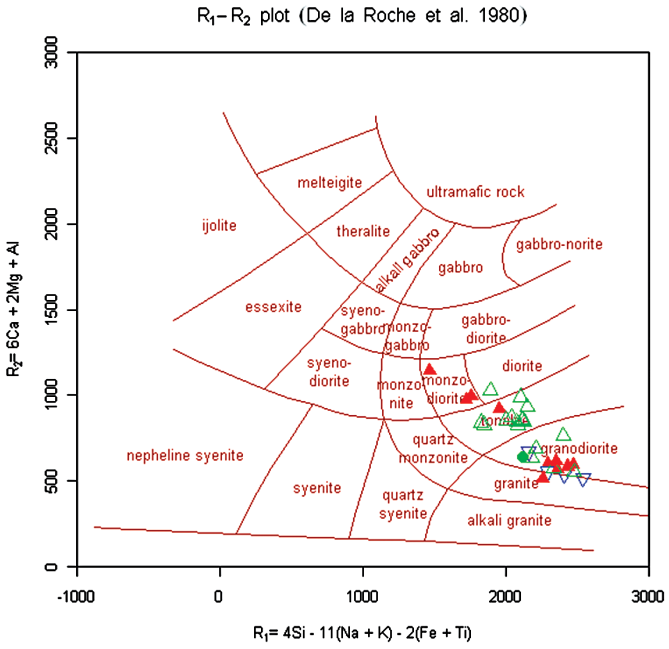

Figure 3.4.2. Fojtka Hybrid Granitoids in the De la Roche R_1/R_2 diagram. Green triangles – Zaječí Důl zone of the hybrid granitoids. Red triangles – Žulový Vrch zone granitoids. Blue triangles – Hrabětice-Novina zone of hybrid granites. Green circle – microgranular mafic enclave (MME).

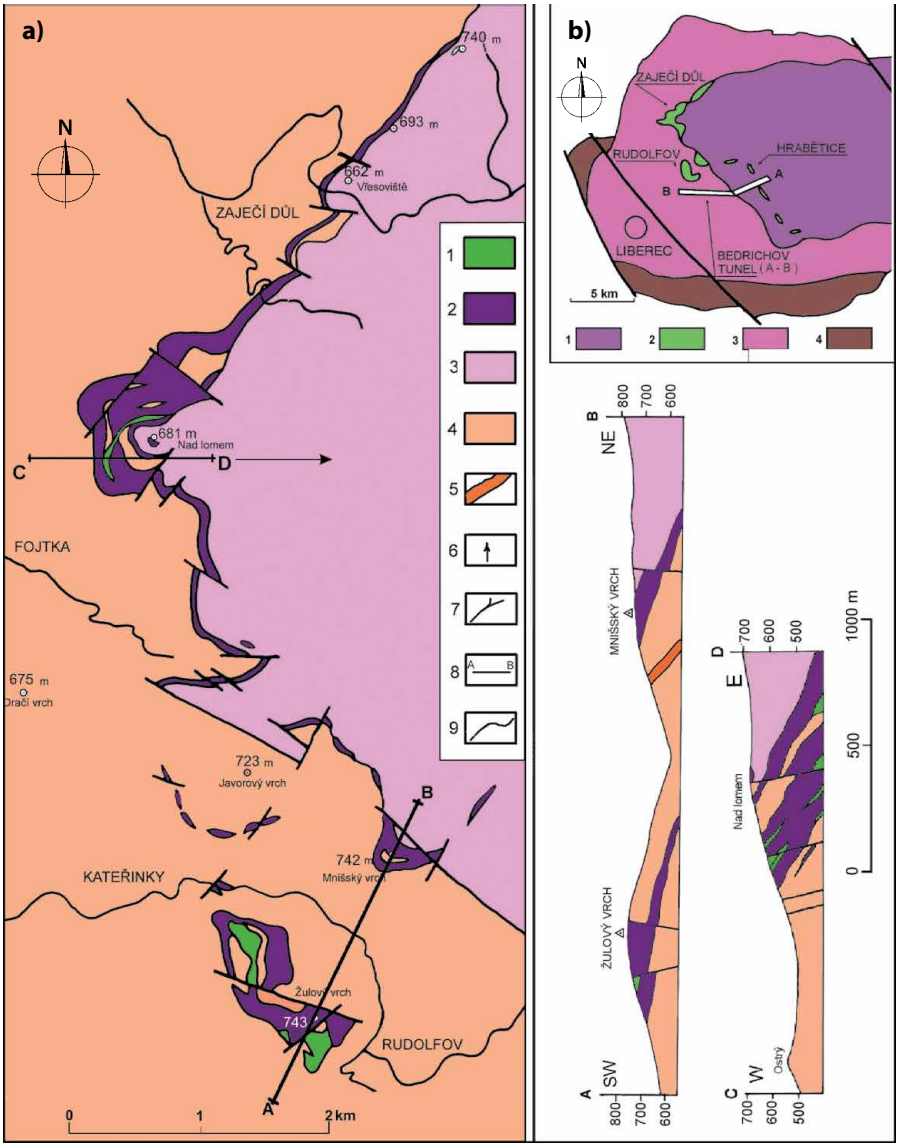

Figure 3.4.3a Geological map of the Fojtka area. Klomínský (2014).
1 – minute grained to medium grained quartz monzodiorite to granodiorite – Fojtka type, 2 – porphyritic minute grained granodiorite – Žulový Vrch type, 3 – Jizera Granite, 4 – Liberec Granite, 5 – fine-grained biotite granite, 6 – brachysynform axis, 7– fault, 8 – geological cross-section line, 9 – road network.

Figure 3.4.3b Geological map of the western segment of the Krkonoše-Jizera Composite Massif. Klomínský (2014). 1 – Jizera Granite, 2 – Fojtka Hybrid Granitoids (FHG), 3 – Liberec Granite, 4 – Tanvald Granite, Double abscissa – A and B water-supply tunnels position in Bedřichov village in the Jizerské hory Mts. FHG in western part of the Krkonoše-Jizera Composite Massif are located in proximity of the Liberec and Jizera contact in the Zaječí Důl, Žulový Vrch, and Hrabětice-Novina zones. These zones are represented by marked range of the rocks from quartz monzodiorite (Fojtka type) up to the most frequent granodiorite (Žulový Vrch type) and monzogranite (Novina type).

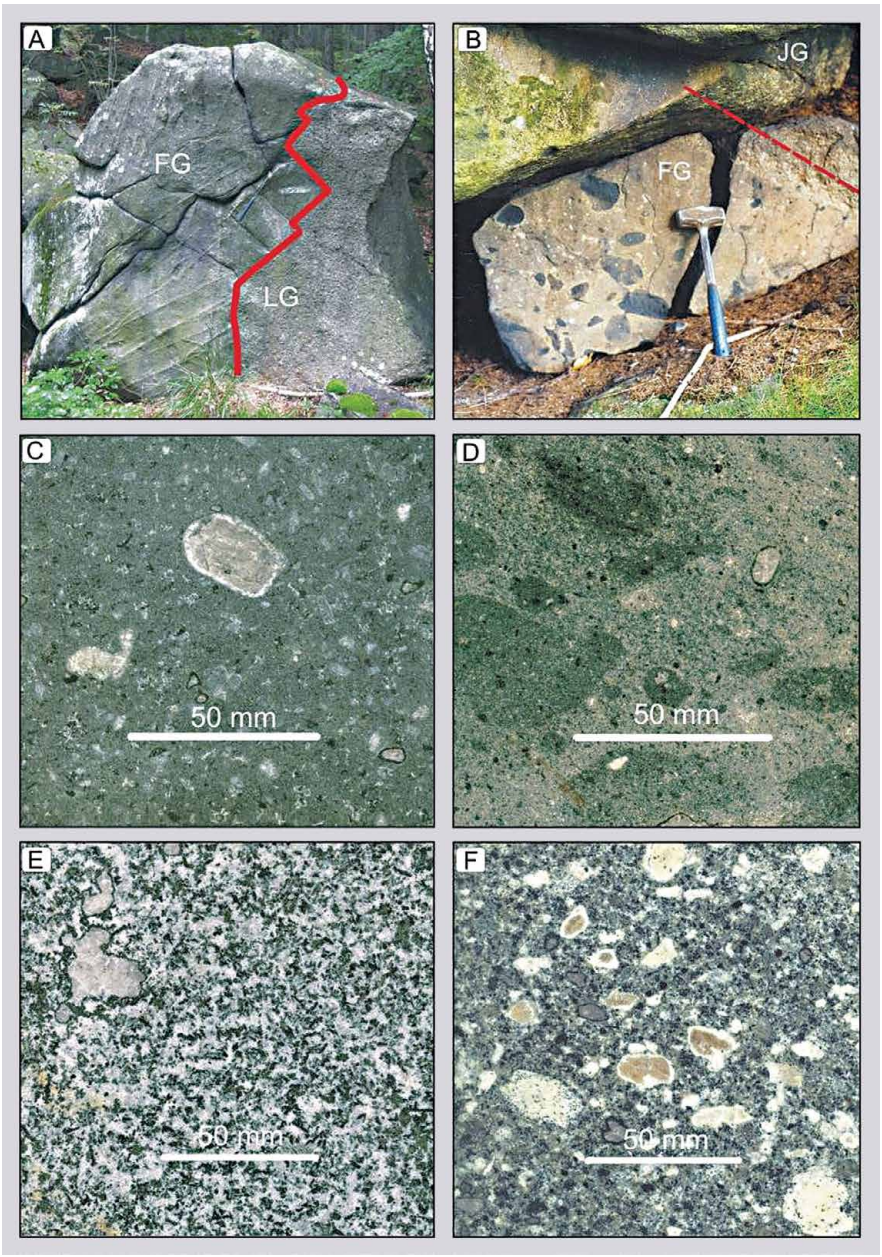

Figure 3.4.4. Fojtka Hybrid Granitoids. Klomínský (2014). A – Contact of the Liberec Granite (LG) and medium grained quartz monzodiorite – Fojtka type (FG), Za-ječí Důl locality. B – Magmatic mixture of Jizera Granite (JG) and minute grained quartz monzodiorite – Fojtka type contact (Mnišský Vrch locality). C – Minute grained quartz monzodiorite – Fojtka type (FG) with Kf-feldspar phenocrysts and oval quartz aggregates with amphibole and biotite rims, Zaječí Důl locality. D – Magmatic breccias of the older MME in minute grained quartz monzodiorite – Fojtka type, Mnišský Vrch locality. E –medium grained quartz monzodiorite – Fojtka type, Zaječí Důl locality. F – Distinctly porphyritic granodiorite – Žulový Vrch type with frequent Kf-feldspar phenocrysts with white plagioclase rims and frequent oval aggregates of quartz with amphibole and biotite rims, Zaječí Důl locality. *(MME – Mafic Microgranular Enclave.)*

Slaby, E. – Martin, H. (2008): Mafic and felsic magma interaction in granites: the Hercynian Karkonosze Massif (Sudetes, Bohemian Massif) – Journal of petrology 49, 2, 353–391.

Vondrovic, L. – Klomínský, J. eds (2015): Základní geologická mapa České republiky 1 : 25 000 03 – 322 Raspenava. Geologické mapy 1 : 25 000 s textovými vysvětlivkami. 57 s. – MS Archive CGS, 202 s. Praha.

Žák, J. – Verner, K. – Sláma, J. – Kachlík, V. – Chlupáčová M. (2013): Multistage magma emplacement and progressive strain accumulation in the shallow-level Krkonoše-Jizera Plutonic complex, Bohemian Massif. – Tectonics, 32, 1493–1512, 34 p.

3.5 Tanvald Massif – relict of the magmatic body in the KJCM

The Tanvald Massif is two large mica alkali feldspar granite intrusions in the Bohemian Massif (Žák et al. 2006). Two spatially separated outcrops of the Tanvald Granite along the Liberec Granite southern and western contact (77–89° dip to S and W respectively) are relics of the formerly larger Tanvald Massif. The southern segment of the Tanvald Massif represents a long and relatively thin slab in size 25 × 4 km at its outcrop, gently dipping to the south under low grade Cambro-Silurian metamorphics (Fig. 1.1.2.).

Both segments of the Tanvald Massif are formed predominantly of medium grained two-mica alkali-feldspar granite and porphyritic biotite alkali-feldspar granite along

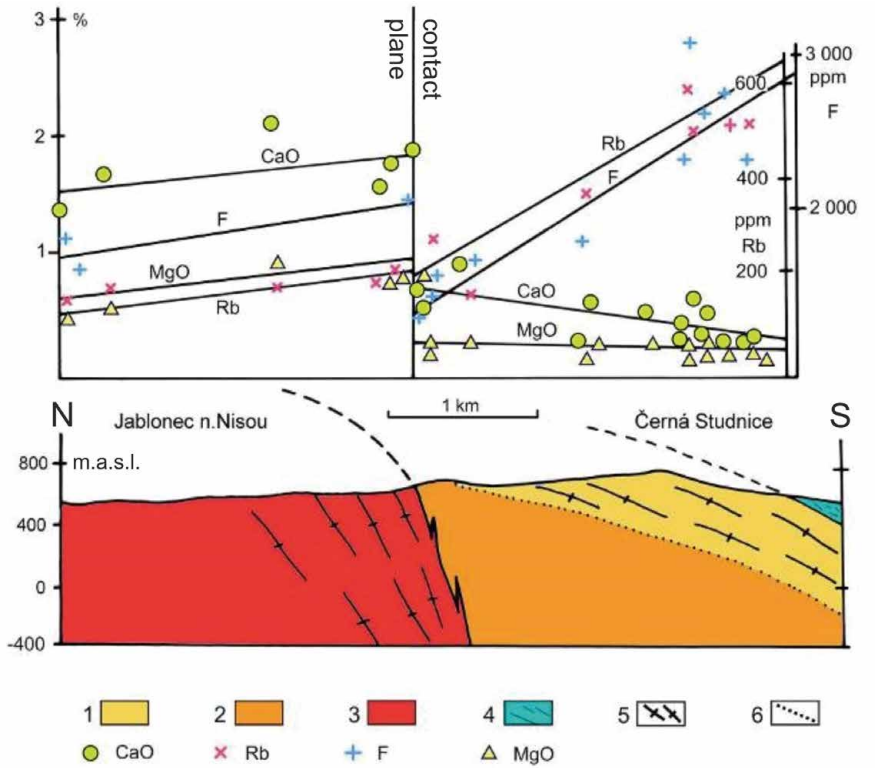

Figure 3.5.1. Geological and geochemical section across southern part of the Tanvald Massif and southern margin of the Liberec Granite (Klomínský et al. 2009).
1 – Tanvald Granite – two-mica facies,
2 – Tanvald Granite – porphyritic biotite facies,
3 – Liberec Granite,
4 – Železný Brod phylites,
5 – magmatic foliation,
6 – lithologic transition.

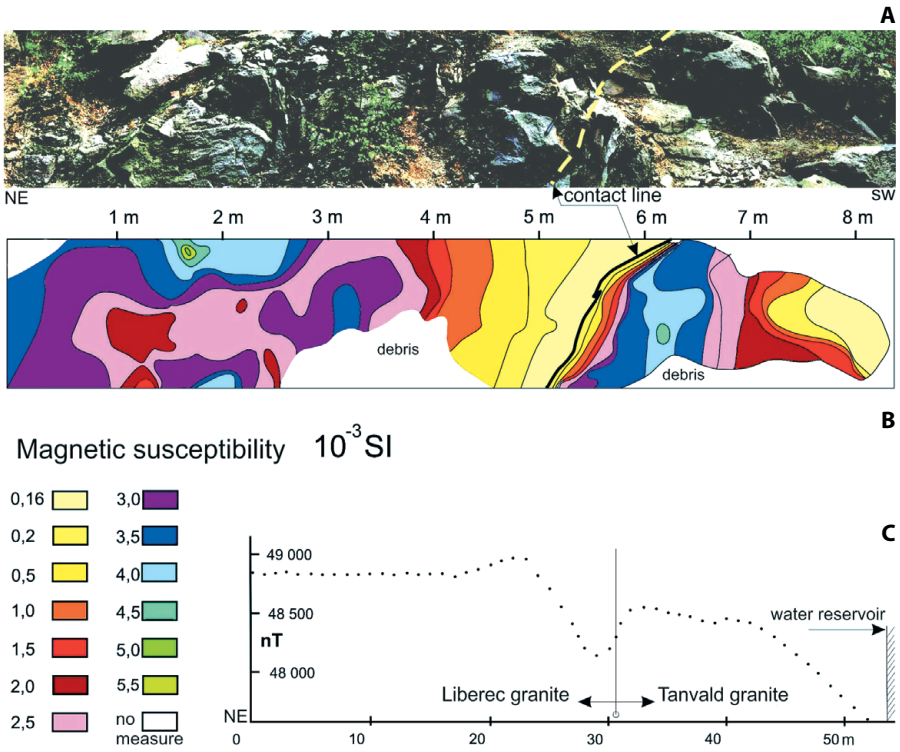

Figure 3.6.1. A – Rock exposure in vicinity of the water reservoir in Nová Ves n.nad Nisou Contact between Liberec and Tanvald Granites is marked by white dash line (situation in 2000). B – Map of the magnetic susceptibility of the rock exposure across the contact of the Liberec and Tanvald Granites. C – Magnetometric profile across the rock exposure. Klomínský et al. (2007).

the northern and western contact with the Liberec Granite. A substantial part of the Tanvald Massif has been disintegrated into rafts and xenoliths by intrusive activity of the younger Liberec Granite. This unusual phenomenon of the magmatic "cannibalism" between the Tanvald and Liberec Granites is documented by contrast in their discordant magmatic fabric and by lithological and geochemical reverse zoning in the Tanvald Granite Fig. 3.5.1 (Klomínský et al. 2009).

REFERENCES

Klomínský, J. – Fediuk, F. – Schovánek, P. – Jarchovský, T. (2009): Tanvaldský masiv – relikt magmatického tělesa v krkonošsko-jizerském kompozitním masivu. – Zprávy. Geol. Výzk. v r. 2008, 158–160.

Žák J. – Vyhnálek, B. – Kabele P. (2006): Is there a relationship between magmatic fabrics and brittle fractures in Massifs? A view based on structural analysis, anisotropy of magnetic susceptibility and thermo-mechanical modelling in the Tanvald Massif (Bohemian Massif). – Physics on the Earth and Planetary Interiors, 157. 286–310.

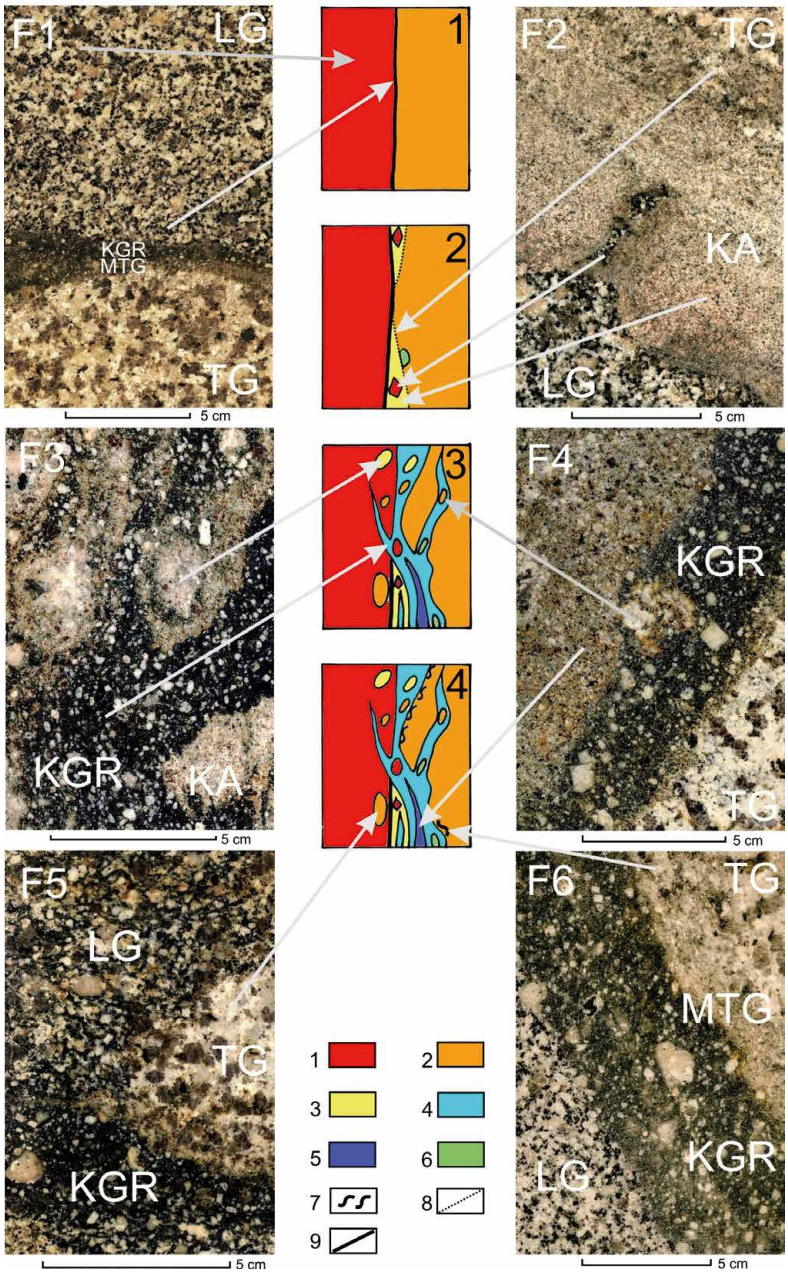

Figure 3.6.2. Relationship between contact rocks and Liberec and Tanvald Granite. (F1 to F6 photos of the polished sections, 1–4 graphic schemes). Klomínský et al. (2007). 1 – Liberec Granite, 2 – Tanvald Granite, 3 – contact aplite, 4 – contact granodiorite dark facies), 5 – contact granodiorite (light facies), 6 – Graphic Granite, 7 – mylonitized Tanvald Granite, 8 – transition between contact aplite and Tanvald Granite, 9 – chilled contact between Liberec Granite and contact aplite, LG – Liberec Granite, TG – Tanvald Granite, KA – contact aplite, KGR – contact granodiorite, MTG – mylonitized Tanvald Granite.

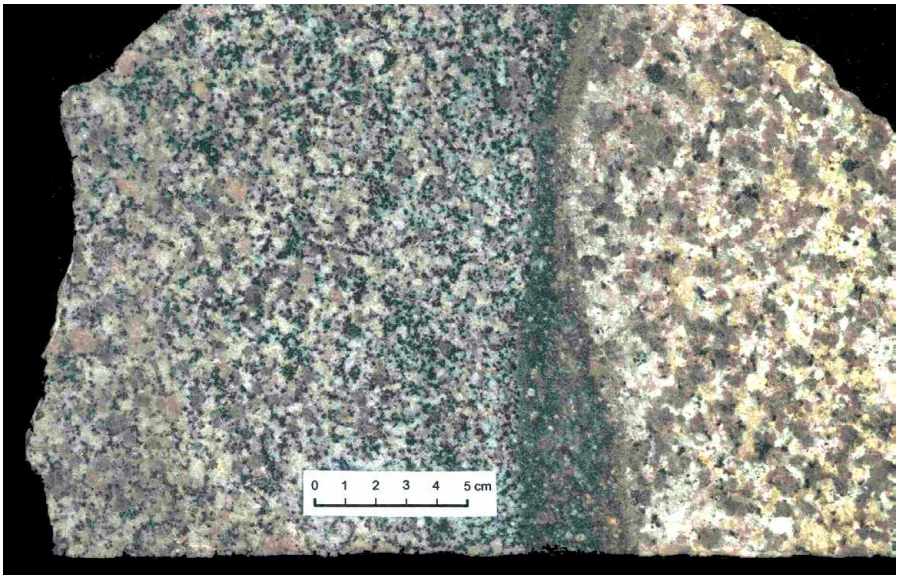

Figure 3.6.3. Liberec (left) and Tanvald Granite contact outcrop near Nová Ves nad Nisou. Klomínský et al. (2007). Contact interface is filled up by younger contact granodiorite. Grain size of the Liberec Granite decreases towards the contact line (chilled margin), Tanvald Granite is mylonitized at the contact with granodiorite.

3.6 Intrusive relationship and interaction between the Tanvald and Liberec Granites

The exposure of the Liberec and Tanvald Granite contact in Nová Ves na Nisou near Jablonec nad Nisou reveals the intrusive relationship and relative age of both granites (Fig. 3.6.1.). This contact illustrates the interaction between hot calc-alkaline granitic magma of the Liberec Granite and already consolidated alkali-feldspar Tanvald Granite (Klomínský et al. 2007). Their concordant interface is occupied by younger contact rocks related to both granites. (Fig. 3.6.2.) The cataclasis, mylonitization (shearing) pseudotachylitic reaction softening (semi-fluid state), protoclasis recrystalization, reaction softening, and up to total remelting of the Tanvald Granite are characteristic features of these rocks (Fig. 3.6.3.).

The younger age of the Liberec Granite is demonstrated by reduction of the grain size and absence of K-feldspar phenocrysts towards the contact (chilled margin) and magnetization of the Tanvald Granite (by thermal impact of the Liberec Granite), and indicated by radiometric dating (321 ± 14 Ma monazite).

The contact between calc-alkaline biotite granite (Liberec Granite) and alkali-feldspar two-mica granite (Tanvald Granite) is an unusual example of the reverse chronological succession of the Variscan granites known in the adjacent Krušné hory Mountains.

REFERENCES

Klomínský, J. – Schovánek, P. – Jarchovský, T. – Sulovský, P. – Toužimský, M. (2007): Kontakt tanvaldského a libereckého granitu u Jablonce nad Nisou. – Zprávy Geol. Výzk. v r. 2006, 24–29.

3.7 Magmatic structures in the Krkonoše-Jizera Composite Massif

The magmatic structures in the Jizera and Liberec Granites preserve field evidence of localized magmatic differentiation, multiphase laminar flow and other physical processes that operated in crystal-rich granitic magma after chamber scale dynamic mixing and hybridization (Figs. 3.7.1. and 3.7.2.). Biotite schlieren-like layers, cognate enclaves and foreign xenoliths, together with potash feldspar phenocrysts, belong to the crucial macroscopic markers of the Krkonoše-Jizera Granite Massif magmatic architecture (Žák and Klomínský 2007, Žák et al. 2009). The frequency, size, shape, and spatial orientation of these markers also serve for modelling the granite massif's primary joint networks. While the biotite schlieren demonstrates the granite magma's active movement upwards, the parameters of the cognate enclaves indicate the stratification of the upper layers of the granite intrusions in the final stage of granite solidification. Planar and linear preferred orientations of K-feldspar phenocrysts (up to 5 cm in size) define magmatic foliation and lineation in the Jizera Granite. Our mapping revealed the presence of three distinct magmatic foliations based on their orientation and overprinting relationships. Two foliations dip steeply and are oriented either ~NE-SW or WNW-ESE to NW-SE. The dominant magmatic foliation, however, dips gently and shows variable orientation.

The most informative examples of the magmatic structures, discovered during our regional mapping and investigations in water-supply and waterway tunnels in the Jizerské hory Mts., seem to fall into several categories and are described in detail below.

Simple and stacked schlieren channels. In the Jizera and Liberec Granites, mafic schlieren are typically defined by accumulation of biotite, having sharp bases and passing gradationally into more felsic granite over a few centimetres (normal grading). These elements are usually rather thin (cm to m) and several metres to tens of metres long, e.g. the Hraničná quarry near Bedřichov (Fig. 3.7.1.). These structures are abundant in the walls of the Souš water-supply tunnel, where Jizera Granite texture exhibits parting parallel to these planar structures (Fig. 3.7.2.). In some cases, the schlieren are both modally-graded and size-sorted, i.e. biotite schlieren pass into a layer with plagioclase phenocrysts (0.5–1 cm in size) which passes into a K-feldspar phenocryst-rich layer (1.5–3 cm in size). Short biotite-rich schlieren with pinnate structure similar to a horsetail are characteristic. The formation of mafic schlieren presumably involved gravitational settling, velocity gradient flow sorting, and interstitial melt escape within

Figure 3.7.1. A cross-section of the composite biotite rich sheet /schlieren) in 2.5 m long block of the Liberec Granite from the Hraničná quarry. Klomínský and Woller (2010).

Figure 3.7.2. Folded composite multiple biotite schlieren in the Jizera Granite. The Souš water-supply tunnel. Photo J. Klomínský.

the crystal mush along flow rims. Mafic schlieren occur either as irregularly scattered single patches or delineate margins of individual channel-shaped structures (schlieren channels) entirely enclosed in the host granite. In many cases, multiple superposed (migrating) concave-upward individual channels delineated by marginal schlieren make up vertical stacks. Figure 3.7.3.b, c depicts a schlieren channel stack, which consists of several superposed troughs and planar or gently curved schlieren and has a lateral extent larger than thickness (the exposed part of the stack is approximately 3-4 m thick and more than 10m wide). The superposed schlieren channels truncate one another as indicated by crosscutting marginal schlieren on the bottom of each channel, and thus closely resemble cross-bedding and scour-and-fill structures in sedimentary rocks. Both modal grading of individual schlieren and younging (defined by schlieren truncation) indicate an upward growth (aggradations) of channel stacks.

Magmatic folds, antiformal (younging unknown) or anticlinal (younging upward) schlieren stacks and folded schlieren channels (Figs. 3.7.3., 3.7.4., 3.7.5.).

In some cases, aplitic dykes, mafic-felsic layers and stacks of superposed schlieren channels have been folded into magmatic folds (with no evidence for subsolidus deformation). These folds occur at variable scales, up to several meters in wavelength, are typically upright and have large interlimb angles (open folds) with a few exceptions of some tightly folded aplite dykes (Klomínský, Woller eds 2010).

A magmatic fold exposed in the Bedřichov water-supply tunnel section A 210 m from its south-western entrance, resembles a schlieren anticline (heading upwards as inferred from schlieren truncations) defined by planar, upward-graded schlieren to form fold limbs with cross-cutting schlieren channels preserved in the summit

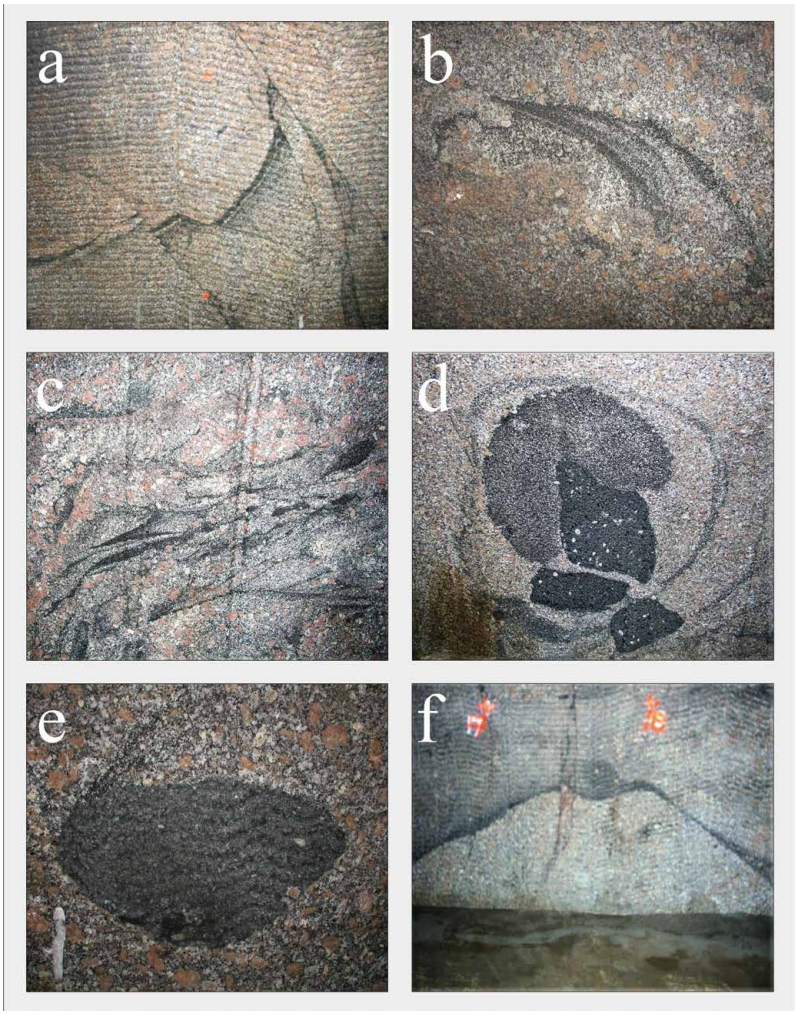

Figure 3.7.3. Examples of magmatic structures and inhomogeneities in granites in the Bedřichov water-supply tunnel. Klomínský and Woller (2010). a - biotite-rich schlieren segmented by joints with significant displacements; b – group of biotite-rich schlieren of horse-tail shape; c – magmatic "channel" filled with biotite-rich schlieren and basic enclaves; d – a relatively plastic intermediate enclave surrounds a basic (more rigid) enclave; e – basic enclave with a tail of biotite-rich schlieren indicating its rotation and magmatic erosion; f – a fold in biotite-rich schlieren showing plastic deformation by a more rigid basic enclave (distance between number 17 and 18 is 1 metre).

part of the anticline (Fig. 3.7.4.). K-feldspar phenocrysts are concentrated above the schlieren of one fold limb, with the schlieren being deflected around the base of the accumulation. A large xenolith of coarse-grained porphyritic alkali-feldspar biotite granite (possibly the Rumburk Granite of the Ordovician age) rests on top and deforms the underlying K-feldspar accumulation (Fig. 3.7.4. and 3.7.8f.). The upper part of this complex structure is formed by a leucocratic (pegmatite, aplite) layer, also being folded roughly parallel to the mafic schlieren. The pegmatite layer is not disrupted

by the xenolith, and thus must represent a feature that postdates the xenolith sinking. The magmatic fold is abruptlytruncated by a submagmatic crack with sharp outer margins delineated by mafic schlieren and filled with the porphyritic Jizera Granite.

Gravitational structures

Some structures can be interpreted as resulting from gravity differentiation of magma. In Fig. 3.7.3.f a mafic enclave in inhomogenous Jizera Granite deformed the underlying schlieren.

The structure shown in figure 3.7.5., exposed 336 m from the south-western entrance of the Bedřichov water-supply tunnel section A, is hosted in the Jizera Granite and is defined by upward-grading biotite schlieren having a sharp base. The structure intersects the opposite tunnel walls, establishing its three-dimensional shape and orientation.

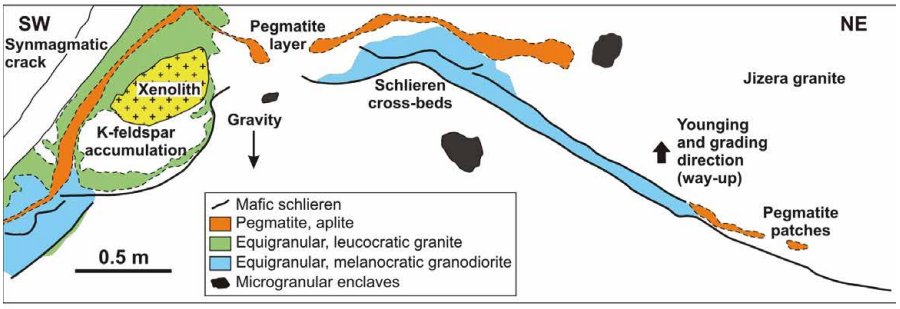

Figure 3.7.4. Magmatic folds and schlieren antiforms in section A of the Bedřichov water-supply tunnel. Klomínský and Woller (2010).

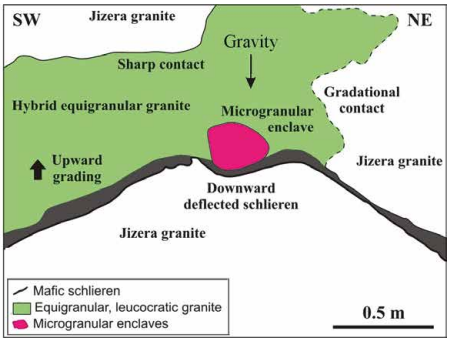

Figure 3.7.5. Mafic enclave in the heterogeneous Jizera Granite deforming the underlying biotite schlieren. Klomínský and Woller (2010).

The overall shape of the structure resembles an antiform (Fig. 3.7.5.) having an axis trending ~120°. The antiform is overlain by darker, medium-grained, equigranular to weakly porphyritic granite to granodiorite. The contact between the host porphyritic Jizera Granite and the darker equigranular granite is mostly sharp but drapes round the K-feldspar phenocrysts within the Jizera Granite. A microgranular enclave rests on the summit of the schlieren antiform (within the darker equigranular granite).

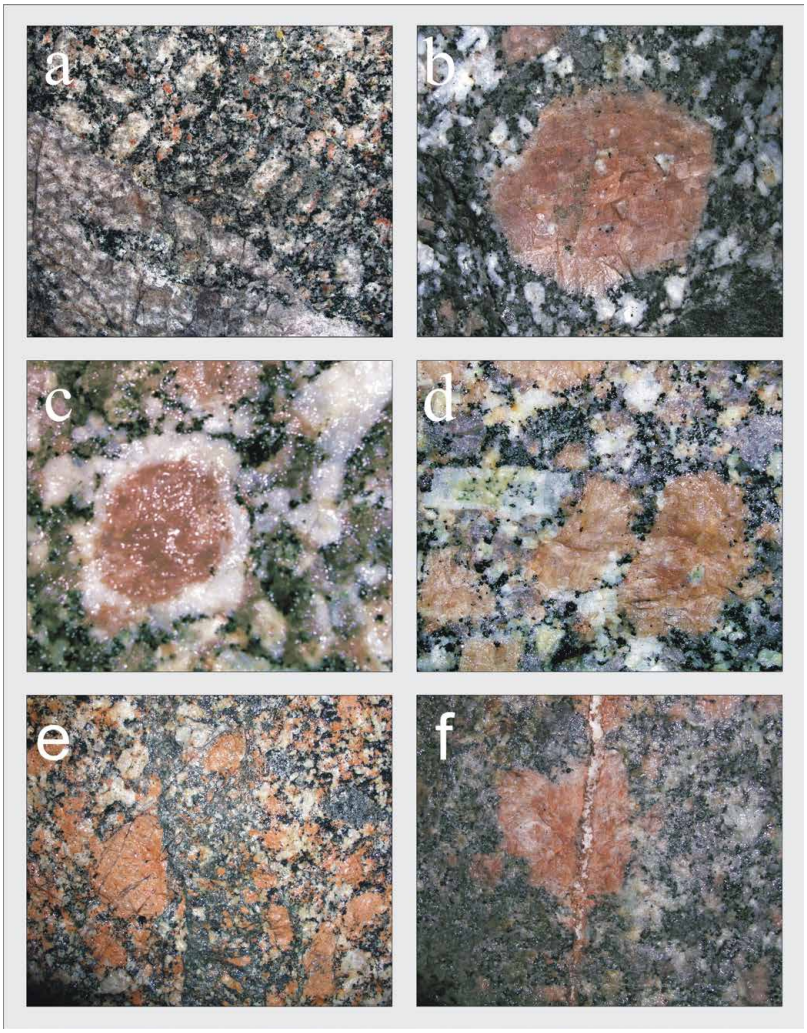

Figure 3.7.6. Examples of K-feldspar phenocrysts in the Jizera Granite of section A of the Bedřichov water-supply tunnel. Klomínský and Woller (2010). a – parallel orientation of K-feldspar phenocrysts, perpendicular to the margin of the aplite dyke; b – flesh-red phenocryst of K-feldspar in medium-grained groundmass composed of plagioclase, quartz and biotitic aggregate; c – oval K-feldspar phenocryst of the rapakivi type with a prominent rim of plagioclase; d – K-feldspar phenocrysts of various size, colour and origin; e – tectonic disintegration of K-feldspar phenocrysts in an early phase of granite solidification; f – segmentation of a K-feldspar phenocryst by a thin calcite veinlet.

Figure 3.7.7. "Subvertical magmatic pocket" – pegmatitic accumulation of "oxidized" feldspar phenocrysts around a cluster of microgranular enclaves in the Souš water supply-tunnel. Photo J. Klomínský. Size of shorter side of picture is 1 metre.

Accumulation (cumulates) of feldspar phenocrysts and their positioning

Accumulation of feldspar phenocrysts (with significantly higher modal ratio of feldspars) is common on meter-scale in both types of porphyritic granite in the Bedřichov water-supply tunnel. Such domains form irregular or platy bodies showing gradational or sharp contacts with adjacent granite. In detail, phenocrysts in these accumulations are very closely packed with a minimum quantity of groundmass between phenocrysts (Fig. 3.7.6.). In some cases the feldspar accumulations pass gradually upward to leucocratic fine-grained granite formed from the intercumulate melt segregated in the process of compaction of the cumulate.

Microgranular mafic enclaves and country rocks xenoliths

Cognate enclaves of acid, intermediate and mafic rocks, and foreign xenoliths together with potash feldspar phenocrysts and biotite schlierens, are the crucial macroscopic markers in the magmatic architecture of each granite massif. The size, shape, and spatial orientation of these markers serve for modelling of the primary joint networks in the granite massifs. While biotite schlieren demonstrate the active upward movement of the granite magma, the cognate enclaves' parameters indicate the stratification and structure of the granite intrusions' upper layers in the final stage of granite solidification.

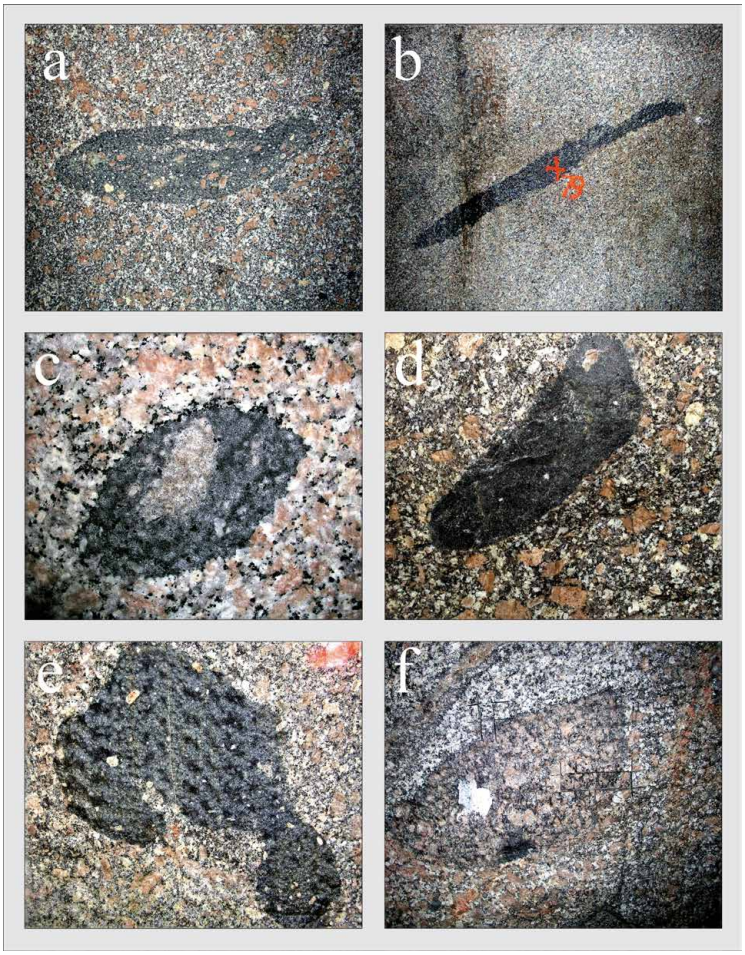

Figure 3.7.8. Examples of enclave sections in the wall of the Bedřichov water-supply tunnel sections A and B. Klomínský and Woller (2010). a – section through a fine-grained porphyritic basic enclave with the horizontal position of the c axis, b – section through a fine-grained basic enclave with a high a/c ratio of axis and dip towards the east, southern wall of tunnel section B; c – a basic fine-grained enclave of elliptic shape encloses a xenolith of microgranite, NW wall of tunnel A; d – oval fine-grained basic enclave with a moderate plunge in the c axis to the SW (NW wall of the tunnel section A); e – section through a fine-grained porphyritic basic enclave with an indication of magmatic corrosion (assimilation) in Jizera Granite, NW wall of tunnel section A; f – section of an oval xenolith of porphyritic coarse-grained biotite alkali-feldspar granite (possibly the Rumburk Granite of the Ordovician age), NW side of the wall of tunnel section A.

The presence of various enclaves, mainly of melanocratic rocks, and biotite-rich inhomogeneities (schlieren) is a typical feature of the Krkonoše-Jizera Composite Massif (Figs. 3.7.3d, e and 3.7.8.). Other inhomogeneities, such as xenoliths of foreign rocks are less abundant. There are largely sharply bound relics of intensively granitized country rocks (granites, orthogneisses, migmatites and contact hornfelses).

The majority of the parental inclusions in granites of the KJCM have intermediate to mafic composition. (Figs. 3.7.7., 3.7.8.). Their dimensions vary from large ones, several

hundred metres, long to small spheroidal or disc-shaped bodies 50 to 5 cm long and smaller. The mode of occurrence of small enclaves, often flattened into fish-like shape due to pressure under conditions of plastic deformation, is highly irregular in both major types of granite. The enclaves include a variable series of rocks, often porphyritic, mesocratic and melanocratic types with variable mineralogical composition, texture and structure, often with large xenocrysts of quartz and porphyrocrysts of K-feldspar. Melanocratic fine-grained enclaves carrying up to several cm long porphyroblasts of biotite set in quartz-feldspathic matrix represent a rare type. Some larger enclaves carry smaller enclaves of a more mafic composition with dark minerals content up to 60 vol. %. Some small mafic enclaves are angular and exhibit a hornfels-like structure. In some cases enclaves form small clusters surrounded by phenocrysts of K-feldspar (Fig. 3.7.7.).

Unusual in the Jizera and Liberec Granites are so-called granite autoliths. They are represented by sharply outlined rounded enclaves of medium to fine grained biotite granite of similar composition to surrounding rocks (Fig. 3.7.9.). More frequent are small mafic inclusions and also voluminous enclaves which used to be mined for building stone (Fojtka Hybrid Granitoids see Chapter 3.4.).

Xenoliths, unlike parental enclaves, represent markedly foreign rock types of different origin and age. These foreign rock types are found in the crystalline complex around the KJCM. Examples of xenoliths enclosed in the Liberec Granite in the Ruprechtice quarry (Figs. 3.7.10, 3.7.11, 3.7.12., 3.7.13.) indicate very variegated lithology of the original roof above the central part of the western segment of the KJCM. These rocks are represented by thermally affected Palaeozoic phylites (hornfelses), Cambrian metagranites and Proterozoic orthogneisses and diatexites.

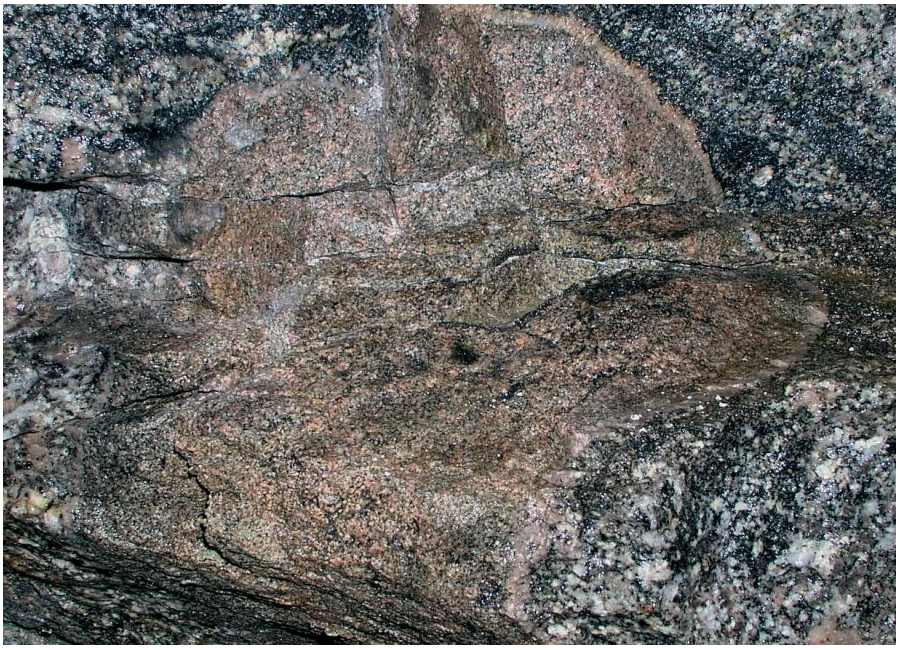

Figure 3.7.9. Microgranular autolith of fine grained biotite granite 30 cm in diameter within the composite schlieren in the Jizera Granite. The Souš water supply tunnel. Photo J. Klomínský.

Figure 3.7.10. Xenolith of Palaeozoic? hornfels in the Liberec Granite, Ruprechtice quarry (half of the original size). Photo J. Šrek.

Figure 3.7.11. Xenolith of Proterozoic augen gneiss in the Liberec Granite. Ruprechtice quarry (half of the original size). Photo J. Šrek.

Figure 3.7.12. Xenolith of Proterozoic oftalmitic biotite diatexite in the Liberec Granite. Ruprechtice quarry (original size). Photo J. Šrek.

> Figure 3.7.13. Xenolith of quartzite with amphibolite in the Jizera Granite. Bedřichov water-supply tunnel section A (real size). Photo J. Klomínský.

> Figure 3.7.14. Xenolith of microgranular mafic rock in the Tanvald Granite showing the reactive interaction between both rocks (real size). Photo J. Klomínský.

REFERENCES

Žák, J. – Klomínský, J. (2007): Magmatic structures in the Krkonoše-Jizera Composite Massif Complex, Bohemian Massif: evidence for localized multiphase flow and small-scale thermal-mechanical instabilities in a granitic magma chamber. – Journal of Volcanology and Geothermal Research 164, 4, 254–267.

Žák, J. – Verner, K. – Klomínský, J. – Chlupáčová, M. (2009): Granite tectonics revisited: insights from comparison of K-feldspar shape-fabric, anisotropy of magnetic susceptibility (AMS), and brittle fractures in the Jizera Granite, Bohemian Massif. – International Journal of Earth Sciences 98, 5, 949–967.

Klomínský, J. – Woller, F. eds (2010): Geological studies in the Bedřichov water-supply tunnel. – Technical report 02/2010. SÚRAO, ČGS Prague. 104 pp.

3.8 Basaltandesite (melaphyre) and trachyandesite dykes

Two basaltandesite dykes 2.5 m and 1.5 m wide were described by Pták (1963) as lapprophyres cutting the Souš water-supply tunnel in 130/80 NE azimuth 384 m and 392 m from the tunnel portal (Fig. 3.8.1.). Their chemical composition and whole

Figure 3.8.1. Trachyandesite dyke 2.5 m wide in the Souš water supply tunnel. Photo J. Klomínský.

Figure 3.8.2. Basaltandesite breccias cemented by white quartz (actual size). Photo J. Klomínský. Vratislavice fault outcrop in the road cut next to Vratislavice Brewery (eastern district of Liberec City).

rock K/Ar dating 169.5 ± 5.6 Ma of Jurassic age (Peczkay 2008) indicates the dykes belong to slightly isotopically resettled (due to hydrothermal alteration) members of the Permian dyke swarm which penetrates the KJCM along the Vratislavice and Harcov tectonic zones (Figs. 3.8.2. and 4.1.2. in Chapter 4.).

3.9 Tertiary volcanites in the Krkonoše-Jizera Composite Massif

Occurrences of neovolcanites penetrating the granites of the KJCM and surrounding crystalline rocks in the form of dykes or small crater pipes have been located during building excavation, quarrying and also by surface magnetometric survey in the Liberec City area (Fig. 3.9.1.) Airborne survey of symmetric bullseye shape magnetic anomalies demonstrate the presence of basaltic neovolcanites rich in magnetite in several places in the Liberec City area (e.g. negative anomaly about –1000 nT in Liberec centre). A similar inversely magnetized (–2300 nT) basaltoid body up to 50 m in diameter has been detected inside the maar or volcanic crater north of Bedřichov (Šalanský et al. 2001). A larger volcanic centre inside an intense isometric anomaly is also located near Krásná Studánka. These Neovolcanites are mainly represented by alkali basalts, basanites, limburgites, olivine nefelinites and dykes of polzenites (olivine melilitites) (Klomínský at al. 2002). The largest volcanic centre in the KJCM comprises the Bukovec Hill nephelinite plug, in association with several diatremes, near Jizerka village. In the past some of these dykes and plugs were quarried, mostly for local building, field fertilisers and road surface works.

Alkaline basaltoids (olivine basanite, olivine nephelinite, limburgite, basalt) comprise a group of dykes and small pipe-like bodies from several decimetres to several meters in thickness (Fig. 3.9.2.). These subvolcanic rocks occur near NW-SE trending fault zones and are now exposed in some small abandoned quarries near Kateřinky, Krásná Sudánka, Mariánská Hill near Josefův Důl, Špičák Hill near Tanvald, Buková Hill near Horní Lučany, Nová Ves nad Nisou, Doubí, Dolina near

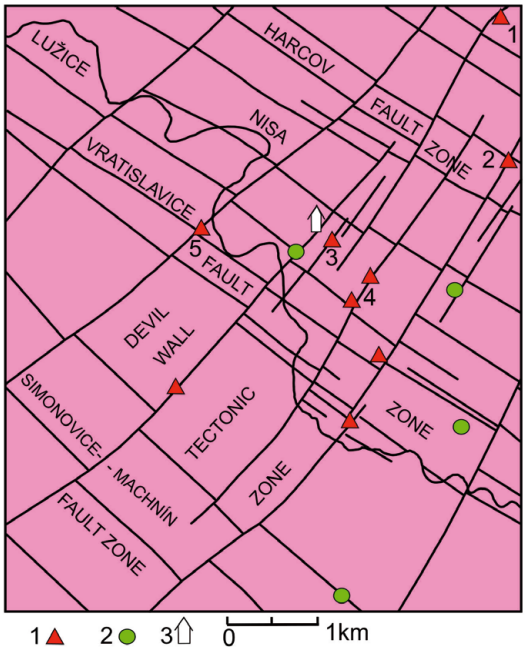

Figure 3.9.1. Model of the tectonic network in Liberec City. Photo J. Klomínský et al. (2016).
1 – location of olivine mellilitite – polzenite: (1 – Ruprechtice Quarry, 2 – Výšina Hill Quarry, 3 – Liberec Castle, 4 – Liebieg Factory, 5 – Žitavská Street),
2 – alkaline basaltoids,
3 – Liberec town hall.

Figure 3.9.2. Deeply weathered basaltoid tuff plug in the highway excavation next to bridge at U sila street. Photo J. Klomínský.
The dyke-like body is parallel to the Vratislavice fault zone.

Figure 3.9.3. Contact of the Jizera Granite with Tertiary olivine basanite in the abandoned quarry in the northern slope of Buková Hill near Tanvald (1/2 size). Photo J. Klomínský.

Figure 3.9.4. Tertiary olivine basanite with olivine xenocrysts and Tanvald Granite xenolith. Photo J. Klomínský. Exocontact of Tanvald Granite Massif in Huť village near Jablonec nad Nisou (1/2 of the original size).

Stráž nand Nisou, Vratislavice nad Nisou, Doubí, Huť near Pěnčín, Hašler Hut near Bedřichov, and Bedřichov water supply tunnel (Fig. 3.9.3. and 3.9.4.). The age of the limburgite 30.0 ± 1.0 Ma (whole rock K-Ar method) from the abandoned quarry next to the Hašler Hut near Bedřichov is reported by Pécskay (2008). Loose boulders of olivine basanite in the exocontact of the Tanvald Granite contain small xenoliths of the Tanvald Granite and Crateceous sediments recently outcropping about 6 km south of Huť near Pěnčín (Fig. 3.9.4.). The Mariánská Hill area is represented by two vertical sheet-like outcrops of nepheline basanite and olivine nephelinite, 60 × 70 m and 90 × 30 m in size (Klomínský et al. 2004). Vertical contact of the olivine basanite with Jizera Granite is exposed in the abandoned quarry on the southern side of Buková

Figure 3.9.5. Xenolith of the Tanvald Granite in olivine basanite (see also Fig. 3.9.4.) with 2 mm rim of glass originating from melting of the granite at the contact with hot basalt magma (2 times of original size). Photo J. Klomínský.

Hill (Fig. 3.9.3.). Both rocks are welded at the sharp vertical contact boundary. Basalt magma thermal effects on the Jizera Granite are most intense several cm from the contact plane. Thermal shock of the granite is recorded in the transformation of

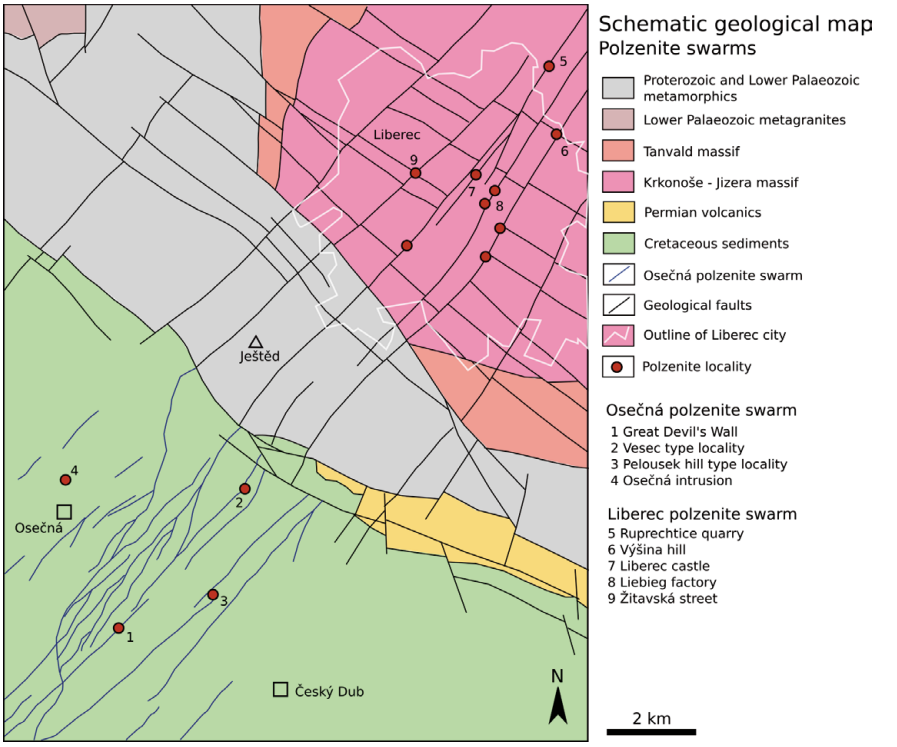

Figure 3.9.6. Polzenite dyke swarm in the Bohemian Cretaceous Basin and the Krkonoše-Jizera Composite Massif (adopted after Paluska et al. 2013). Bukovská et al. (2017).

biotite into a fine film of magnetite, and partly K-feldspars into the glass and mullite melt. This mineral association indicates the temperature at contact was about 1000 ºC (Kaczor et al. 1988). Magnetic susceptibility of the contact granite (13.5 . 10^{-3} SI) is similar to basanite (12 . 10^{-3} SI).

Polzenite dykes

Alkaline and ultra-alkaline rocks with melilititic association of upper Cretaceous up to Paleogene age are of mantle origin and represent products of magmatic activity of the Eger rift (Ulrych et al. 1988, 2001). A swarm of polzenite dykes occurs in the KJCM along NE-SW cross faults showing interconnection with the "Devil's Walls" tectonic structures in the Bohemian Cretaceous Basin (Fig. 3.9.6.). These polzenite dykes have been exposed in a different geological environment and probably at much deeper crustal level then their equivalents in the Osečná Volcanic Centre (Paluska et al. 2013, Coubal et al. 2015). A critical demarcation between the sandstone and granite environments of the polzenite swarm is marked by the Lusatian Fault Belt (Fig. 3.9.6.).

These subvolcanic rocks are older than the alkaline basaltoids (Peczkay 2008) and have been found in granite quarries at Ruprechtice and next to Výšina Hill in Liberec city as well as during construction of housing in Liberec centre (Liebig factory, Žitavská street, Liberec castle cellar, Gränzer 1929, Sedlář et al. 1982).

One of these olivine-melilititic dykes (approx. 70 cm thick) outcropped in an abandoned quarry in Liberec Granite (Gränzer 1929) on Výšina Hill in Liberec. The dark grey olivine melilitite with porphyritic texture consists of olivine, augite, melilite and biotite, magnetite, perovskite and haüyn (Tab. 3.9.1.). Idiomorphic

Figure 3.9.7. Shock reaction of the Liberec Granite xenolith to the hot the olivine mellilitite (polzenite) magma. Photo J. Klomínský. Granite is hydraulically fractured, malleably deformed and partially melted (granite glass is represented by the grey area). Abandoned quarry, Vyšina Hill in Liberec City (actual size).

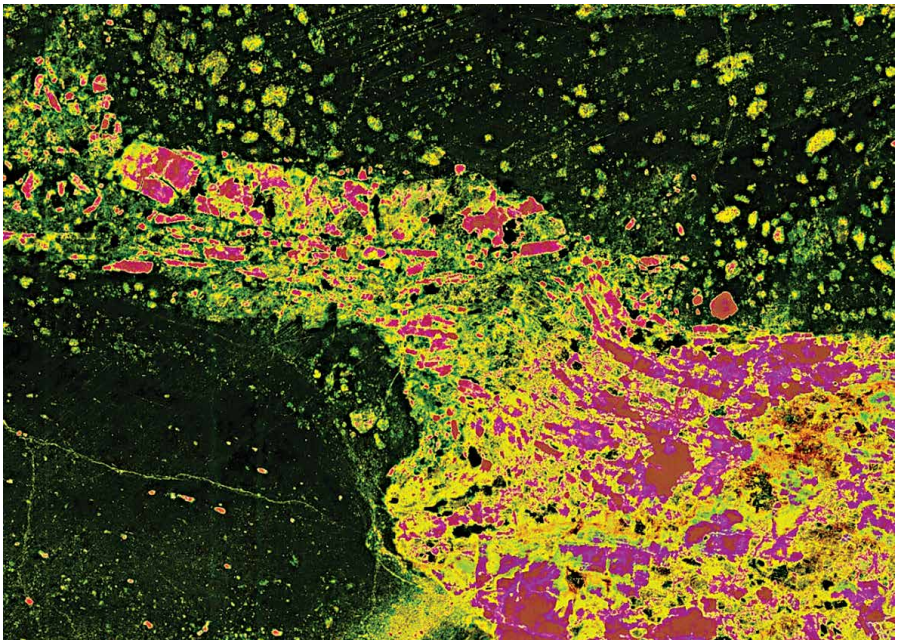

Figure 3.9.8. Shock reaction of the Liberec Granite xenolith to the hot the olivine mellilitite (polzenite) magma in false colour image. Photo J. Klomínský. Granite is hydraulically fractured, ductually deformed and partially remelted. Red grains are mostly fractured K-feldspars, yellow grains in polzenite (black) are olivines. Granite glass is represented by greenish colour. Polished slab from the abandoned quarry, Vyšina Hill in Liberec City (natural size).

crystals of olivine (up to 2 mm) are completely serpentinized; pyroxenes are zoned. This melilitite dyke is 61.9 ± 3.0 Ma old according to K-Ar dating (Pécskay, 2008), and it encloses xenoliths of Liberec granite of Variscan age (320 Ma, U/Pb zircon age) with tracks of 'pyrometamorphic destruction' (Grapes 2006). Thermal shock in the granite caused by melilitite emplacement is recorded by volume expansion, hydraulic cracking, microfracturing and local melting (Bukovská et al. 2017). This is evident from transformation of biotite to magnetite, partial melting of alkali feldspars, and occurrence of glass and mullite (Figs. 3.9.7. and 3.9.8.). This mineral association may show a temperature of over 1000 °C at the exocontact, and also very rapid solidification of both rocks (Kaczor et al. 1988).

New chemical analysis (Tab. 3.9.2.) and K-Ar whole rock dating (61.9 ± 3.0 Ma) has been performed on the polzenite from the abandoned Liberec Granite quarry on Vyšina Hill in Liberec City (Fig. 3.9.7. and 3.9.8.). This dyke about 70 cm wide is represented by olivine melilitite showing a strong thermal and tectonic impact on the neighbouring Liberec Granite. The contact zone in the granite is more than one metre wide and contains traces of thermal alteration hydraulic fracturing, and partial melting resembling pseudotachylite structure (Fig. 3.9.7.). A similar polzenite dyke over 1 meters wide has been found by horizontal drilling in Wagner II Ruprechtice quarry (Tab. 3.9.2.). A new locality of the olivine melilitite (polzenite) dyke 70 cm wide is exposed in Žitavská street near the Liberec centre (Tab. 3.9.1., Figs. 3.9.9., 3.9.10.).

Table 3.9.1. Mineralogical composition in vol. % of Neovolcanic rocks in Liberec area (Gränzer 1929).*

Locality	Rock	olivine	augite	melilite	nefeline	biotite	perovskite	haüyn	magnetite	remarks
Výšina Hill	ol. melilitite	20	15	35		10	5	3	10	dyke thickness 50 cm
Liberec – Textilana	ol. melilitite	20	35	25		5	2	3	10	dyke thickness 100 cm
Ruprechtice	ol. melilitite	30	10	30		15	3	5	5	dyke thickness 30–60 cm
Kateřinky	nefelinite	20	60		10				10	dyke thickness 10 m
Stráž nad Nisou – west	nefelinite	15			10				10	matrix 65% + augite
Vratislavice	ol. limburgite	20	20							matrix 40% + magnetite
Hašler Hut	ol. limburgite	20	20							matrix % + magnetite
Liberec – town	nefelinite									dyke thickness 200 cm

* incomplete data

Figure 3.9.9. Olivine melilitite (polzenite) dyke 70 cm wide. Photo J. Klomínský. Exposure in Žitavská street, Liberec City.

Figure 3.9.10. Cross-Nikols photomicrograph showing black olivine xenocrysts in thin section of olivine melilitite (polzenite) dyke exposure in Žitavská Street in Liberec City. Photo J. Klomínský.

Table 3.9.2. Chemical analyses of Neovolcanites in the Krkonoše-Jizera Composite Massif.

Locality	Rock	SiO_2	TiO_2	Al_2O_3	Fe_2O_3	FeO	MgO	MnO	CaO	Na_2O	K_2O	P_2O_5	CO_2	$H_2O(+)$	$H_2O(–)$
Žitavská street	polzenite	35.61	2.79	10.0	8.06	3.99	17.41	0.244	4.67	0.30	1.38	1.264	0.15	8.3	4.59
Výšina Hill Q	polzenite	33.90	2.22	7,,38	4.71	5.23	15.81	0.188	13.89	0.77	1.09	0.62	7.27	4.05	2.10
Ruprech-tice Q	polzenite	34.80	3.14	9.05	5.32	5.58	14.35	0.23	13.50	0.790	1.32	0.84		8.16	1.68
Rochlice Q	polzenite	39,93	2.28	9.99	4.60	6.51	14.31	0.21	11.96	2.0	1.48	1.0	1.08	3.56	0.33
Huť	basanite	43.59	2.04	12.46	3.50	7.17	13.23	0.223	11.08	3.20	1.23	0.742	0.04	0.631	0.27
Dolina Q	nefelinite	43.13	2.04	14.94	6.02	6.07	6.09	0.262	11.76	3.98	1.26	1.18	0.07	1.87	0.40
Proseč Q	basanite	45.07	2.47	12.63	4.01	5.53	8.05	0.194	11.26	2.43	1.40	0.819	0.11	4.27	1.18
Kateřinky Quarry	nephelinite	43.15	2.53	12.15	5.04	5.78	8.95	0.198	12.10	2.64	1.01	0.825	0.39	3.87	0.98
Souš tunnel	trachande-site	61.48	1.17	14.87	3.68	1.55	2.34	0.059	1.74	1.91	7.56	0.587	0.57	2.02	0.28
Hašler Hut Q	limburgite	44.38	1.94	12.53	2.93	7.74	13.6	0.21	9.95	3.12	1.26	0.572	0.07	1.09	0.30
Mariánská Hill	basanite	40.75	2.93	11.82	3.77	7.60	11.53	0.202	14.07	3.01	0.91	0.95	0.61	0.95	0.33

REFERENCES

Bukovská, Z. – Larikova, T. – Klomínský, J. (2017): Deformation and metamorphic interaction at the contact of olivine mellilitite dyke with granite, the Krkonoše-Jizera Massif, Czech Republic. In: L. Šimon, M. Kovačiková, S. Ozdinová, J. Michalík, D. Pivko et al.: Zborník abstraktov a exkurzný sprivodca Otvoreného geologického kongresu Vysoké Tatry 2017, s. 12. – Slovenská geologická společnosť. ISBN 978-80-972667-7-6.

Coubal, M. – Málek, J. – Adamovič, J. – Štěpančíková, P. (2015): Late Cretaceous and Cenozoic dynamics of the Bohemian Massif from the paleostress history of the Lusatian Fault Belt. – Journal of Geodynamics, 87 (2015) 26–49.

Grapes, R. (2006): Pyrometamorphism. – Springer-Verlag Berlin Heidelberg. 275 p.

Gränzer, J. (1929): Tertiare vulkanische Gesteine in der Umgebung von Reichenberg in Bohmen. Mitteilungen des Vereines der Naturfreunde in Reichenberg 51. Jahrgang. 12–27.

Kaczor, S.M. et al. (1988): Disequilibrium melting of granite at the contact with a basic plug: A geochemical and petrografic study. Journal of Geology, 1988,vol. 96, p. 61–78.

Klomínský, J. – Adamová, M. – Bělohradský, V. –-Burda, J. – Kachlík, V. – Lochmann, Z. – Manová, M. – Nekovařík,Č. – Nývlt, D. – Šalanský, K. (2004): Vysvětlivky k základní geologické mapě České republiky 1 : 25 000 03-143 Liberec. 68 s. – ČGS. Praha. ISBN 80-7075-623-3.

Klomínský. J. – Mrázová, Š. – Šalanský, K. (2002): Neovulkanity v okolí Liberce, jejich geofyzikální indikace a regionálně geologický význam. – Zprávy o geologických výzkumech v roce 2001, 36–39.

Mrázová, Š – Klomínský J. – Adamová, M. – Burda, J. – Jarchovský, T. – Kachlík, V. – Kořán, V. – Kříbek, B. – Manová, M. – Nekovařík, Č. – Šalanský, K. (2006): Základní geologická mapa České republiky 1 : 25000 s Vysvětlivkami, 03 – 323 Jablonec n. N. – 62 s. ČGS. Praha.

Paluska, A. – Rapprich, V. – Veselý, P. – Ulrych, J. (2013): Field trip 1: Upper Cretaceous/ Paleogene ultramafic volcanism in the Osečná and the Ploučnice area (North Bohemia). 244–271. In Basalt 2013 – Cenozoic magmatism in Central Europe, (eds) Büchner, J. – Rapprich, V. – Tietz, O. Abstracts & Excursion Guides, Senckenberg scientific conference. 24th to 28th April 2013, Görlitz / Germany.

Pécskay, Z. (2008): K/Ar age determination on intrusive magmatic rocks of SURAO project 2008 – Institute of Nuclear Research of the Hungarian Academy of Sciences (ATOMKI), Debrecen, Hungary. Research report.

Pták, J. (1963): Lamprofyrové žíly jizerského žulového masivu a jejich vztah ke granittektonice – Zpr. Geol. Výzk. v r. 1962. 71–75.

Sedlář, J. et al. (1982): Surovina : dekorační kámen. Závěrečná zpráva Ruprechtice 0178 1126. Geoindustria. – MS Geofond. Praha. Sign. P 36975.

Šalanský, K. – Klomínský, J. – Fediuk, F. – Mrázová, Š. (2001): Bazaltoidy v krkonošsko--jizerském masívu – nové výskyty. (Basaltoids in the Krkonoše-Jizera Composite Massif – new occurences) – Zprávy o geologických výzkumech v roce 2000, 108–111.

Ulrych, J. – Adamovič, J. (2001): Memorandum to the classification of the ultramafic melilite lamprophyres and related alkaline lamprophyres from the type localities in northern Bohemia. MS Geol. Institute, Czech Academy of Sciences, Prague.

Ulrych, J. – Povondra, P. – Rutšek, J. – Pivec, E. (1988): Melilitic and Melilite-bearing subvolcanic rocks from the Ploučnice river region, Czechoslovakia. Acta Univ. Carol. – Geologica, 2, 195–231.

Verner, K. – Mrázová, Š. – Břízová, E. – Buriánek, D. – Holub, F. – Klomínský, J. – Malík, J. – Martínek, K. – Pecina, V. – Rambousek, P. – Rukavičková, L. – Skácelová, D. – Skácelová, Z. – Štor, T. – Vrána, S. – Žáčková, E. (2013b): Vysvětlivky k Základní geologické mapě České republiky 1 : 25.000, list 03-142 Hejnice a 03-231 Jizerka. 143 s. MS Archiv CGS Praha.

Vondrovic, L. – Klomínský, J. eds (2015): Základní geologická mapa České republiky 1 : 25 000 03 – 322 Raspenava. Geologické mapy 1 : 25 000 s textovými vysvětlivkami. 189 s. – MS Archive CGS, 202 s. Praha.

4. Tectonic network in western segment of the Krkonoše-Jizera Composite Massif

The western part of the Krkonoše-Jizera Composite Massif exhibits a certain regularity in tectonic segmentation, particularly similarity in orientation of structures. The fundamental network of brittle deformation is characterized by systems of Sudetic trend (NW-SE) and Krušné hory Mountains/Erzgebirge trend (NE-SW) several tens of kilometres long (Figs. 1.1.2., 1.1.3.). The main intersection of the Sudetic and Erzgebirge faults is situated in the area of Liberec City (Fig. 4.1.). The most dominant Sudetic faults are the Harzov, Vratislavice, Šimonovice-Machnín, Držkov and Harrachov faults further east. The frequency of occurrence of these structures exhibits a hierarchic pattern from individual fractures in fresh granite to fracture swarms in hydrothermally altered granite, with a tendency to intense fracture grouping and coalescence in tectonic zones many metres wide (Figs. 4.2., 4.3.). In the western part of the KJCM the Sudetic structures are dominantly older than the Krušné hory Mountains trending structures. The Sudetic structures are dilation faults with rather variable mineral filling. The Vratislavice fault may serve as an example (Klomínský et al. 2005). Hydrothermally altered Liberec Granite is affected by brittle deformation of variable intensity grading to mylonitization. In domains of this type there are dykes of Permian basaltandesites up to several meters wide (so-called melaphyres, Gränzer 1929). Due to repeated movements along these faults (Fig. 4.5.), the dykes were transformed, probably during the Mesozoic, to tectonic breccias impregnated by several generations of quartz, often with hematite-rich pigment. The densest Sudetic fracture swarm up to 3 km wide is outlined by the Machnín and Harcov faults in the Liberec City area (Figs. 4.1., 4.1.2.).

There are Permian "melaphyres" (basaltandesites) intensively shattered and hydrothermally altered up to and including mineable iron ore (Figs. 4.1.1., 4.1.2.).

Some of these faults later served as conduits for Cainozoic alkaline Neovolcanic rocks, related to later stages of evolution of the Ohře/Eger rift structure. Faults of this type, trend and regional extent functioned for prolonged periods as loci for the transmission of earthquake waves generated in relatively remote epicentres (Gränzer 1901). Such structures function as collectors of ordinary meteoric water and mineralised water (e.g. the Vratislavice mineral water spring), including CO_2 and radon from local degassing loci.

As indicated by the geomorphology of the area between Stráž na Nisou village and the western margin of Liberec City, the zone of NW-SE trending faults is disrupted by younger faults trending NE-SW, representing the continuation of the Čertovy zdi (Devil's Walls) fault zone from the Osečná magmatic centre in the Bohemian Cretaceous Basin (Fig. 3.9.6.). Faults of the same trend around Liberec are accompanied by small basalt plugs and short dykes of ultrabasic melilitites (polzenites). These occurrences are localized in a 25 km wide belt trending SW-NE, across the western part of the Krkonoše-Jizera Composite Massif and its northern

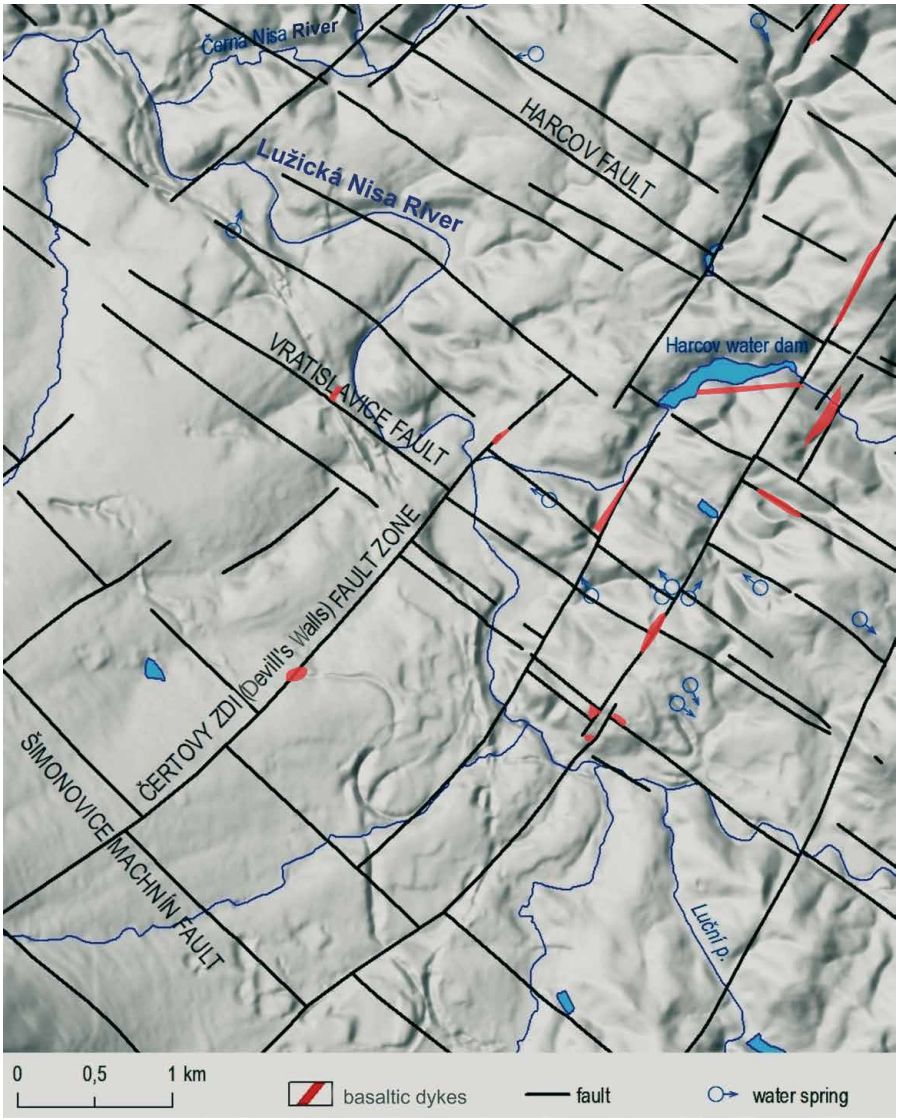

Figure 4.1. Model of the tectonic network in correlation with swarm of basaltic dykes and water springs in the DMR 5G LIDAR surface morphology of the Liberec City centre. Klomínský et al. (2016).

periphery, with springs of carbon dioxide saturated water near the towns of Libverda Spa, Nové Město pod Smrkem and Świeradow Zdroj (see Fig. 4.5.2.).

The tectonic structures of the Krušné hory Mountains trend (NE-SW) in the western segment of the KJCM are of compressional character, and they have limited mineral and rock filling. They are therefore less prominent water conduits compared to the faults of the Sudetic trend.

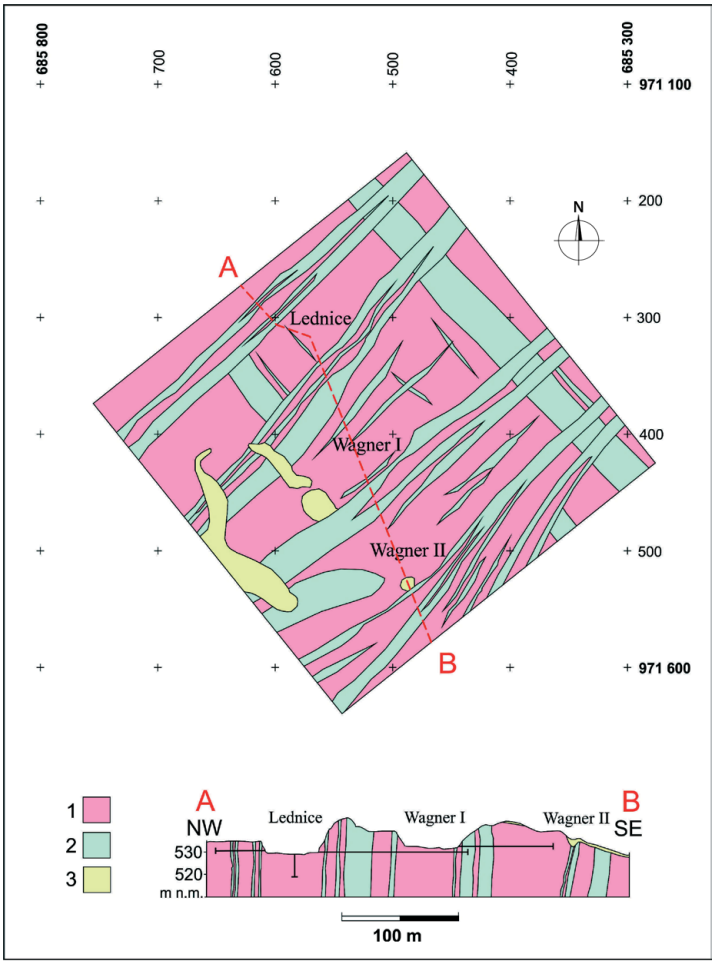

Figure 4.2. Geological map and profile of the Ruprechtice quarry in Liberec City with Lednice, Wagner I and Wagner II sections (Sedlář et al. 1982).

1 – fresh Liberec Granite,
2 – geological faults with dominant fracturing and/or hydrothermal alteration of the Liberec Granite,
3 – main dump of the quarry.
Horizontal lines in the geological profile A–B are horizontal drillings.

Figure 4.3. NE-SW zone of the tectonic fracturing and hydrothermal alteration of the Liberec Granite between the Lednice and Wagner I sections of the Ruprechtice quarry. Klomínský et al. (2016).

Figure 4.4. The intense hydrothermal alteration of the Liberec Granite 20 m wide in the NE-SW zone between the Lednice and Wagner I sections of the Ruprechtice quarry. Photo J. Klomínský.

Figure 4.5. Subhorizontal striation on the SW-NE fault surface of the Erzgebirge direction. Road cut near Lukášov SE of Liberec City. Photo Vl. Bělohradský.

4.1 Vratislavice fault zone – an example of the tectonic dilatation of the Liberec Granite

The Vratislavice fault zone of the Sudetic direction (NW-SE) has been exposed in a new road cut on the eastern outskirts of Liberec City (Fig. 4.1.2.). It can be classified as a normal dilatational groundwater saturated semiparalel fracture network with a multi-stage rock fracturing and repeated cementation of the quartz-hematite matrix. It consists of a zone over 100 m wide including several "melaphyre"dykes 0.5 to 5m wide and quartz vein stockworks.

These tectonic structures show widening toward the surface demonstrated by intense brecciaing of the older "melaphyre" dyke filling (Fig. 4.1.1.) and by Cretaceous sandstone xenoliths up to 20 cm in size (sediments of Cretaceous formation crop out recently 10 kilometres to the south) (Klomínský et al. 2005).

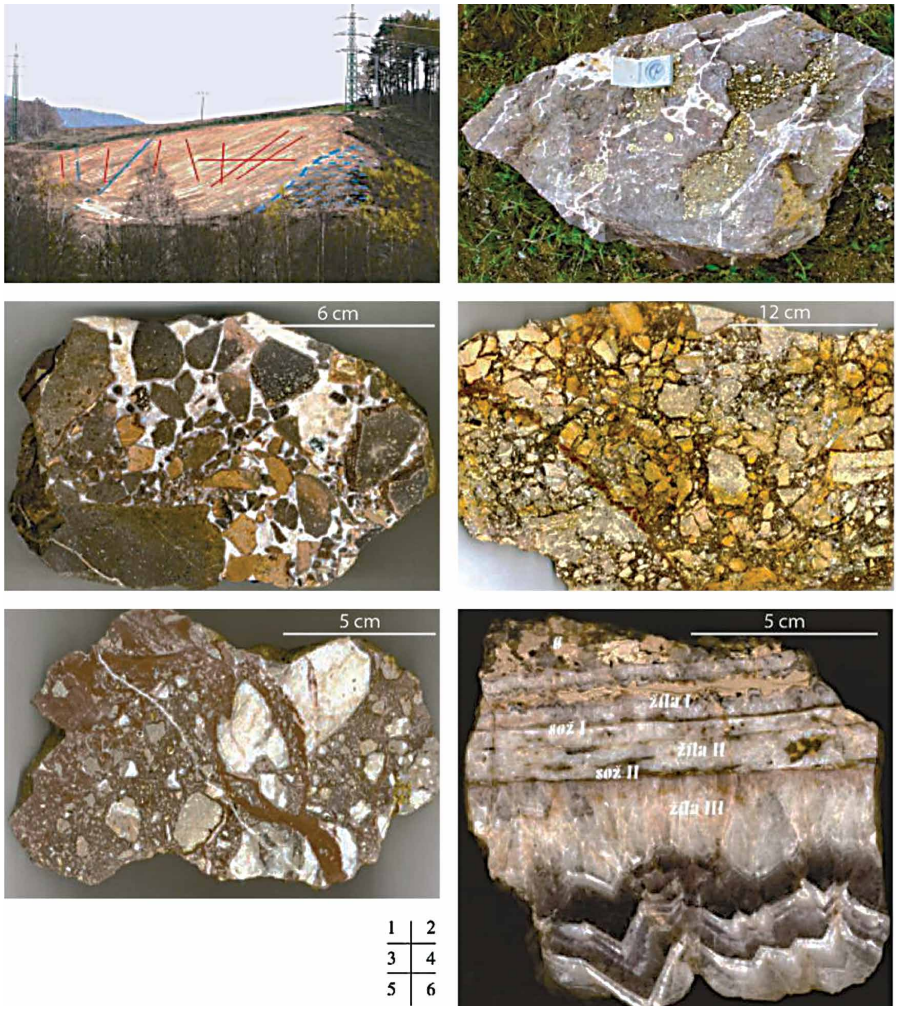

Figure 4.1.1.
1 – Exposure of the Vratislavice tectonic zone near Vratislavice Brewery (view from west), blue – melaphyre dykes, red quartz vein network.
2 – "melaphyre" with quartz breccias,
3 – detail of the "melaphyre" breccia texture with white quartz matrix,
4 and 5 – detail of the "melaphyre" breccias with hematite-quartz matrix,
6 – Composite quartz veins of different ages and colours (see violet amethyst). Klomínský et al. (2005).

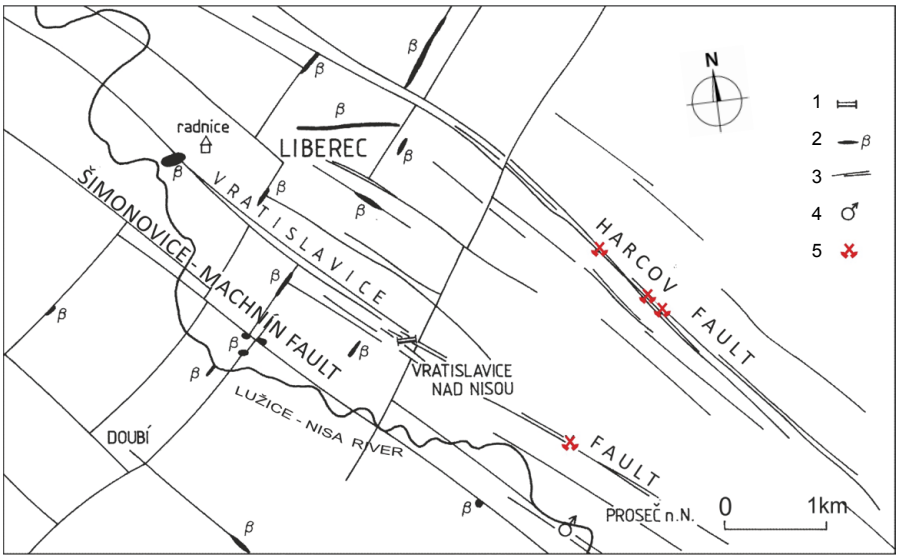

Figure 4.1.2. Geological faults network in Liberec city area with traces of iron ore mining. Klomínský et al. (2005).

1 – exposure of the Vratislavice fault zone near Vratislavice brewery,
2 – dykes and plugs of basaltic Neovolcanites,
3 – geological faults,
4 – Vratislavice mineral water spring,
5 – abandoned iron ore mine

The Vratislavice fault zone is a part of the dominant tectonic network breaking up the western segment of the Krkonoše-Jizera Composite Massif into several autonomous blocks.

The infrastructure of the tectonic faults in granites usually reflects the sensitivity of these types of rocks to bridle deformation soon after their consolidation and much earlier than their exhumation onto the Earth's surface. These fault zones usually have significant length and sufficient depth to create a favourable environment for seismic vibration propagation. The high competence of granites enables shallow earthquakes to evoke the large scale transport of fluids inside and around fault zones (Simson et al. 1975). This seismic pumping of the groundwater along tectonic fractures is recorded in the composition and textures of fracture filling in the Vratislavice fault zone (Fig. 4.1.1.).

Analysis of the dilatational fault parameters (direction, length, width, seismicity, infrastructure, hydrogeological role and tectonothermal activity) is a basic requirement for identification of monolithic polygons suitable for construction of underground radioactive waste repository.

4.2 Fractures in the granite outcrops of the KJCM

The fracture network in the fresh granites of the western segment of the KJCM is characterized by the presence of systematic steep fractures, locally variable non-systematic fractures, and sub-horizontal fractures. The steep fractures (70-90° dip) form two prominent regional sets that are present on the majority of outcrops that are widespread throughout the KJCM (Fig. 1.1.2.). The two sets are nearly perpendicular, or at a high angle to each other; one set strikes NE-SW and the other NW-SE, both having some minor deviations from the dominant strike (see Fig. 4.1.).

On outcrops, each set typically consists of multiple individual fractures that are approximately planar and subparallel to one another with spacing that varies between 1 cm and several meters. Fractures in a given set predominantly do not interact with one another even at small spacing. No consistent relative time relationships (e.g., termination of fractures of one set at fractures of the other set, curvature of one joint set towards the other) between the two sets have been observed. Where fractures of one set meet the other, they provide ambiguous time relationships. Most commonly, on subhorizontal exposure vertical fractures of the two sets are straight and intersect at high angles with no changes in orientation. Fractures are barren on most outcrops but in some places are coated by thin films of chlorite, epidote and hematite, or veined with quartz and calcite. Typically, the vertical fractures of both sets crosscut microgranitoid enclaves or aplitic dykes without offsetting them. Also, at the grain-scale, the fractures consistently crosscut individual grains without any even very small offset. The majority of steep fractures show no shear offset of grains parallel to fracture planes. Moreover, where fractures are healed by quartz or calcite veins, the displacement of fracture surfaces occurs perpendicular to the fracture wall. Only a small number of fractures in the study area bear slicken lines or slicken fibres on their surfaces and thus may represent minor shear fractures or reactivated pre-existing opening-mode fractures (faulted joints). The sub-horizontal fractures could be in many cases be interpreted as late sheeting or exfoliation joints, as they are closely spaced (with even less than cm spacing), follow the present-day topography, cut across the steep fractures, and are confined to the near-surface level (Fig. 4.2.1.).

Figure 4.2.1. The fracture network in the Hraničná granite quarry, 3 km south of the Bedřichov water-supply tunnel A. Klomínský and Woller (2010. The exfoliation planes in the near-surface zone, which has a limited continuation in the interior of the granite massif, represent the youngest set of fractures.

4.3 Seismicity in the western segment of the Krkonoše-Jizera Composite Massif

In the Jizerské hory Mts. seismicity occurs at a maximum intensity of 6° MSK-64. An earthquake of measurable intensity can be registered by people inside as well as outside buildings as displacements of lighter and heavier items (for example furnishings), plaster damage, fractures in walls, landslides, chimney damage and also water table variation. The immediate earthquake epicentre 40 km from Liberec is the Hronov-Poříčí geological fault next to Náchod in northeast Bohemia, with frequent earthquake events in intensity up to 7 grade of the International macroseismic EMS-98 scale (Fig. 4.3.1.).

The Sudetic earthquake in January 1901, well documented by Gränzer (1901), affected the whole Liberec region at M6 intensity according to the ten grade scale (Fig. 4.3.1.). Recently several weak earthquakes have been recorded near Liberec and Frýdlant with magnitudes from 1.6. to 4.6. (Málek et al. 2008).

Figure 4.3.1. Map of the localities between Liberec and Jablonec nad Nisou affected by the Sudetic earthquake on 11 January 1901 according to Gränzer (1901). Geological legend see Cháb, J. – Stráník, Z. – Eliáš, M., eds (2007).

Figure 4.3.2. Tectonic zone of the Sudetic direction in the Liberec Granite, 50 meters wide in construction site near Na Bídě town district (Perštýn locality). Photo J. Klomínský.

The outline of the Liberec tectonic graben is formed by the broad Sudetic fault zone with a NW-SE direction, consisting of the Šimonovice-Machnín, Harcov and Vratislavice faults (Fig. 4.3.2) which are the most important conductors of seismic events from near and distant epicentres (Fig. 4.3.1).

Tectonic breccia textures in Fig. 4.3.3. in the Vratislavice fault zone demonstrate multiphase destructive impact of earthquakes on the original rock filling (hydrothermaly altered Permian melaphyre cemented by fine grained heamatitic quartz matrix).

4.4 Recent seismicity survey in the Bedřichov water-supply tunnel section A

The instrument used for long-term monitoring of deformation of the rock-massif resulting in micro displacements on fracture planes is the TM71 fracture gauge (CZ

Figure 4.3.3. Tectonic breccia textures from the Vratislavice fault zone demonstrating multiphase destructive impact of earthquakes on the original rock filling (hydrothermaly altered Permian melaphyre cemented by fine grained hematitic quartz matrix). Photo J. Klomínský.

patent No. 131631 and 246454, author Ing. B. Košťák, CSc. ÚSMH AV ČR Institute). The instrument operates on the principle of mechanical interference (Fig. 4.4.1.). Its construction permits long-term, highly accurate 2.5 D measurements of displacements even under climatically unfavourable conditions. Its sensitivity is 0.05 to 0.0125 mm in the direction of all three axes. Its sensitivity to rotation is 3.2. 10^{-4} rad. This type of instrument has been used for several decades, mainly for monitoring slow slope deformations of block type. Once the interpretation possibilities were tested and verified, measurement of micro displacements on fracture planes started. At present the instruments are used for monitoring micro displacements of various origins at numerous local and foreign localities (e.g., Peru, Canada, Germany, Italy, Greece, Poland, Slovakia, Bulgaria, Slovenia and Kyrgyzstan).

TM71 fracture gauges were installed in 2004 at footages of 792 m and 881 m from the SW portal of the tunnel section A on tectonic fractures of the Sudeten trend (NW-SE) and the Krušné hory Mountains (Erzgebirge) trend (NE-SW), Figs. 4.4.3. and 4.4.4. Another two gauges were installed in November 2005 at footages of 235 m and 278 m (from the tunnel portal section A). Measurements started on 30 November 2005.

Figure 4.4.1. TM71 device positioned on the NW wall of the Bedřichov water-supply tunnel section A. Photo J. Klomínský.

Seismic observations at the Bedřichov earthquake monitoring station

Local seismic background noise is caused mainly by movement of vehicles and people close to the station. Continuous long period noise consists of microseisms with a period of approximately 6 seconds, as observed at all seismic stations in central Europe.

The nearest registered blasts take place at the Krásný Les basalt quarry near Frýdlant (Fig. 4.4.6.). The majority of recorded events are made up of mine tremors from ore mines near the Polish town of Lubin (Fig. 4.4.2.). These induced earthquakes exhibit the highest amplitude of all the regional earthquakes up to a distance of 500 km. The station also registers earthquakes in the Alps and other seismically active regions. The station has sufficient sensitivity to register earthquakes worldwide. The highest vibration velocity was measured during the Kuril Islands earthquake with a magnitude of M_w 8.1, 13 January 2007 (Fig. 4.4.2.). Remote earthquakes reach the highest amplitudes usually in terms of surficial waves for periods of 15–20 seconds.

Microdisplacements on tectonic fractures in granite of the Bedřichov water-supply tunnel A (Klomínský, Woller 2010)

All four TM71 fracture gauges installed in the tunnel registered displacements (Figs. 4.4.3. and 4.4.4.).

The individual displacements registered during the period 2004–2012 are of the order of 0.1mm in the horizontal and vertical directions (Figs. 4.4.3. and 4.4.4.).

Displacements registered in discontinuities of the same tectonic trend (2 devices installed on faults of the Krušné hory Mts. trend, i.e. NE-SW, and 2 devices installed on faults of the Sudetic trend, i.e. NW-SE) are in mutual agreement. This suggests that the registered displacements can be identified with a high probability as being of tectonic origin.

An analysis of successive displacements, taking account of the cumulative displacements of local blocks for a period of three years 2004–2007 results in a displacement velocity of 0.22 mm per year along discontinuities of the Krušné hory Mts. trend and 0.16 mm per year in the granite massif along those of the Sudetic trend.

All the fracture gauges registered displacements corresponding to oblique overthrusts, with thrusting of the southern blocks over the northern blocks.

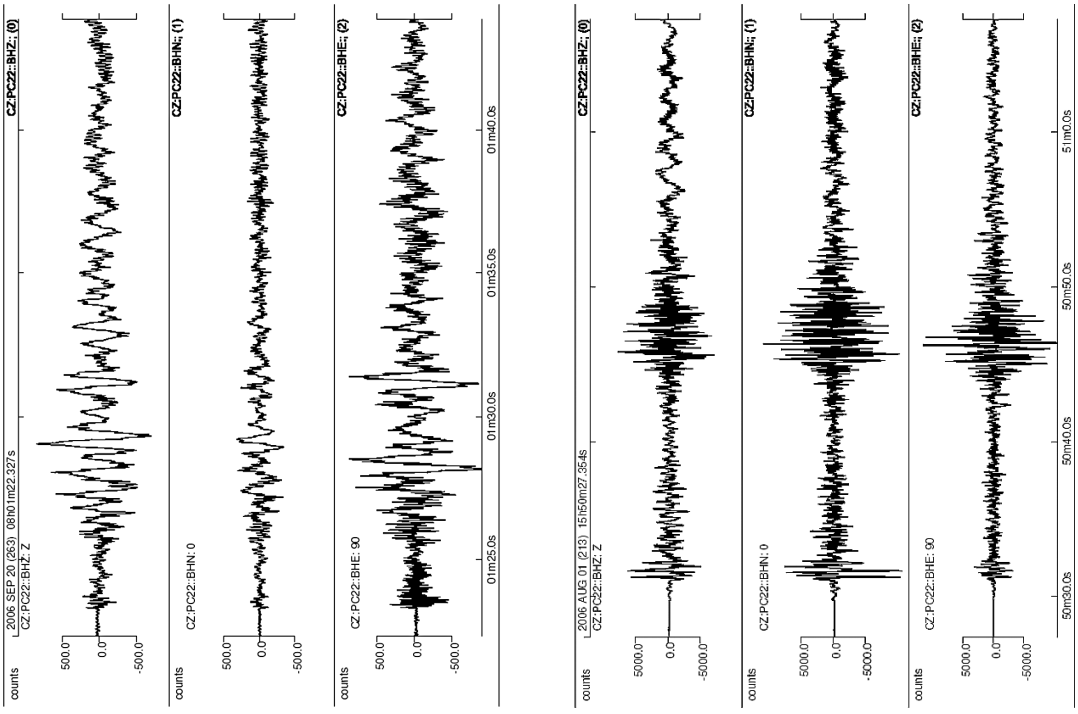

Figure 4.4.2. Record of mine tremors (left 3 traces) from a regional earthquake in ore mines near Lubin (Poland), 100km NE of the Bedřichov water-supply tunnel. Klomínský and Woller (2010). Record of a strong earthquake (right 3 traces) in the Kuril Islands with a magnitude of 6.5.

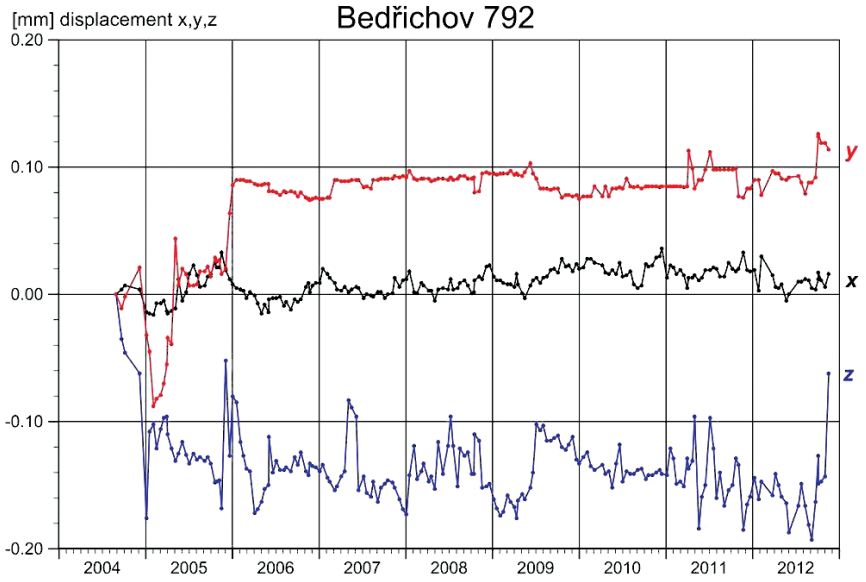

Figure 4.4.3. 2.5 Dimensional micro displacements recorded at location 792 m from the Bedřichov water-supply tunnel SW portal section A on the NE-SW Erzgebirge trend tectonic fault between 1. 8. 2004 to 1. 5. 2012. Hokr et al. (2014). × – Horizontal motion across the fault, y – horizontal motion along the fault, z – vertical motion along the fault.

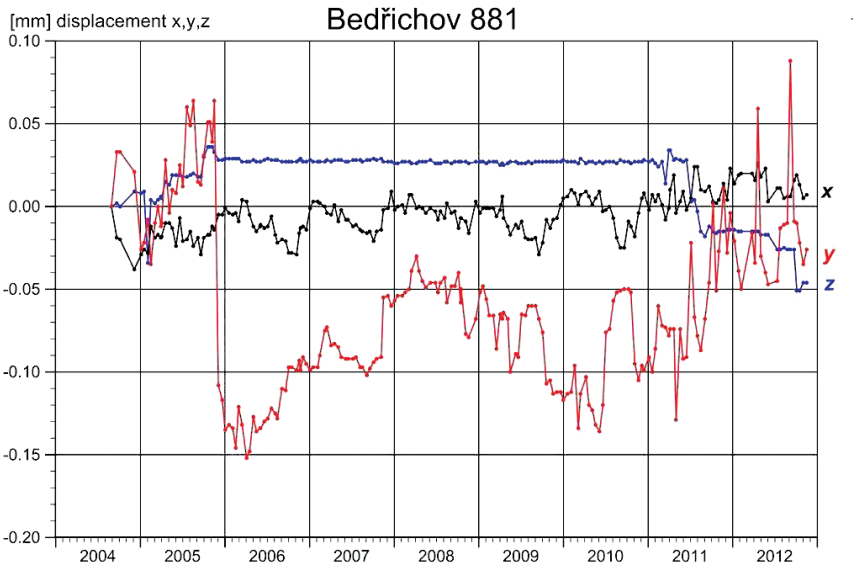

Figure 4.4.4. 2.5 Dimensional micro displacement recorded at location 881 m from the Bedřichov water-supply tunnel section A SW portal on the NW-SE Sudetic trend tectonic fault between 1. 8. 2004 to 1. 5. 2012. Hokr et al. (2014). × – Horizontal motion across the fault, y – horizontal motion along the fault, z – vertical motion along the fault.

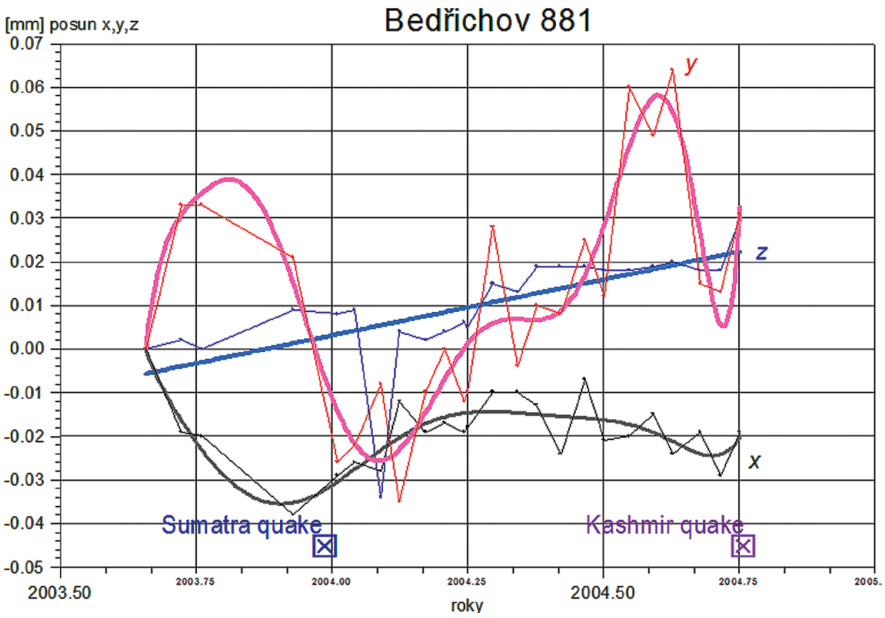

Figure 4.4.5. Detail of micro displacements recorded at location of 881 m on the NW-SE Sudetic trend fault in the the Bedřichov water-supply tunnel SW portal section A registered during a major earthquake near Sumatra (26 December 2004; M = 9.3) followed by a catastrophic earthquake in Kashmir (8 October 2005; M = 7.7). Klomínský and Woller (2010).

The displacements measured correspond to a stress field model with a compression axis tending north-south and with overthrust displacements towards the north. This orientation of compression possibly corresponds to residual pressure resulting from the southerly transport of the continental glacier and the pressure exerted by its front against the buttress of the Jizerské hory Mts. and Krkonoše Mountains.

The sum of the displacement rates inside the granite massif in the period of 2004–2012 amounted to 0.22 mm/yr along the NE-SW faults (the Krušné hory Mts. fault system) and 0.16 mm/yr along the NW-SE faults (the Sudetic fault system). Displacements with an oblique reverse-fault character, with southern blocks thrusting over northern blocks, were observed along the above-mentioned directions. The character of the displacement corresponds to the compression stress model in an approximately N-S direction with north-verging over-thrusting. A comparison was done of the occurrence of seismic phenomena with the greatest amplitude of vibration velocity and the time course of micro-displacements on fractures, which were monitored with TM71 gauges in the Bedřichov water-supply tunnel section A. The greatest amplitude of seismic waves of 13 January 2007 (Kuril Islands earthquake) correlates well with change of the trend on the × – axis of the A792 gauge.

In the course of monitoring two prominent impulses or peaks were recorded, associated with increased rate of microdislocations. The first impulse (Fig. 4.4.5.) was recorded shortly after the monitoring started, near the turn of 2004/2005. It correlates with the earthquake near Sumatra at the end of December 2004. The recorded peak

apparently reflects the stress changes accompanying this earthquake of global character (M_W = 9.3). The record of this impulse is better documented in detail (Fig. 4.4.5.). The character of the impulse is different from later displacements registered until November 2007. Another important impulse is linked with the catastrophic Kashmir earthquake (Islamabad, October 8, 2005; M = 7.7).

According to Málek et al. (in Hokr ed. 2014) in the period 2004 to 2012 various displacements have been recorded on all four gauges installed in the Bedřichov water-supply tunnel. in order of 0.1 mm along vertical and horizontal direction of the NW-SE and SW-NE fault structures.

Seasonal component of the massif dilation mainly was recorded on the component of the horizontal opening / closing of the fault with a maximum amplitude of 0.1 mm. Distinct dilatation in the component of horizontal strike-slip displacement is just on the fault closest to the entrance (stationing 235). An important finding is that dilatation (seasonal opening of the fault) toward the massif continuously decreases from 0.1 mm to 0.04 mm. The component of the opening / closing displacement is not important for the interpretation of the jump (pulse) displacements that affect other components of fault movements.

Seismic activity in the surroundings of the Bedřichov water-supply tunnel

A wide-band (0.03-50 Hz) three-component seismic station was installed in May 2006 below the Josefův Důl dam. This station, equipped for continuous registration, was selected for registration of local, regional and distant seismic events. It has a CMG-40T (GURALP) seismic recorder with the registration aperture RUP2004 (ÚSMH AV ČR). Accurate synchronisation is achieved using the signal from the satellite GPS navigation system. The station was put into operation on 10 May 2006 and it is integrated into the regional PASSEQ network. In 2011 two seismic sensors are placed at the location of 235 m and 278 m from the SW portal of the water-supply tunnel (section A) in Bedřichov. These positions were chosen close to tectonic faults. At 235 m, the tunnel is intersected by NW-SE trending fault and at 278m by SW-NE fault. The wide-band characteristic of the stations permits registration of a wide-range of seismic phenomena:

Local seismic disturbances caused by car traffic near the station. Sporadically, movement of people near the station is registered. Another significant source of undesirable noise is a small water power plant (SWPP) in front of the portal to the gallery and connected through water pipeline DN 800.

Continuous long-period noise corresponds to microseisms with the period approximately 6 seconds, which is common to all stations in central Europe.

Regional seismic events

A few tens of weak seismic events (mostly with highest amplitude < 1 μm/s, occasionally < 3 μm/s) were probably caused by mining works in quarries nearby (quarry Bezděčín 14 km, quarry Krásný Les 17 km, quarry Smrčí 20 km, quarry Košťálov 30 km, quarries Studenec, Tachov, Chlum 38 to 47 km). Seismometers in Bedřichov tunnel detected 30 events per month from copper mines in Lubin

(approx. 70 km in Poland). Usually once or twice a month, a Lubin earthquake has magnitude 3.5 or higher. Weak tectonic earthquakes with location in the Czech Republic were detected very rarely. At the time of activity in west Bohemia (earthquake swarm in 2011), only events with magnitude higher than 3 were detected because of the distance of 200 km. Quite often there were events from coal mining in Ostrava (approx. 250 km) and from the Upper Silesian basin in Poland (250 to 300 km). There were around tens detected a year however they had amplitudes not exceeding 1 μm/s. Other detected events were sporadic tectonic earthquakes from Poland, Slovakia, Hungary, Slovenia, Austria and Germany (200 to 400 km). Maximum amplitudes of seismic waves of these events from central Europe were in the order of μm/s, occasionally in the first tens of μm/s. Other detected events included those from the active parts of south Europe (Italy, Greece and Croatia) where earthquakes occur sometimes with magnitudes even around 5. These strong earthquakes cause seismic vibrations in massif with velocity amplitudes in tens of μm/s and their impact on the massif is incomparable with the effects of stronger quarry earthquakes from Lubin. The last group of detected events includes far away (global) earthquakes. There were tens of them detected per year but only parts of the arriving waves were registered because of the characteristics of the seismometers (frequencies from 1 Hz). Amplitudes reach at maximum the first tens of μm/s in the measured frequency range. The installed seismometers reliably measure local and nearby low or moderate periodic events whereas long waves of faraway events are registered either badly or not at all. No local earthquake has been detected (event in hypocenter location < 3 km).

Seismic event registered in the Bedřichov water-supply tunnel on December 5, 2012

The nearest detected microearthquake was a seismic event on 5th December 2012 at 08:30:29 UTC (Fig. 4.4.6.). The hypocenter was determined in distance of 11 km below the valleys of the Bílá Desná river and the Černá Desná river in the area between the Souš water reservoir and the Desná village in the depth of the first few kilometers.

Blasting in the Krásný Les quarry near Frýdlant.

Registration of the blast is shown in Fig. 4.4.6. The seismograms show a prominent surface wave in addition to the P and S waves. In fact, there were two blasts on 14 August 2007, separated only by 10.61 seconds. Special monitoring was conducted at the time of these blasts. One seismograph was located 100 metres from the blast site and recorded the exact time of the blast, another seismograph was positioned in the quarry 200 m from the blast site; it recorded the character of the tremors near the source. The time of P-waves propagation (3.15 s) and S-waves propagation (5.68 s) was calculated from comparison of data from the quarry with the Bedřichov seismic station. The epicentre distance was 17.52 km.

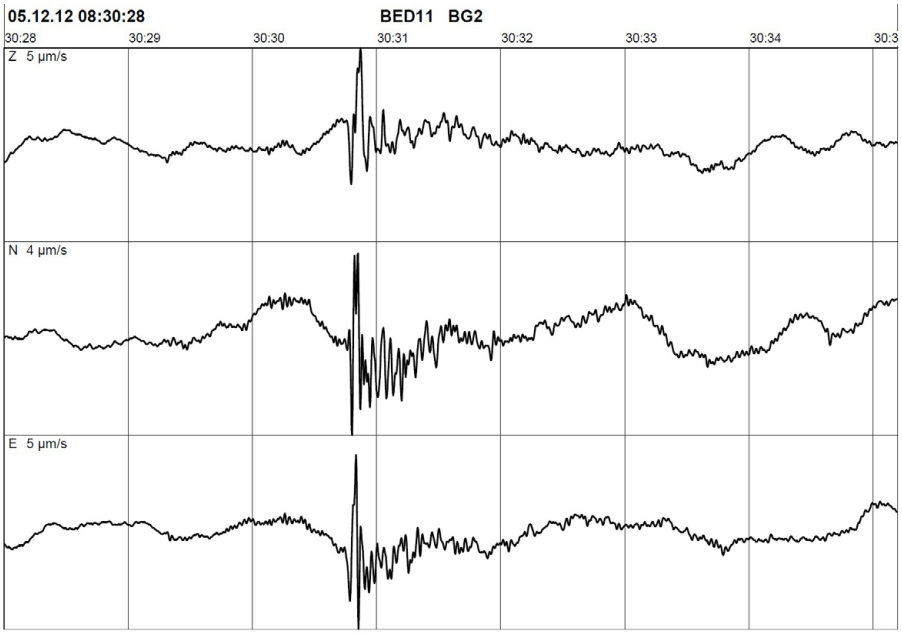

Figure 4.4.6. Record of the microearthquake by sensor LF-24 in the Bedřichov water-supply tunnel on on 5th December 2012 at 08:30:29 UTC. Hokr et al. (2014).

REFERENCES

Cháb, J. – Stráník, Z. – Eliáš, M. eds (2007): The geological map of the Czech Republic 1 : 500 000 – Czech Geol. Survey, Prague.

Gränzer, J. (1901): Das sudetische Erdbeben vom 10. Jänner 1901, Mittheilungen aus dem Vereine der Naturfreunde in Reichenberg, 1901, Jahrgang 32, S. 3–109.

Hokr, M. ed. (2014): Tunel 2011 – Závěrečná zpráva březen 2014. Technická universita v Liberci. 166 str. MS SÚRAO Praha, TUL.

Klomínský, J. ed. (2008): Studium dynamiky puklinové sítě granitoidů ve vodárenském. tunelu Bedřichov v Jizerských horách. Etapa 2006–2008. – MS Čes. geol. služba. Praha.

Klomínský, J. – Bělohradský, V. – Fediuk, F. – Schovánek, P. (2005): Vratislavický zlom – nový odkryv u Liberce v severních Čechách. – Zprávy o geologických výzkumech v roce 2004.

Klomínský, J. and Woller, F. (2010): Geological studies in the Bedřichov water supply tunnel. SÚRAO Technical Report 02/2010. 103 s. – Česká geologická služba. Praha. ISBN 978-80-7075-760-4.

Málek, J. – Stejskal, V. – Zedník, J. (2008): Seismický roj na hronovsko-poříčském zlomu v lednu 2008.

Stemberk, J. – Košťák, B. (2007): 2.5 D trend of aseismic creep along active faults in western part of the Gulf of Corinth, Greece. – Acta Geodyn. Geomat., 4, 1 (145), 53–65. Praha. ISSN: 1214-9705.

Stemberk, J. – Košťák, B. (2008): Recent tectonic microdisplacements registered in Bedřichov water-supply tunnel "A" in the Jizerské Hory Mts. (N. Bohemia). – Acta Geodyn. Geomater.,5, 4 (152), 377–388.

4.5 Geothermal field of the Krkonoše-Jizera Composite Massif

According to Čermák (1975, 1981), the average heat flow in the Bohemian Massif reaches 68 ± 24 μW.m^{-2}. The highest values of heat flow in the northern part of the Bohemian Massif 80 to 100 μW.m^{-2} are related to higher radioactivity of the late Variscan granites of the Smrčiny-Krušné hory Mts. Batholith and the Krkonoše-Jizera Composite Massif. According to Rybach (1976) total radiogenic heat generated by average granite contributes to the Earth heat flow 2.5 μWm^2 in each one km of the granite layer. If one unit of the heat production (HGU) corresponds to 0.417 μWm^3 = 3.16 cal/m^3 in one year then 1 m^3 of the Krkonoše-Jizera granite produces around 14 HGU or 45 cal/m^3 in one year. The KJCM volume of several thousands of cubic kilometers and the geological age of about 320 Ma produces a gigantic amount of thermal energy (around 90 Gcal/year).

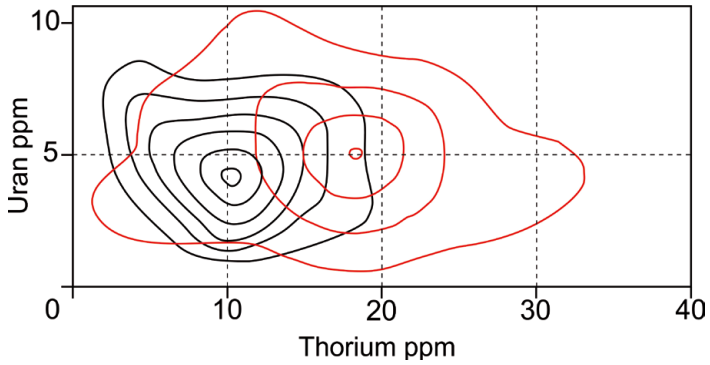

Figure 4.5.1. Uranium and thorium concentration in Jizera Granite (black) and Liberec Granite (red) in western segment of the Krkonoše-Jizera Composite Massif.

Average content of radiogenic elements was for western segment of the KJCM assessed at 7.84 ppm U and 19.9 ppm Th (Fig. 4.5.1.) and for the eastern (Polish) part of the KJCM at 11.7 ppm U and 24.2 ppm Th (Černík and Goliáš 2014). Most of the heat produced in these granites comes from the radiogenic alpha-decay of U. The heat production of granites can significantly influence the regional heat flow pattern. The Jizera and Krkonoše Mountains region has long been well known for mineral, thermal and radioactive (radon) water springs (Fig. 4.5.2.). Spring locations are both within the KJCM and on its periphery on both sides of the Czech border with Poland (e.g. Libverda Lázně Spa, Vratislavice, Nové Město pod Smrkem, Bilý Potok mineral springs on the Czech side, and Swieradow Zdroj and Czerniawa Zdroj on the Polish side). There is a 29 °C thermal spring at Janské Lázně Spa and a 44 °C thermal spring at Cieplice Lázně Spa near Jelenia Gora in Poland. According to Dowgiallo (2002) there is similar geothermal energy resource potential in other parts of the granite massif such as the Liberec basin (Fig. 4.5.2.).

The deepest borehole (C-1) ever drilled up to now into a granite body in the Bohemian Massif, located at Cieplice Lázně Spa near Jelenia Góra in Poland

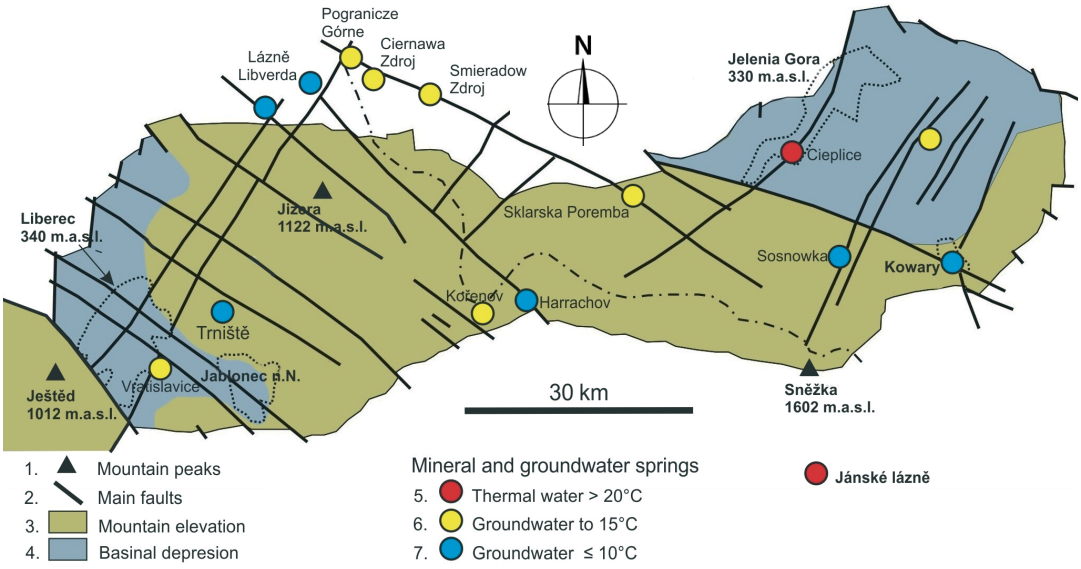

Figure 4.5.2. Temperature of the mineral and groundwater springs in the Krkonoše-Jizera Composite Massif area and their relationship to KJCM major geomorphologic structures. Klomínský (2006).

(approximately 85 km ENE from Liberec City), encountered, at a depth of 2 km, thermal water with a temperature of 97.7 °C and an inflow of 15 l/s. The borehole is located in Liberec type porphyritic granite in the Krkonoše-Jizera Composite Massif and the main inflow of thermal water issues from the tectonic zones of the Sudetic (NW-SE) and Krušné hory Mts. (NE-SW) trends. The high radiothermal heat yield of KJCM (6–8 μWm^3) is considered to be the main source of heat for the thermal groundwater.

One of the most important factors when considering the thermal potential of granite massifs is the value of heat production. Methods used for the analysis of the thermal gradient of granitic bodies based on their heat production and terrestrial heat flow can be used in the classification of intrusive bodies from the point of view of suitability for the disposal of highly radioactive material.

The discovery of the deep circulation of high temperature thermal water within the tectonic zones of the Krkonoše-Jizera Composite Massif, with water temperatures reaching 60 ºC at an approximate depth of 500 m (Bujakowski et al. 2016).

Groundwater heating in the Krkonoše-Jizera Composite Massif is due to both the Earth heat flux and the decay of uranium, thorium and potassium radioactive isotopes. The high content of these elements ranks the Krkonoše-Jizera Composite Massif in the High Heat Production (HHP) granites.

In the wider surroundings of Bedřichov, various types of water occur, including natural mineralised waters from the Vratislavice and Libverda Lázně Spa springs and from Nové Město pod Smrkem. Vratislavice mineral water has the highest mineralization, containing a total of 2288 mg/l total dissolved solids (TDS).

This mineral water is classified as the Na-K-HCO_3 type, with 6.28 pH, dissolved hydrogen-carbonates and CO_2. The mineral water from the Libverda Lázně Spa is of the Ca-HCO_3 type, containing 1070 mg/l of TDS. Similar to the Vratislavice mineral water, it has a relatively low pH of 6.58. The mineral water from the town of Nové Město pod Smrkem is weakly mineralized with 967 mg/l TDS, but it has an interesting chemical composition. It is of the Mg-HCO_3 chemical type. Its pH of 6.72 is weakly acidic. The water from Bedřichov, with 516 mg/l TDS, is moderately mineralized. It is of the Ca-Na-SO_4 chemical type. The elevated content of SO_4 ion indicates relatively shallow circulation in the oxidation zone, with a prolonged period of residence in the massif. The Bedřichov water has a pH of 7.51 and 0.97 Na+K/Ca ratio. The water from the Hašler Hut near Bedřichov has a chemical composition similar to that from Bedřichov, but it has low mineralization with 143 mg/l TDS. It is also of the Ca-Na-SO_4 type and the Na+K/Ca ratio is 1.08. It is probable that waters from Bedřichov and the Hašler Hut are closely related, but water from the Hašler Hut has a shallower circulation. The strikingly low pH of 4.72 is most probably caused by decomposition of organic material with subsequent infiltration into a near-surface zone.

The water from Karlov, near Bedřichov, has a low mineralization of 141 mg/l TDS and it is of the Ca-SO_4 type. It features properties similar to water commonly found in the near-surface zone. It has a pH of 6.14. The above data indicate the presence in the Bedřichov area of waters which are closely related in origin, as well as waters of different types. The differences in chemical composition indicate differences in the

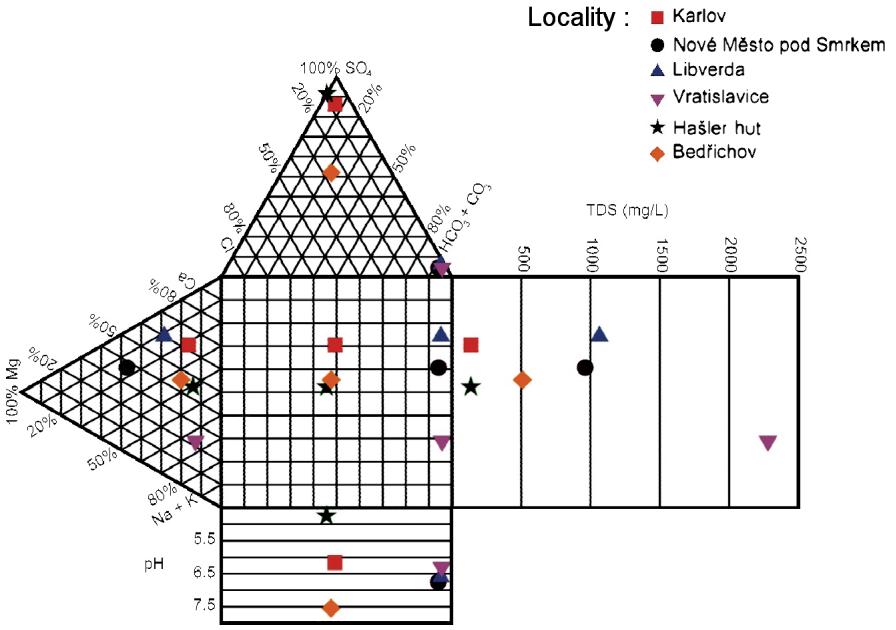

Figure 4.5.3. Durov diagram showing composition of the groundwater springs and mineral waters from the study area. Klomínský and Woller (2010).

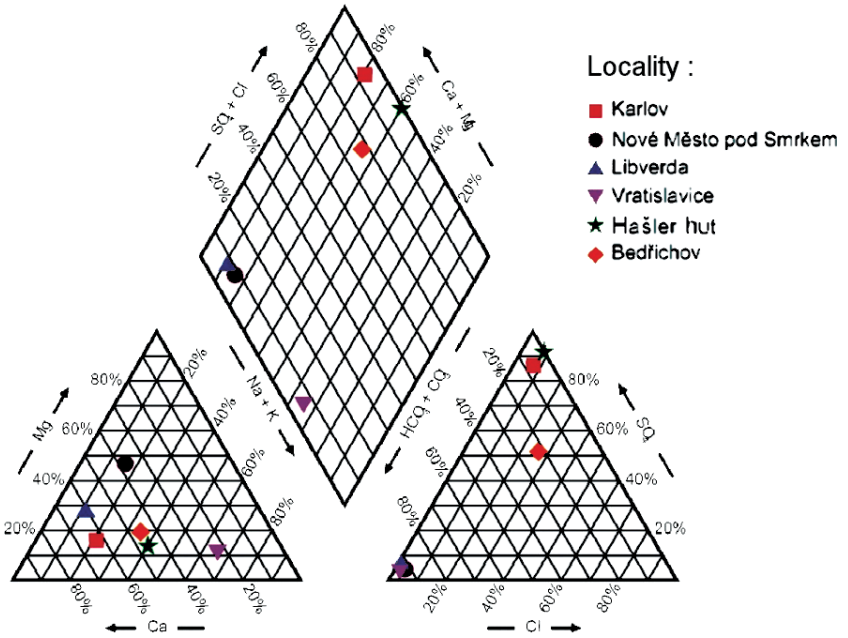

Figure 4.5.4. Piper diagram showing composition of the groundwater springs and mineral waters from the study area. Klomínský and Woller (2010).

Figure 4.5.5. Fragment Vratislavice fault zone quartz vein with frequent open caverns (half of actual size). Photo J. Klomínský.

composition of the rock environment and differences in chemical processes involved in evolution of the waters. Figs. 4.5.3. and 4.5.4. present Durov and Piper diagrams with plots of chemical composition of the water springs discussed above.

Vratislavice nad Nisou mineral spring

The Vratislavice mineral and CO_2 rich water spring is found in the SE corner of the Liberec tectonic graben. This water, with 240 to 340 ppm TDS and temperature about 13.0 °C, emerges from the Vratislavice fault zone of the Sudetic direction (Figs. 4.5.2 and 4.5.5.) through hydrothermally altered Liberec Granite and melaphyre dyke. Vratislavice mineral water was commercially tapped until recently.

A new cluster of water springs of the Na-Cl type, with high radioactivity up to 2300 Bq/ ^{222}Rn, 1,5 g/l TDS, 22 l/min flow rate and temperature of 11.6 °C, was recently found north of Albrechtice next to the main road from Liberec to Frýdlant (Goliáš et al. 2014).

REFERENCES

Bujakowski, W. – Barbacki, A. – Miecznik, M. – Pajak, L. – Skrzypczak, R. (2016): A structural-thermal model of the Krkonosze Pluton (Sudetes Mountains, SW Poland) for hot dry rock (HDR) geothermal use. – Arch. Min. Sci. Vol. 61 (2016), No 4, p. 917–935.

Čermák, V. (1981): Heat flow investigation in Czechoslovakia. In: Zátopek, A, (ed.): Geophysical syntheses in Czechoslovakia. 427–439, Veda, Bratislava.

Čermák,V. (1975): Combined heat flow and heat generation measurement in the Bohemian Massif. – Geothermica, 4, 19–26, Piosa 1975.

Černík, T. – Goliáš, V. (2014): Radioactivity of granitoids of the Krkonoše-Jizera Pluton. – Statistical analysis of archival data. (In Czech). – Zprávy o geol. výzk. v roce 2013, 103–106.

Goliáš, V. – Hrušková, L. – Čermák, T. – Bruthans, J. – Najkládal, P. – Churáčková, Z. – Kula, A. (2014): Albrechtický chloridový okrsek. Zprávy o geol. výzk. v roce 2013. 165–170.

Dowgiałło, J. (2002): The Sudetic geothermal region of Poland. Geothermics vol 31, 3, 343–359.

Gränzer, J. (1901): Das sudetische Erdbeben vom 10. Jänner 1901, Mittheilungen aus dem Vereine der Naturfreunde in Reichenberg, 1901, Jahrgang 32, S. 3 – 109.

Gränzer, J. (1929): Tertiare vulkanische Gesteine in der Umgebung von Reichenberg in Bohmen. Mitteilungen des Vereines der Naturfreunde in Reichenberg 51. Jahrgang. 12–27.

Klomínský, J. (2006): Geotermální pole v západní části krkonošsko-jizerského masivu – fikce nebo realita? – Zprávy o geol. výzk. v roce 2005. 179–182.

Klomínský, J. – Bělohradský, V. – Fediuk, F. – Schovánek, P. (2005): Vratislavický zlom - nový odkryv u Liberce v severních Čechách. – Zprávy o geologických výzkumech v roce 2004.

Klomínský, J. – Woller, F. (2010): Geological studies in the Bedřichov water supply tunnel. SÚRAO Technical Report 02/2010. 103 s. – Česká geologická služba. Praha.

Málek, J. – Žanda, L. – Štrunc, J. – Brož, M. – Briestenský, M.: in Hokr, M. ed. (2014): TUNEL 2011 – Final Report March 2014. MS TU Liberec and SÜRAO Prague.

Málek, J. – Stejskal, V. – Zedník, J. (2008): Seismický roj na hronovsko-poříčském zlomu v lednu 2008. In: Marková, E. (ed). Člověk ve svém pozemském a kosmickém prostředí. Úpice 20 – 22. 5. 2008. ISBN 978-80-86303-14-7.

Rybach, L. (1976): Radioactive heat production and its relation to other petrographic parameters. – Pure appl. Geophys. 114, 309–318.

Simson, R. H. et al. (1975): Seismic pumping – a hydrothermal fluid transport mechanism. – J. Geol. Soc. London. 131, 653-659.

Stemberk, J. – Košťák, B. (2007): 2.5 D trend of aseismic creep along active faults in western part of the Gulf of Corinth, Greece. - Acta Geodyn. Geomat., 4, 1 (145), 53–65. Praha. ISSN: 1214-9705.

Stemberk, J. – Košťák, B. (2008): Recent tectonic microdisplacements registered in Bedřichov water-supply tunnel "A" in the Jizerské Hory Mts. (N. Bohemia). – Acta Geodyn. Geomater.,5, 4 (152), 377–388.

5. Water-supply tunnels in the Jizerské hory Mts.

5.1 Tunnels parameters

At the beginning of the 20th century, several waterway and water-supply tunnels were constructed, using traditional mining methods, to regulate water streams in the Jizerské hory Mrs. (e.g. the Souš water-supply and the Mšeno water-way tunnels, Fig. 5.1.1.). Their main function was to protect the valley towns of Tanvald and Jablonec nad Nisou against floods during rainstorms. In the early 1980s two new water supply tunnels were constructed to transport raw and treated water to and from the treatment plant in Bedřichov (Klomínský et al. 2003, 2005). The Mšeno water-way tunnel is 1.758 m long with second branch of the Mšeno dam tunnel 636 m, the Souš water-supply tunnel 1100 m and the two sections (A and B) of the Bedřichov water-supply tunnel total about 6780 m (Fig. 5.1.1.).

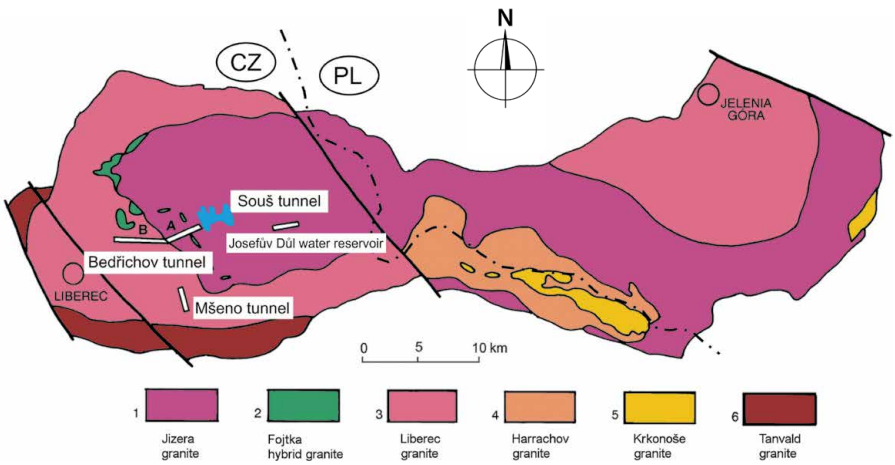

Figure 5.1.1. Geological map of the Krkonoše-Jizera Composite Massif with location of the water-supply and water-way tunnels. Klomínský et al (2005).

The **Souš water-supply tunnel** (Figs. 5.1.1., 5.1.2. and 5.1.3.) was constructed in 1914 using traditional mining technology to transfer water from the Bílá Desná dam to the nearby Černá Desná river valley if there was a danger of flooding when the dam water level rose too high. It is 1100 m long with a 1 % incline. Today the Souš water-supply tunnel serves as the underground water conduit to fill the Souš water dam. The Souš water-supply tunnel intersects porphyritic medium grained biotite granite (Jizera Granite). The granite is very inhomogenous in lithology and texture. These features have been documented in the tunnel as multilayered biotite schlieren up to several meters in thickness. Their subhorizontal stratification and lithology resemble migmatites. The schlieren have the form of flat domes with N-S elongation. Thickness

of the tunnel overburden fluctuates around 100 m. Two dykes of the alkali-feldspar quartzsyenite or trachyandesite (width of 1.8 and 1.9 m) of Permian age penetrate the Souš water-supply tunnel in NW-SE direction at distances of 370 m and 384 m from the western tunnel portal. These rocks were described by Pták (1963) as lamprophyres. The tectonic zone of the larger thickness and high groundwater inflow (60 l/min) in azimuth NE-SW is located between 750 to 900 m from the Souš water-supply tunnel's western portal. A similar tectonic zone of NW-SE direction cuts the tunnel 650 m from the western tunnel portal (Fig. 5.1.3.).

The **Mšeno water-way tunnel** was constructed in 1914 with a length of 1 758 m from the bed bottom of the Lužice Nisa river to the Mšeno water dam in Jablonec nad Nisou The tunnel walls are completely covered by brickwork. The surface of the tunnel walls is in patches covered by white powder of opal.

Figure 5.1.2. Interior of the Souš water-supply tunnel in the Jizerské hory Mts. Water runs over the tunnel ground. Klomínský et al. (2005).

Bedřichov water-supply tunnel (sections A and B)

The Bedřichov water-supply tunnel in the Jizerské hory Mts. is in one of only a limited number of underground drifts in the Czech Republic, which intersects the Krkonoše-Jizera Composite Massif (Figs. 5.1.1. and 5.1.6.). The tunnel's importance in this respect is especially due to its unusual length (over 6 km) and the technical attributes of the method of construction (a combination of the tunnel boring method – TBM – and the drill and blast technology used in tunnel driving). The tunnel walls are particularly appropriate for the study of granite jointing and the long-term monitoring of the "metabolism" of the rock environment. The results of such observations allow models to be created of the evolution of both far-field and excavation-damaged zones (EDZ)

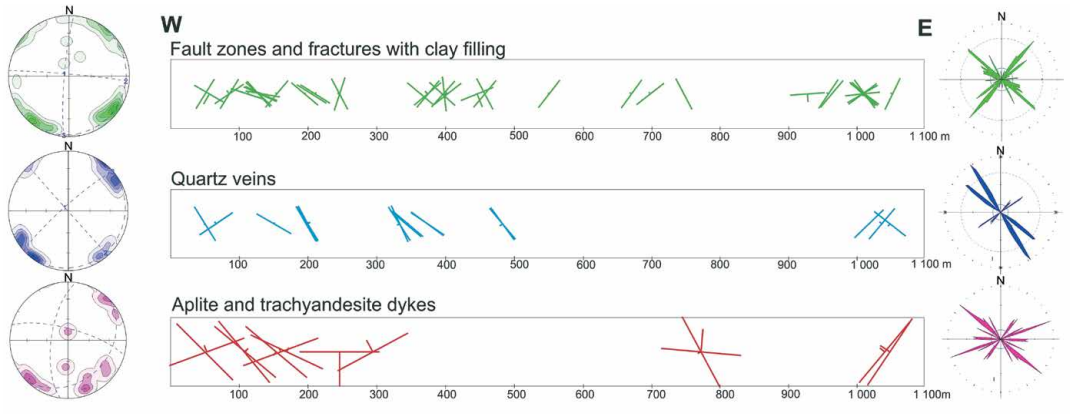

Figure 5.1.3. Diagrams of fracture networks in the map of the Souš water-supply tunnel. Klomínský et al. (2005).
Green fractures with clay filling, blue – quartz veins, red – trachyandesite and aplite dykes.

for follow-up studies of underground radioactive waste repository candidate areas and localities, as well as to describe and demarcate the geological barriers assisting to retard or reduce radionuclide migration from the repository into the biosphere. The long-term monitoring of the hydrogeological regime, temperature conductivity and recent micro-displacements of the tectonic network in the Bedřichov water-supply tunnel provides input data for models of granite fracturing, groundwater transport and the evolution of tunnel stability in a granite massif.

The Bedřichov water-supply tunnel (sections A and B) was built in 1981–1987. The tunnel, with a total length of about 6780 m and circular diameters of 3.6 m (section A) and 2.1 m (section B), were driven into the Liberec and Jizera Granite as much as 200 m below the surface (Fig. 5.1.4). Two different technologies were used to drive this tunnel. About one third of section A was driven in a classical destructive way and the other two thirds were driven non-destructively using DEMAG (TBM) type tunnelling technology (Fig. 5.1.5.). An iron water pipe with diameters of 80 cm (section A) brings the raw water from the Josefodol water dam to the water treatment plant in Bedřichov and trought the water pipe in diameter of 60 cm drinking water runs through the tunnel section B to the central tank in outskirts of Liberec City.

Bedřichov water-supply tunnel section A is part of the water-supply system for the water-treatment plant in Bedřichov transporting water from the Josefův Důl dam to the processing plant Klomínský and Woller 2010). The tunnel axis is linear with an azimuth of 70° and 1.562 % incline to the west. The length of section A is 2600 m including the section below the water level of the dam. The height of the tunnel overburden fluctuates between 26 m and 141 m (except portal gate sections) with a mean value of 90–110 m and the tunnel at 800 m from the portal lies at the maximum depth below the surface of 141 m (Fig. 5.1.4. and 5.1.5.).

The temperature and humidity of air in the Bedřichov water-supply tunnel was regularly monitored in 2005–2007. Temperature measured at 100, 800, 2000 and 2450 m from the western tunnel portal fluctuates in a narrow range from 6.5 to 4.5 ºC.

Figure 5.1.4. Topographic cross-section along the Bedřichov water-supply tunnel – A section showing the depth of the tunnel beneath the present-day surface. Cross-section the tunnel axis. The tunnel has the inner diameter of 3.6 m. Klomínský et al. (2005).

This temperature stability is caused by the water-supply conduit, in which cold water of a stable temperature flows. The conduit functions as a cooler of the tunnel interior. The humidity of the air in the tunnel was monitored at the 800 m monitoring station and is stabilized at a level of 98 % total humidity for the major part of the year.

Bedřichov water-supply tunnel section B was constructed with TBM technology along its whole length. It transports processed water into a central underground water reservoir on the periphery of Liberec City. The Bedřichov portal of section B is situated at the bottom of a 15 m shaft next to the water treatment plant (626.34 m above sea level (a.s.l.) and its opposite portal is located next to the Hotel Orion (556,61 m a.s.l), distance of 3 670 m to the west in azimuth 87° with an inclination of 2.072 %.

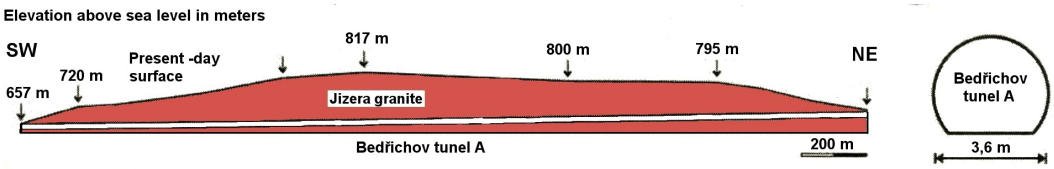

Figure 5.1.5. Bedřichov water-supply tunnel – section A. Klomínský and Woller (2010). 1 – boundary of bored and blasted sections, 2 – concrete casing with no infiltration of groundwater, 3 – concrete casing of tectonic zone with sinters and stalactites of newly formed calcite, 4 – blasted section with uneven and bare tunnel walls.

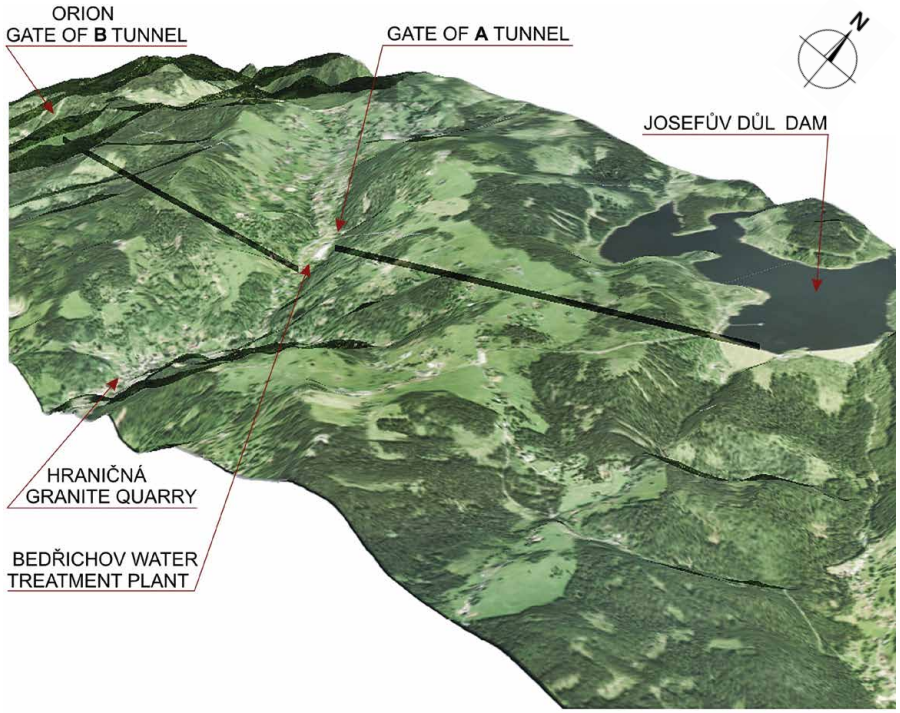

Figure 5.1.6. Topography and morphology of the area around the Bedřichov water-supply tunnels. Klomínský and Woller (2010).

Thickness of the tunnel overburden fluctuates between 66–194 m (except portal gate sections) with a mean value of 100–140 m. At 2035 m from the eastern portal tunnel section B lies at the maximum depth below the surface.

5.2 Geology of the Bedřichov water-supply tunnels (section A and B)

The Bedřichov water-supply tunnel of over 6 km in length penetrates both major granites of the Jizera and Liberec types of the KJCM (5.1.1.). Magmatic structures in both granites are represented by mostly planar schlieren, magmatic folds and gravity-dependent structures. The dominant set of fractures trending NE-SW and NW-SE (in terms of joint abundance) displays an orientation of 22–55/70–90° SE and 120–150/75–90° NE (Fig. 5.2.1.). These two orthogonal systems are developed regularly throughout the area, without any lateral or vertical gradient in distribution and frequency of fractures. The exfoliation planes in the near-surface zone, which has a limited continuation in the interior of the granite massif, represent the youngest set of fractures (see Fig. 4.2.1.).

Rock lithology in the Bedřichov water supply tunnel section A

Section A of the Bedřichov water-supply tunnel is mostly located in the distinctly porphyritic, medium-grained to coarse-grained biotite Jizera Granite. Fine-grained to

medium-grained granite makes up a minor lithology in the form of local bands close to biotite-rich schlieren. Dykes of aplite, aplopegmatite and medium-grained leucogranite are relatively common in certain parts (Fig. 5.2.1.). Three dykes of olivine basalt, 0.3 to 2 m wide, were exposed in section A of the tunnel at locations 817–846 m and 872–875 m from the Josefův Důl dam. All the basalt dykes are covered by a concrete casing. In addition, two dykes of basaltandesite (melaphyre) 30 and 20 cm wide and strongly hydrothermally altered occur at location 130 m from the tunnel SW portal.

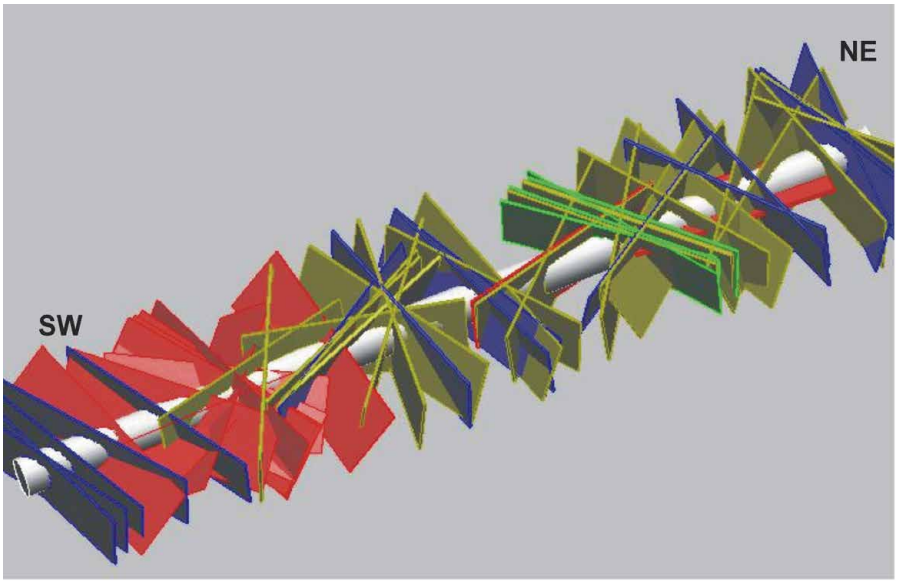

Figure 5.2.1. Model of the tectonic network in the Bedřichov water supply tunnel section A (view from the southwest). Klomínský et al. (2005).
Red – aplite dykes, blue – quartz veins, green – dykes of Cainozoic basalt, yellow – zones of mylonitization and cataclastic crushing.

Generally, the tectonic disturbance of the granite massif exposed in section A is considered slight or weak. Relatively long sections of fresh and very strong granite (20 to 90m long and exceptionally 256 m long) alternate at short intervals, exhibiting widely-spaced fracturing (10 to 40 m, exceptionally 256 m), along with relatively long intervals of granite exhibiting moderate to strong fracturing and numerous tectonic zones. The granite in these zones is densely fractured and in places shows brittle cataclastic deformation grading locally to sand-like incoherent material. In such locations the rock shows kaolinization and chloritization of variable intensity.

Clay-bearing and kaolinitic material fills the fractures and voids between the rock fragments so that certain narrow tectonized zones include material similar to sand-clay soil. Some fault zones include segments of cataclastic or mylonitic granite. Domains filled with grey to dark grey fine-grained material comprising crushed feldspars, quartz and chlorite vary from several centimetres to 20 cm in width. Any strong alteration of minerals is accompanied by the reddish colouration of K-feldspars, the kaolinization of feldspars and the chloritization of biotite; iron oxi-hydroxides and hematite partly impregnate altered rocks.

Individual fractures were opened up at some point in geological history, as indicated by mineral filling (Fig. 5.2.2). The width of quartz, calcite, ankerite, chlorite, and clay veinlets typically varies from less than 1mm to 10mm. Fault zones are sometimes accompanied by quartz veins several millimetres to 30 cm in width. Variations and transitions from fractures just millimetres wide to tectonic zones 200 to 400 cm wide can be observed at locations 2174 and 2155 m from the Josefův Důl water dam.

Seventy-five tectonic zones of widths exceeding 57 cm have been documented, including 29 zones wider than 100 cm. Three approximately perpendicular sets of joints are evident in close proximity to section A. The most prominent set of joints (in terms of joint abundance) displays an orientation of 22–55/70–90º SE. The second most significant joint set displays 120–150/75–90º NE.

Oriented dykes of Cainozoic basalt and the majority of veins of hydrothermal quartz lie parallel with this system. Along the whole length of the tunnel moderately densely packed sub horizontal joints can be found tending E-W with a shallow dip of 0–30° to the south and north.

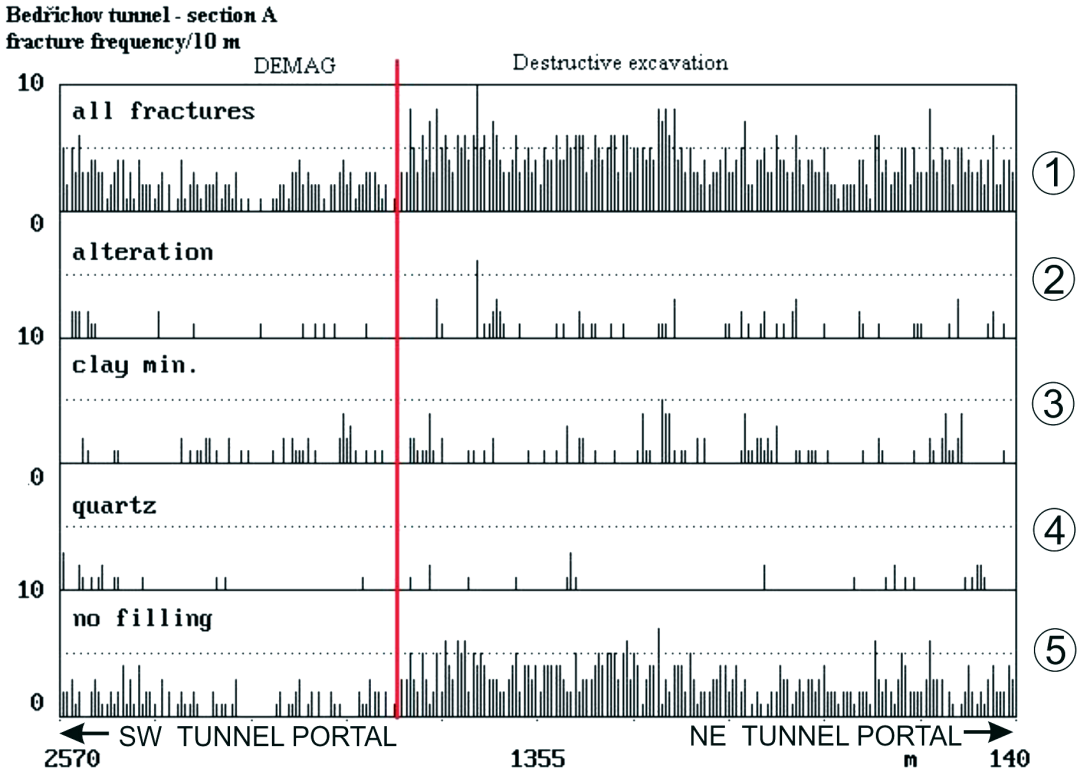

Figure 5.2.2. Bedřichov water.supplytunnel section A – map of fracture network with fractures classified according to the type of fracture filling. Klomínský and Woller (2010). 1 – all fractures, 2 – hydrothermal alteration, 3 – fractures filled by clay and accompanied by cataclastic deformation, 4 – quartz veins, 5 – no filling (open fractures); red vertical line – boundary between TBM excavation technology and blasting method.

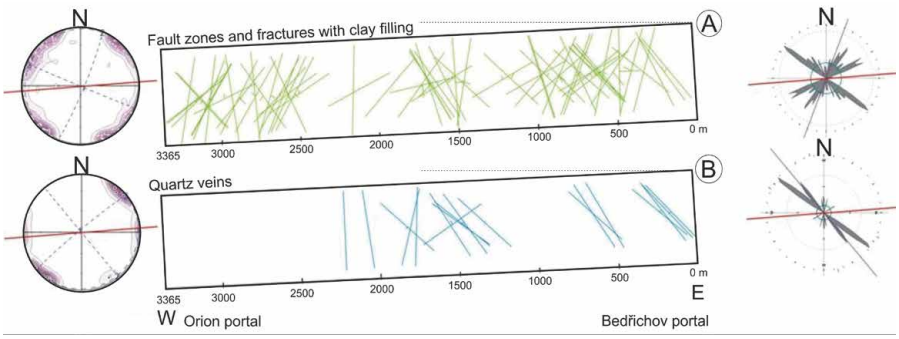

Figure 5.2.3. Diagrams of fracture networks in the map of the Bedřichov water-supply tunnel section B. Klomínský et al. (2005). Black – all fracture structures, green – fractures with clay filling, blue – quartz veins.

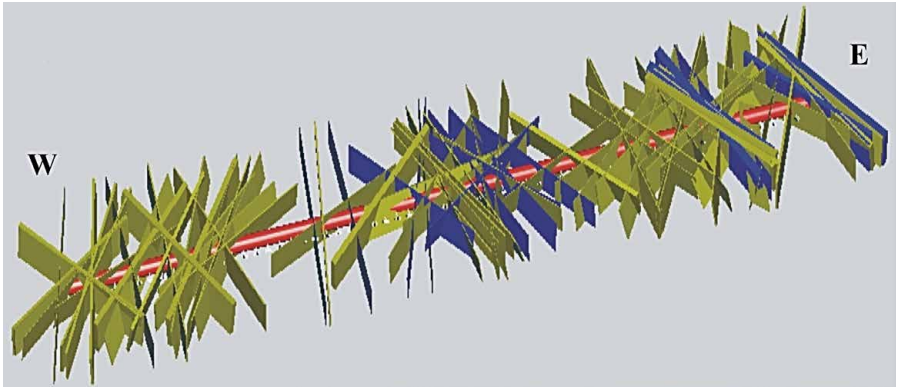

Figure 5.2.4. Model of the major structures in the Liberec Granite in the Bedřichov tunnel section B. Klomínský et al. (2008). Yellow – cataclastic structures, blue – quartz veins.

Bedřichov water supply tunnel section B mostly intersects porphyritic medium to coarse grained biotite granite (Liberec Granite). The NE boundary of this granite is demarcated by a swarm of quartz veins 14 to 105 m (azimuth 120–135/85–85 and thickness10–30 cm) from the eastern tunnel portal (Fig. 5.2.3.).

Tectonic fracturing of the granite is overall moderate or weak. Long sections of the fresh and sparsely fractured granite (20–90 m) alternate with shorter sections (10–40 m to maximum 110 m) where the granite is moderately to densely fractured and penetrated by numbers of tectonic zones.

These fault zones are frequently filled by quartz veins from several mm to 30–40 cm in thickness and sporadically up to 110 cm between 516–527 m from the NE portal (Fig. 5.2.4.). There are 84 quartz veins and fault zones with a thickness of 10 cm and more. There are 29 fault zones with a thickness over 100 cm. Bedřichov tunnel section B is abundant in groundwater resources. An estimate of the total groundwater outflow from the tunnel was 410 l/min in 1984.

In both sections of the Bedřichov water-supply tunnel there are frequent carbonate veinlets only several millimetres wide. Some of them have a zoned structure with quartz along the margin and a central carbonate fill. Zoned carbonate veins carry calcite at the margin and ankerite, siderite or rhodochrosite in the centre.

Magnetic susceptibility of the Jizera and Liberec Granites in Bedřichov water-supply tunnel sections A and B

Magnetic susceptibility (MS) is one of the quantitative parameters for the field discrimination of the Jizera and Liberec Granites (Klomínský ed. 2008). This petrophysical parameter represents the amount and proportion of paramagnetic biotite and ferromagnetic minerals, probably magnetite, in the granites. MS values $> 0.5 \cdot 10^{-3}$ SI are characteristic for the Liberec Granite, whereas values $< 0.5 \cdot 10^{-3}$ SI are typical for the Jizera Granite. MS mapping in both sections of the Bedřichov water-supply tunnel was used to detect the gradual boundary between the Jizera and Liberec Granites. Magnetic susceptibility (MS) in both sections of the tunnel was measured by portable kappameter SM-20 at 1 to 2 metres spacing on the NW wall of section A and on the S wall of section B. Gaps in MS measurements represent missing data. In Figs. 5.2.5. and 5.2.6. the data trend indicates partly gradual fluctuation and partly leaps of the MS values from $< 0.12 \cdot 10^{-3}$ SI in the NE end of section A to $1.5 \cdot 10^{-3}$ SI at the Orion portal of the Bedřichov tunnel. According to the MS data, the Jizera and Liberec granite boundary can be demarcated in the middle of the Bedřichov tunnel section B around 2300 m from the Bedřichov portal, where MS values permanently jump up above $0.5 \cdot 10^{-3}$ SI (Fig. 5.2.6.). This demarcation line of the Jizera and Liberec Granites corresponds with some petrographic parameters such as decrease of the number K-feldspar phenocrysts per m^2 and their triclinity (Fediuk in Klomínský et al. 2005).

Systematic magnetic susceptibility fluctuation along sections A and B, in combination with size of the K-feldspar phenocrysts and their density, allows construction of a model of the gradation contact between the Liberec Granite on ground and the Jizera Granite declining in a shallow angle towards the North (Fig. 5.2.7.). Both granites are separated by a 100m thick layer of transition zone represented by granite having magnetic susceptibility at the lower limit for the Liberec Granite

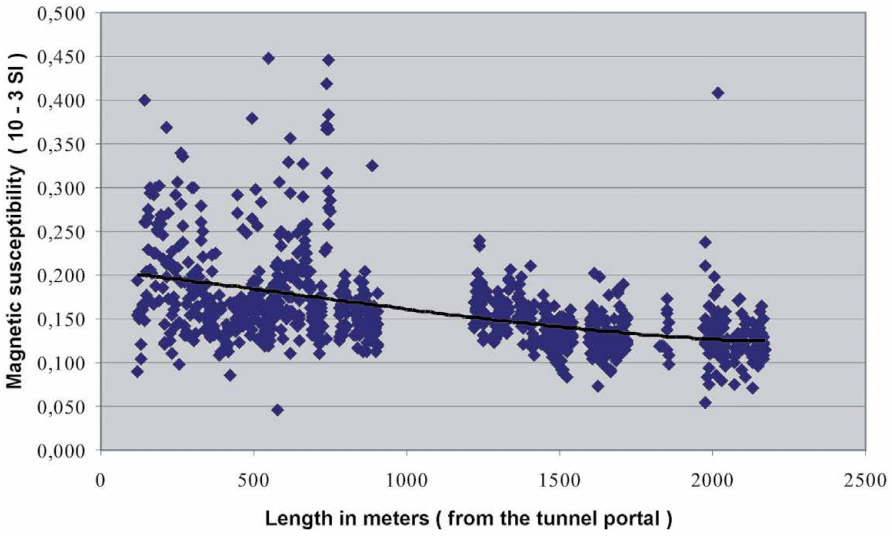

Figure 5.2.5. Fluctuation of magnetic susceptibility of the Jizera Granite in the Bedřichov water-supply tunnel section A from the Bedřichov portal (0 m) to the Josefův Důl Dam (2500 m). Klomínský and Woller (2010).

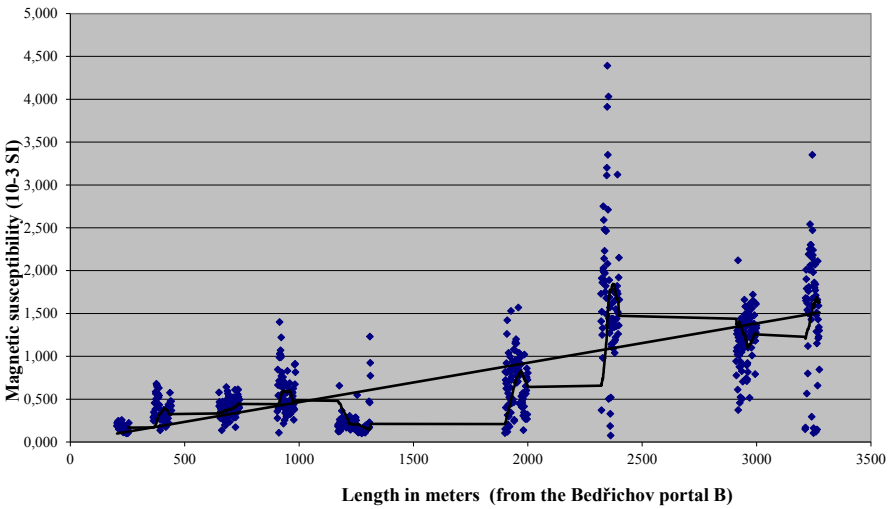

Figure 5.2.6. Fluctuation of magnetic susceptibility of the Liberec Granite in the Bedřichov water-supply tunnel (section B) from Bedřichov portal (0m) to the Orion portal (3500 m). Klomínský et al. (2005).

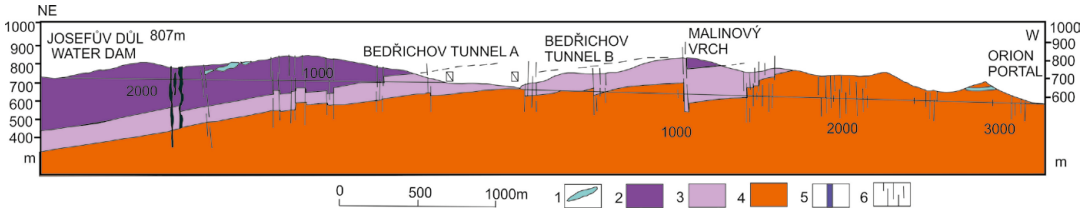

Figure 5.2.7. Model of the geological profile along the Bedřichov water-supply tunnel (A and B sections) based on the magnetic susceptibility survey and K-fedspar phenocrysts measurement. 1 –Fojtka Granitoids, 2 – Jizera Granite, , 3 – Transitional Granite (marginal facies of the Liberec Granite), 4 – Liberec Granite , 5 – Basaltoid dykes, 6 – tectonic zones.

and the upper limit for the Jizera Granite (about 0.5 . 10^{-3} SI) in combination with size of K-feldspar phenocrysts characteristic of the Jizera Granite.

Anisotropy of the magnetic susceptibility (AMS)

Anisotropy of the magnetic susceptibility (AMS) was studied in part of section A between locations 120m from portal. The mean susceptibility of Jizera Granite in this section is from 120.2 to 893.5 × 10^{-6} [SI]. The AMS is due to the presence of both paramagnetic biotite and ferromagnetic minerals, probably magnetite. The degree of anisotropy, 1.007–1.239, and a shape parameter of between 0.827 and 0.958, indicate both linear and planar fabric. Magnetic foliations are somewhat homogeneously oriented and dip steeply to the NE or SW. Magnetic lineations are largely sub horizontal and tend to the NW or SE.

The magnetic fabric of granite (due probably to magnetite) is different from the fabric of K-feldspar phenocrysts. AMS analysis indicates that the magnetic fabric probably records the last increments of deformation before the final crystallization of the granite.

Orientation, density and kinematics of fracture systems in the Bedřichov water-supply tunnel section A

The analysis and classification of structural data included 5,500 readings from both parts (sections A and B) of the Bedřichov water-supply tunnel, from the point of view of deformation kinematics and stress field orientation (Fig. 5.2.8 and 5.2.9). Fresh fracture planes identified as having formed in the process of tunnel excavation, mainly during blasting, were removed from the data set. These discontinuous, small to moderate size planes with a coarsely structured or moderately coarse surface were processed separately. The planes are largely steep, tending ENE-WSW (parallel to the tunnel wall) or NE-SW (at an angle to the tunnel wall).

The natural joint network in the granite massif in the Bedřichov water-supply tunnel area shows three distinct maxima: steep joints tending NW-SE, NE-SW and N-S (mainly in tunnel section B). The formation of the steep joints tending NE-SW and NW-SE cannot be explained solely by contraction fracturing in the process of the cooling of the massif. It is obvious that joints with these orientations were formed and re-activated later in the history of the granite massif. The fractures tending NW-SE and N-S often carry a newly formed mineral fill. This indicates a significant extension component in the activity of the fractures. In contrast, fractures tending NE-SW exhibit mineral filling only exceptionally and indicate association with brittle cataclastic zones which could indicate the activity of shear displacements. There is a significant difference in typical intervals between the joint planes: the NW-SE joints are densely spaced with intervals of 10–20cm, joints tending NE-SW have typical intervals of 200–210cm.

Fracture and joint spacing

One-dimensional spacing data were collected along the examined section of the tunnel wall of the section A (120–320 m from SW portal). The scan-line was thus 200 m long and its azimuth was 64° (azimuth of the tunnel). We consider only joints or veins attributed to one of the two regional sets; other non-systematic joints were excluded from this analysis. We present Terzaghi-uncorrected data; the "true" joint spacing could not be exactly determined as the adjacent fractures are not parallel and their orientations vary even within a single set. However, given that the scan-line is linear and of constant direction, the data obtained allow comparison of spacing characteristics of the two regional fracture sets.

The results indicate that both sets have irregular spacing ranging from several centimetres to metres. Most of the spacing values of fractures of the NW-SE set fall in the range of 10 to 100 cm; spacing greater than 120 cm is much less frequent. Mean spacing is 131 cm; mode is 12 cm. Spacing values of the NW-SE set show a clustered distribution. On the other hand, the NE-SW set is characterized by more widely spaced fractures with mean spacing 415 cm and mode 490 cm. The frequency distribution is approximately uniform. The spacing characteristics of the two regional joint sets thus differ significantly; the NW-SE fractures are more abundant and tend to be more closely spaced than the NE-SW fractures, which is in line with the orientation distribution statistics shown in the rose diagram in Fig. 5.2.8.

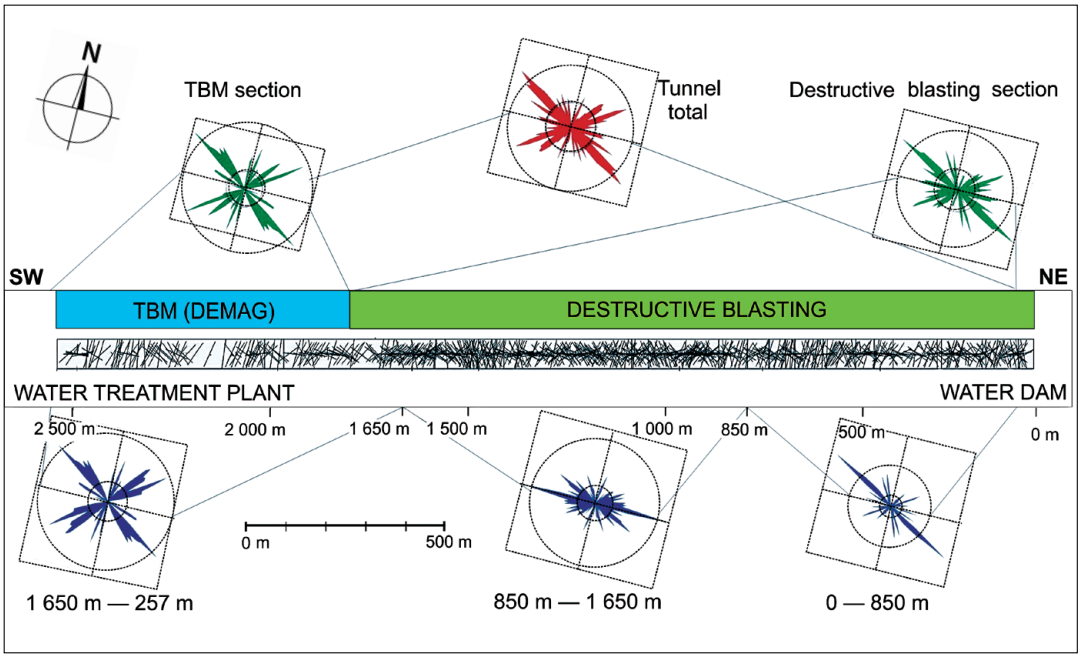

Figure 5.2.8. Diagrams of fracture networks in the A section of the Bedřichov water-supply tunnel with the preferred orientation and according to their characteristics in the three tunnel sections. Klomínský and Woller (2010).

Dilatation of the Jizera Granite in the Bedřichov water supply tunnel section A

The frequency of joints and tectonic zones shows two maxima, at azimuth values 40° and 130° (Fig. 5.2.8. and Tab. 5.2.1.) The extension of the granite massif culminates at azimuth 120 – 150° (approximately 40 m) with a maximum of 140° (11 m) and in the interval 10 – 60° (approximately 43 m) with a maximum of 40° (approximately 10 m). These partial figures indicate that fillings classified as cataclastic zones (approximately 75m) dominate. The second location corresponds to quartz veins (14.3 m), followed by aplite dykes (7.3 m) and basalt (3.1 m). The total combined width of the fillings in the 2.6 km long tunnel section A is approximately 100 metres. This suggests an expansion of the granite massif during its post-magmatic history of 4% of its total volume.

The partial totals indicate that the greatest width reached by fillings classified as cataclastic zones is around 75 metres. In second place are quartz veins (14.3 m), followed by aplite dykes (7.3 m) and finally basalts (3.1 m). The total width of filling materials in the 2.5 km section A is around 100 metres. This value suggests that this particular part of the granite massif probably expanded during its postmagmatic history. This situation could be caused by the following processes:

- Contraction of the intrusive body due to cooling,
- Dilation of granite due to hydraulic fracturing in the process of heat release from the granite heat production,

Table 5.2.1. Width of fractures and tectonic zones and their filling in the A section of the Bedřichov tunnel according to their trend (azimuth interval 10º, width in cm). Klomínský and Woller (2010).

Filling / azimuth	10º	20º	30º	40º	50º	60º	70º	80º	90º
quartz+crushing+alteration	20	20	0	60	0	5	0	0	0
mylonitization+cataclasis	550	609	678	934	548	800	87	119	161
aplite dykes	2	0	3	8	3	70	0	455	0
basalt dykes	0	0	0	0	0	0	0	0	0
Total width	**572**	**629**	**681**	**1002**	**551**	**875**	**87**	**574**	**161**

Filling / azimuth	100º	110º	120º	130º	140º	150º	160º	170º	180º
quartz+crushing+alteration	0	18	2	265	325	396	12	110	0
mylonitization+crushing	42	187	937	395	681	548	56	341	5
aplite dykes	1	27	10	25	77	5	70	0	0
basalt dykes	0	0	295	15	0	0	0	0	0
Total width	**43**	**232**	**1244**	**700**	**1083**	**949**	**138**	**451**	**5**

- Dilation of the water saturated fractures due to cryogenic (permafrost) conditions.
- Drop in hydrostatic pressure due to prograding erosion of the granite massif,
- Tectonization of the granite massif caused by imposed stress (e.g. dynamics of episodic earthquakes).

The cataclastic zones belong to the youngest tectonic structures disturbing the coherence of the granite massif. Their prevalent width indicates intensive tectonization of the massif during the last stage of its geological evolution, approximately the last several million years.

Palaeostress of tectonic network in tunnel section A

Palaeostress analysis shows that the whole fault system is heterogeneous and evolved by means of the superposition of deformation events rather than via a single stress field. Dominant effects show the stress field is characterized by a sub horizontal position or shallow plunging of the σ_1 axis tending ENE-WSW and the sub horizontal or shallow plunging of the σ_3 axis tending NNW-SSE (Fig 5.2.10.).

Position of the Bedřichov water-supply tunnel section A in the tectonic network models of granite massif

The natural joint (fracture) network which crosscuts the porphyritic medium-to coarse-grained biotite granite (Jizera and Liberec Granite) in the Bedřichov water-supply

tunnel area is characterized by three distinct trends (two of which are perpendicular to one another): steep planes in the NW-SE, NE-SW and N-S directions. The steep fractures in the NW-SE and N-S directions were healed much more frequently and contain filling which is indicative of the important extensional character of the activity of these structures. The planes running along the NE-SW direction, on the other hand, were healed only exceptionally; in contrast, accompanying crushed zones are more common which could point towards an activity associated with shear displacements.

The correlation of the azimuth of the tunnel sections with the tectonic network is an important step in the evaluation of construction stability of the tunnel sections and in minimizing the costs of tunnel maintenance. The position of section B of the tunnel is very near to the proposed orientation with respect to the tectonic network. On the other hand, the azimuth of section A is at 13º anti-clockwise to the orientation of tectonic network (Fig. 5.2.10.). The optimal azimuth is similar for both tunnel sections at 83º–88º.

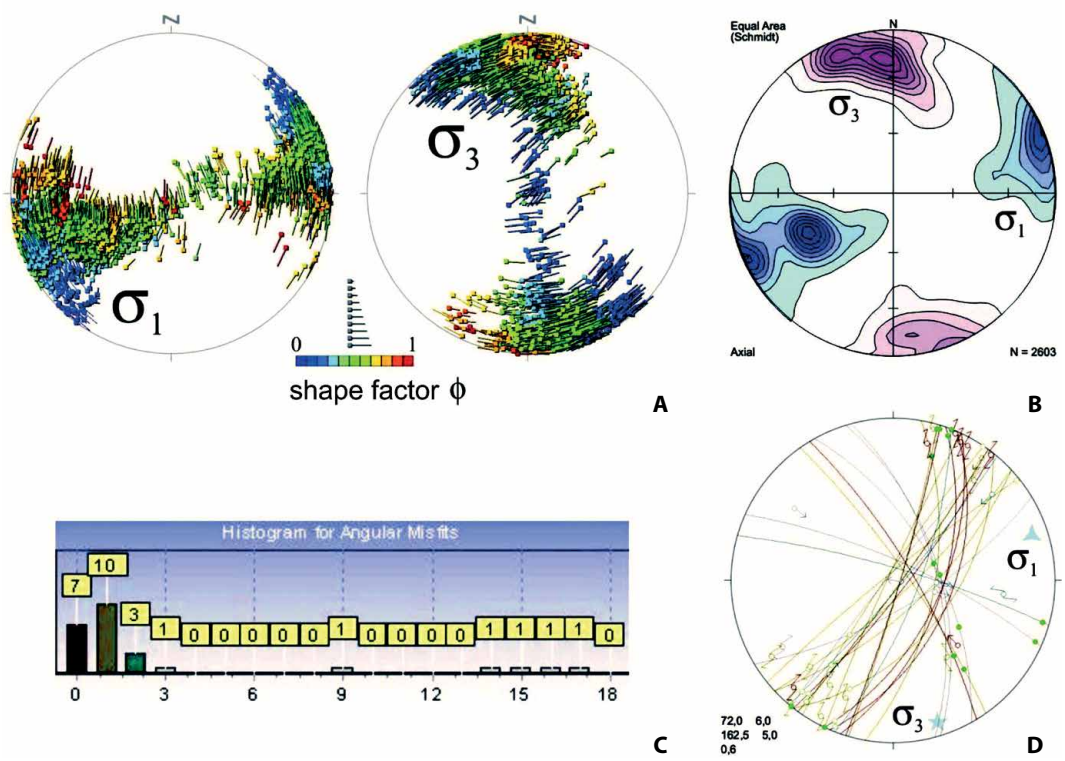

Figure 5.2.9. Results of palaeostress analysis of fractures with striations in section A of the Bedřichov tunnel. Klomínský and Woller (2010). A – Diagram of 2603 partial solutions obtained by the method of multiple inversion. B – contour diagram of σ1 and σ3 orientation for 2603 partial solutions; C – diagram of angular deviations between theoretical and measured glide vector on fractures (faults) for solution σ1 = 72/6, σ3 = 163/5, shape factor σ = 0,6; D – diagram of analysed fractures and their relation to the solution σ1 = 72/6, σ3 = 163/5, shape factor σ = 0,6, which fits 20 out of 26 analysed faults.

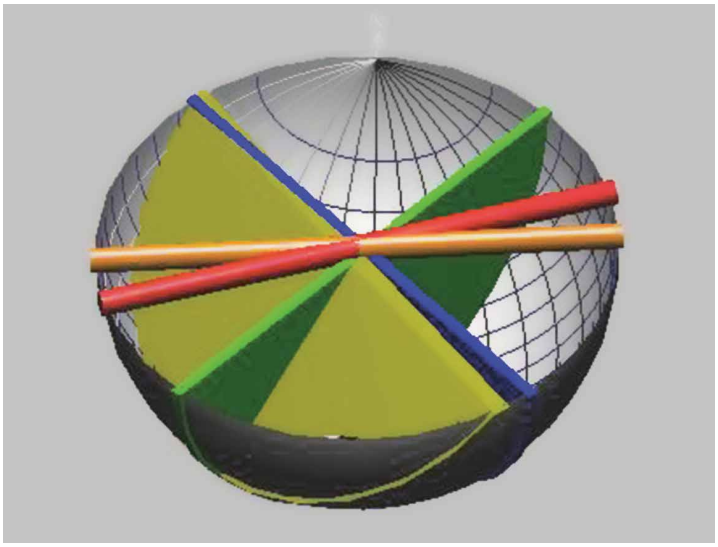

Figure 5.2.10. Tunnel section A azimuth (red). Proposed azimuth of tunnel section A (yellow) with respect to the tectonic network of the granite (L joints – yellow green, Q joints – blue, S joints – green) in the lower hemisphere projection. Klomínský and Woller (2010).

5.3 Spatial visualisation of the Bedřichov tunnel section A wall topography

The available digital technology of panoramatic scanning permits transformation of surface irregularities on the exterior surface. 2.5 D visualisation of section A of the Bedřichov water supply tunnel is an example of documenting the tunnel surface. Models of the tunnel walls represent application of this method to underground constructions. The model depicts a 27 metres long section at the boundary of the drilled and blasted part of the tunnel (12 m and 15 m) in Fig. 5.3.1. The laser scanning method is based on measurements with a laser beam. The recorded data include distance and horizontal plus vertical angular position of the laser beam. The polar co-ordinates are transformed to the Cartesian system of X, Y and Z co-ordinates (Klomínský, Woller eds 2010).

The procedure of 2.5 D visualisation of the tunnel surface included the following steps:

- Panoramatic scanning of the tunnel walls with the RIEGL LMS-Z360i scanner in bands 11.5 m wide with 50% overlap. The laser instrument produces a spot model and images of the scanned object with a digital camera with a high resolution. The accuracy of distance measurement is ± 6 mm with a speed of measurement of 812,000 points/s. The total number of points in the measured part of the tunnel is 1,865,694. The point density is 0.005 m. The trace dimension of the laser beam on the tunnel wall is around 4 × 3.5 mm.
- Calibration of the projection centre of the digital camera and colour coding of laser spots.
- Conversion of "laser clouds" into a spot model (876,039 spots between the locations of 880 and 892 m in from SW portal tunnel section A the part driven by drilling, and 989,655 spots between the locations of 892 and 907 metres in the part driven by blasting.

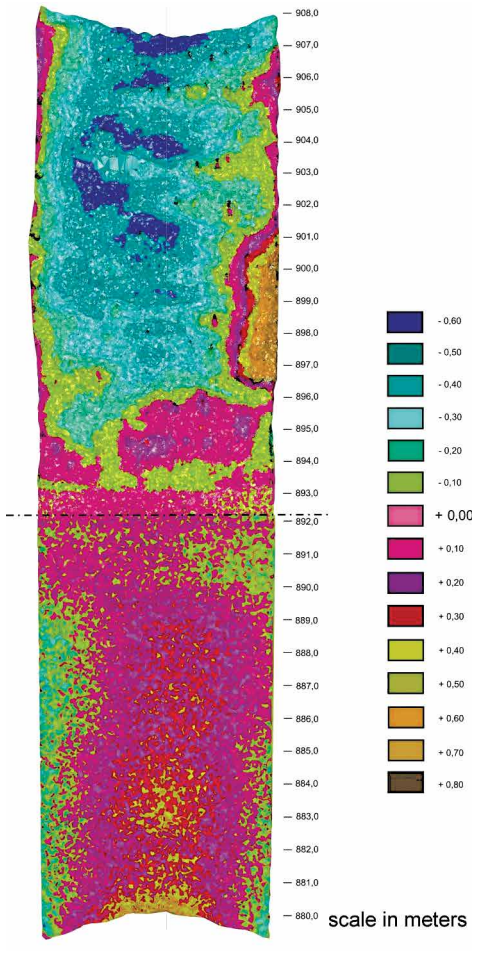

- Deconvolution of the "laser clouds" onto a plane with (hypsometric) isoline visualisation of 2.5 D surface in the drilled and blasted parts of the tunnel, with isoline step of 3 cm or alternatively 10 cm.
- Distance between the individual spots and the tunnel axis was calculated from the laser data.
- A coloured isoline map of the deconvoluted surface of the tunnel with hypsometric visualisation from a cylindrical reference surface was projected on the surface of a rotational cylinder. The resulting 2.5 D models were derived with the use of the Phong method.
- 2.5 D models of the tunnel wall morphology. Data were loaded separately for the blasted and drilled parts of the tunnel into the Voxler program (Golden Software Company) and visualized at various scales for both drilled and blasted parts of the tunnel.

The 2.5 D model of the tunnel wall morphology produced from results of laser measurements is presented in Figs. 5.3.2 and 5.3.3.

A comparison of hypsometric maps of the drilled and blasted tunnel parts shows a similar asymmetry in orientation of the ceiling axis in relation to the general tunnel axis. This deviation toward the east is around 57° and it can correspond to orientation of the magmatic fabric of granite (e.g. orientation of the longer axis of K-feldspar phenocrysts). The transverse ridges in the ceiling

Figure 5.3.1. Isoline presentation of the uneven surface of the tunnel wall in the blasted section of the Bedřichov water-supply tunnel A section (top) and the drilled part (bottom). Klomínský and Woller (2010). The hypsometry data document uneven surface in the range of –0.60 m to +0.80 m with isoline step of 3 to 10 cm. The absolute height exaggeration in tunnel morphology is 1.75 m.

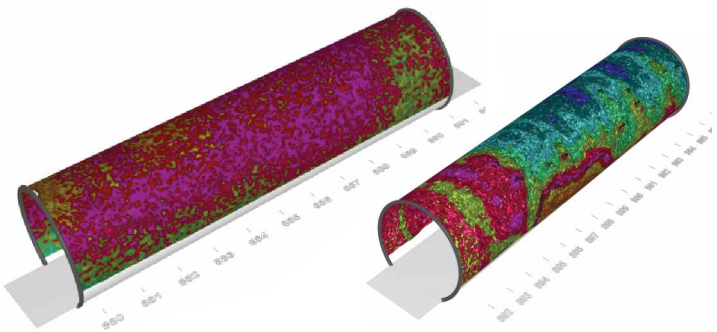

Figure 5.3.2. Contour map layout on the tunnel A section model of the TBM section (left) and the blasted section (right). Klomínský and Woller (2010). Hypsometry represents the tunnel wall morphology in range from +0,99 m to –0,73 m with contour space of 10 cm (maximum drop in the tunnel wall morphology is 1.75 m).

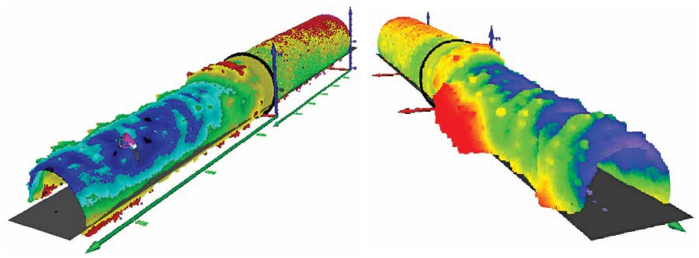

Figure 5.3.3. 2.5 D model of the Bedřichov water-supply tunnel A wall morphology. A view from the north (in left picture) and from the west (right picture). Klomínský and Woller (2010). Colours represent differences in the tunnel wall morphology. Blue colour shows rock spurs into the tunnel and red colour represents spurs out of the tunnel or asymmetric tunnel profile widening.

morphology of the blasted part of the tunnel are caused mainly by location of the individual sets of drill holes.

5.4 Spacial visualisation of the geological scene of the tunnel section A walls

The present digital technology permits transformation (projection) of a geological picture of tunnel walls on its exterior surface (Klomínský et al. 2008). 2.5 D visualisation of a section of the Bedřichov water-supply tunnel section A wall is presented as an example of this method. Projection of lithological boundaries, ductile structures, brittle deformation or hydrothermal alteration phenomena provides a new kind of information on the structure and state of the granite massif containing the tunnel. This kind of model of the tunnel represents the first use of this geological-structural technology for mapping in the Czech Republic (Kopačková and Klomínský 2012). The sequence of visualisation is presented in Fig. 5.4.1.

The 2.5 D visualisation of geological situation on the tunnel walls includes the following steps:

- Covering the tunnel wall with a square network of reference points with steps of 1 × 1 m,
- Taking pictures of the individual squares by digital camera with resolution of 2560 × 1920 pixels,
- Joining of the individual pictures into bands oriented normally to the tunnel axis, representing bands 6.5 m long and 1 m wide,
- Adjustment of colours and contrasts within photo bands,
- Joining of the individual bands into a seamless photo mosaic with a total surface of 6.5 × 11 m of the tunnel surface,

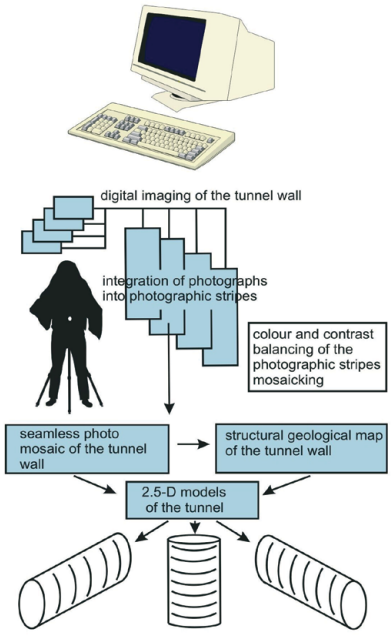

Fig. 5.4.1. Diagram of the sequence of steps in 2.5 D visualisation of geological situation of the wall of the Bedřichov water-supply tunnel. Klomínský et al. (2008).

- Formation of deconvoluted image of the inner surface of the tunnel wall in the Corel Photo-Paint program (Fig. 5.4.2.),
- Formation of deconvoluted geological-structural map of the inner surface of the tunnel wall on the background of the "seamless" photo mosaic,
- Inversion of the photo mosaic and the digital image of the geological-structural map of the tunnel wall in the Corel Photo-Paint program on the exterior side of the tunnel wall,
- Construction of 2.5-D models of the tunnel in the MicroStation program as an orthogonal projection of the exterior image of the tunnel ceiling, left and right wall,
- Transfer of the photo mosaic and the digital image of the geological-structural map onto the surface of 2.5 D body of the tunnel in the JPEG true colour format with 5000 × 2270 pixels. The resulting 2.5-D pictures were formed via rendering by the Phong method (Fig. 5.4.3.).

The "seamless" photo mosaic of the inner side of the tunnel (Fig. 5.4.2.), comprising around 72 pictures, has a size around 6.5 × 11 metres and represents about 60 % of its segment from the margin of the concrete pathway along the NW tunnel wall up to the upper margin of the waterworks pipe next to the SE wall.

The section A wall exposes the Jizera Granite (dark grey background) with abundant lithological inhomogeneities of magmatic origin. Swarms of biotite-rich schlieren (dark red areas and light blue lines) and abundant nests of enclaves (blue and green) accompanied by hybrid granitoids (violet and brick-red areas) are arranged in two fold structures of a rather complicated shape (Fig. 5.4.2.). The youngest members are sills and nests of pink aplite grading to aplopegmatite (yellow areas).

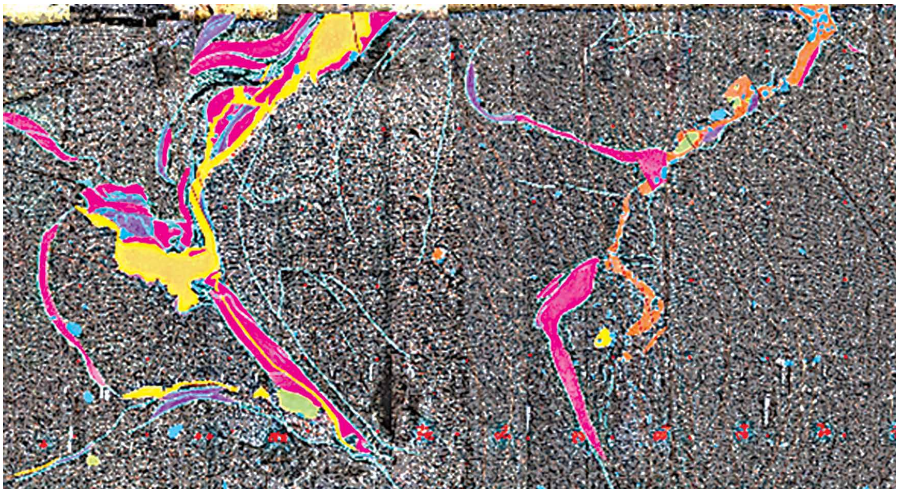

Figure 5.4.2. A "seamless" photo mosaic of the tunnel A wall deconvoluted onto a plane with dimensions of 11 × 6.5 m and with projection of the geological structures as viewed in vertical direction from outside of the tunnel, at the location 203 to 215 metres from SW portal of the tunnel section A (the upper edge of the image depicts the water-supply pipe, the lower edge corresponds to the tunnel floor). Klomínský and Woller (2010). Orientation of the photo mosaic: NE at the left, SW at the right. Red medium grained hybrid granite, yellow and orange aplite, pale green granite xenolith, violet melanocratic hybrid granite, pale blue schlieren.

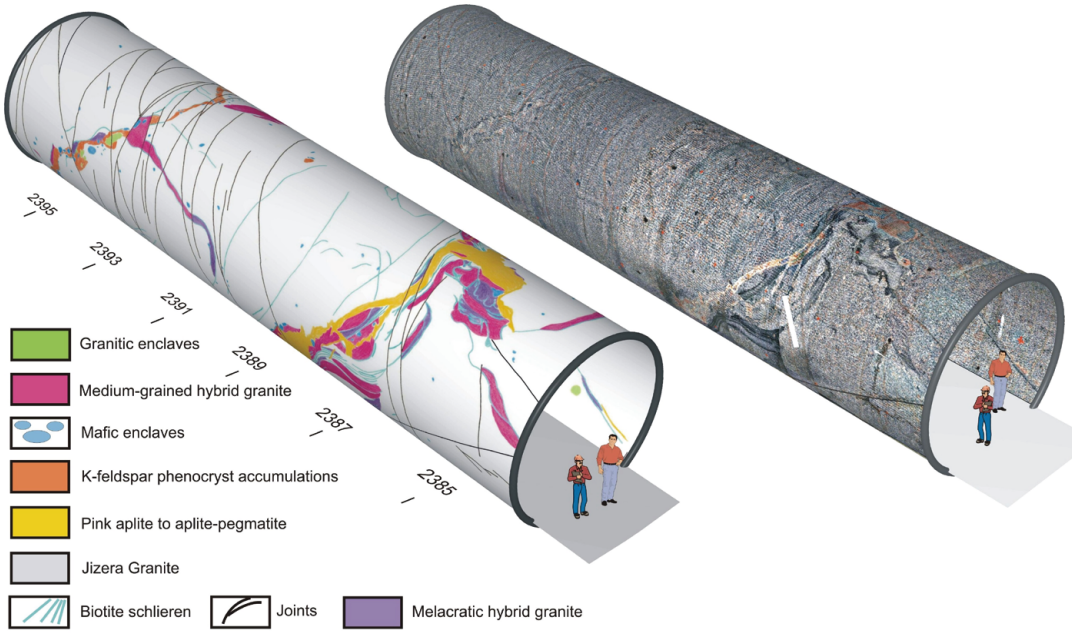

Figure 5.4.3. 2.5-D models of the geological image of the tunnel A wall and the projection of the digital internal surface image of the tunnel on the outer surface of the tunnel in true colours (right picture) projected on surface of rotational cylinders. Klomínský and Woller (2010). The tunnel walls consist of the porphyritic biotite granite of the Jizera type) with abundant lithological heterogeneities of magmatic origin. The swarms of biotite-rich schlieren and nests of numerous enclaves accompanied by hybrid granitoids are arranged in two fold structures of a rather complicated shape. The youngest members are sills and nests of pink aplite to aplopegmatite. The numerous nearly vertical fractures rimmed by alteration zone are locally filled by hydrothermal quartz and calcite. The light grey area is the pathway at the tunnel floor (the distance in metres corresponds to the distance from the Josefův Důl dam).

Numerous nearly vertical fractures, rimmed by zones of hydrothermal alteration, are locally filled by vein quartz and calcite. They show the same trend as the axes of magmatic antiforms (black lines). Red marks indicate one metre intervals on the tunnel wall.

5.5 Computer-based image analysis of granite alteration in the Bedřichov water-way tunnel (section A)

Recent digital photography technology permits automated processing and interpretation of pictures of geological objects down to microscopic scale (thin sections and polished sections of rocks and minerals). Due to differences in absorption and reflection of light (electromagnetic spectrum) of variable wavelength, it is possible to distinguish various rock-types and their minerals in digital pictures of geological objects. The automated analysis of images can be used for visualisation and qualitative classification of the intensity of secondary alteration of the rock-massif.

The walls of the Bedřichov water-supply tunnel consist of the Jizera Granite with abundant lithological inhomogeneities. Swarms of biotite-rich schlieren and nests of enclaves (xenoliths) accompanied by hybrid types of granite represent processes of magma movement, mixing and plastic deformation. In images of tunnel walls this magmatic structure is disturbed by a fracture network, which served for transport of hydrothermal fluids, CO_2 and groundwater during the long time interval from granite massif solidification to the present day. Veins and veinlets of quartz and carbonates document the activity of fluids.

The movement of fluids with variable composition and temperature results in alteration or destruction of the primary minerals of granite close to, and in the wider surroundings of, the fractures. The changes in mineralogical and chemical composition of the original granite result in changes in physical-mechanical properties such as strength, permeability, porosity and volume. The visual manifestation of granite alteration includes mainly colour changes. Shades of red colour indicate gradual alteration of biotite to chlorite. Red pigment of Fe_2O_3, which is formed as a by-product of biotite alteration, penetrates the altered granite via diffusion and it preferentially impregnates K-feldspar phenocrysts.

We used the method of supervised image classification employing mathematical operations with defined algorithms. This procedure examines the ability of image pixels to form clusters. Pixels of one class are located in proximity in multidimensional space, whereas pixels belonging to other surfaces have different spectral properties and can be well separated. With the use of uniformly selected parameters this approach permits identification of subtle differences in spectral properties and recognition of different surfaces. Numerous minerals, e.g. biotite, chlorite, K-feldspar, amphibole, plagioclase, can be identified in digital photographs consisting of RGB bands (red, green and blue components) in the visible part of the electromagnetic spectrum (EMS).

The sequence of the analysis of the geological picture of the tunnel walls is as follows:

- Covering the tunnel wall with horizontal reference planes parallel to the tunnel axis, with 1 m interval,
- Digital photography of the tunnel wall from a distance of 3 m in a direction perpendicular to the tunnel axis, with interval of 1 m, using adigital camera with resolution HQ 2 560 × 1920 pixels,
- Formation of seamless pictures with 5 m intervals, oriented parallel to the tunnel axis (Zoner Panorama Maker),
- Inserting 2.5 D co-ordinates of the tunnel axis in the metric system x,y (rectification, ArcGIS environment; ArcEditor),
- Production of a mosaic of the individual 5 m bands (ad 3), production of a seamless "photo mosaic" in the Erdas Imagine environment, unification of colour shades of the individual bands, illumination correction – calculation of new RGB values for pixels positioned in the photographic shade resulting from artificial illumination,
- Automated processing of the digital picture of the tunnel wall (statistical classification of the digital picture),

- Qualitative evaluation of the picture and application of artificial colours (expert classification) – Fig. 5.5.1.,
- Conversion to vector data,
- Transfer to GIS database,
- Geostatistical analysis (construction of lithological boundaries and isolines of the content of the individual minerals (intensity of granite alteration) – Fig. 5.5.2.

REFERENCES

Klomínský, J. ed. (2003): Geologická a strukturní charakteristika granitoidů z vodárenských tunelů v Jizerských horách. Etapa 2003. – MS Čes. geol. služba. Praha.

Klomínský, J. ed. (2005): Geologická a strukturní charakteristika granitoidů z vodárenských tunelů v Jizerských horách. Etapa 2004–2005. – MS Čes. geol. služba. Praha.

Klomínský, J. ed. (2008): Studium dynamiky puklinové sítě granitoidů ve vodárenském tunelu Bedřichov v Jizerských horách. Etapa 2006–2008. – MS Čes. geol. služba. Praha.

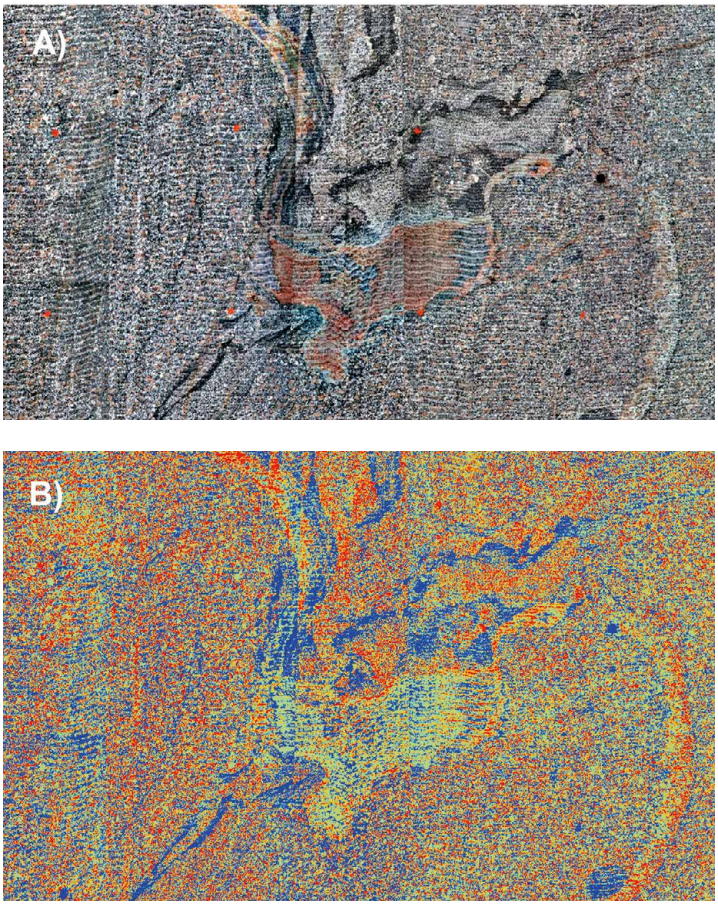

Figure 5.5.1. Qualitative (lithological) classification of the digital picture (photograph) of the wall of the Bedřichov water-supply tunnel section A (location 203 to 215 metres from SW tunnel portal. lomínský and Woller (2010).
A – Photo mosaic of the deconvoluted tunnel wall into a plane represents a picture of lithological inhomogeneities in the Jizera Granite. B – Classification of lithological elements in artificial colours: blue – biotite schlieren and basic enclaves, yellow – aplite, deep red – fine-grained hybrid granodiorite.

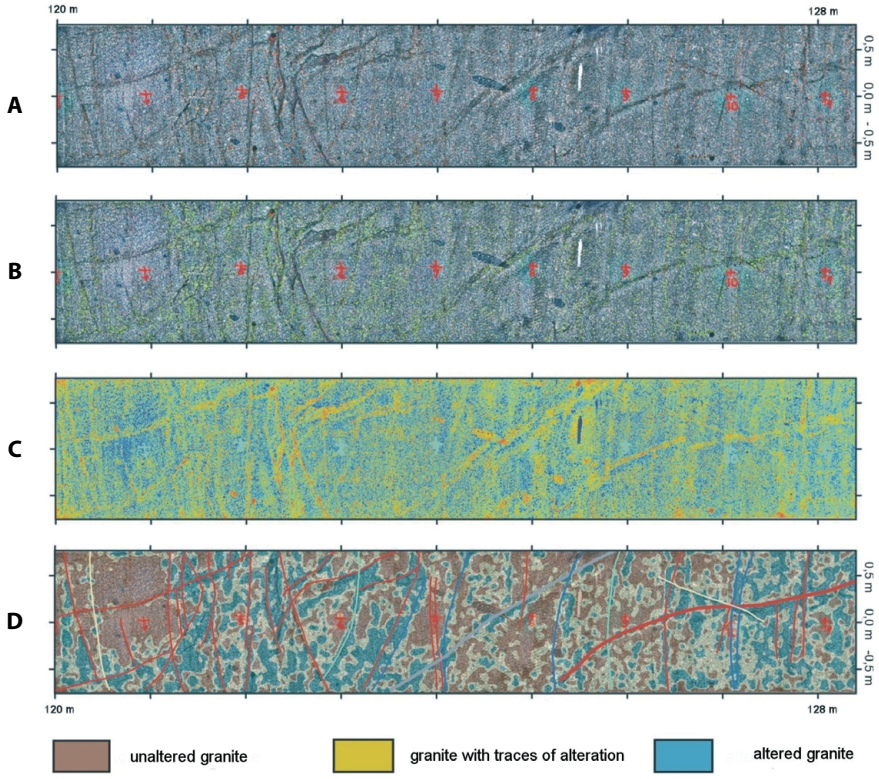

Figure 5.5.2. Qualitative classification of the alteration intensity image in the NW wall of the Bedřichov water-supply tunnel section A (location 120 to 123 m from SW tunnel portal. Klomínský and Woller (2010).
A – digital photograph of the tunnel wall, B – digital photograph of the tunnel wall with chlorite occurrence, C – automated classification of the digital picture of alteration in the tunnel wall in artificial colours, D – qualitative classification of granite alteration intensity based on distribution of chlorite (see explanation).

Klomínský, J. – Woller, F. eds (2010): Geological studies in the Bedřichov water supply tunnel. Technical report 02/2010. SÚRAO, ČGS Prague. 104 pp.

Kopačková, V. – Klomínský, J. (2012): Automatická analýza obrazu stěny bedřichovského tunelu v Jizerských horách – klasifikace intenzity alterace granitu. – Zprávy o geologických výzkumech v roce 2011, 45, 177–180.

Pták, J. (1963): Lamprofyrové žíly jizerského žulového masivu a jejich vztah ke granittektonice – Zprávy Geol. Výzk. v r. 1962. 71 – 75.

6. Mineralogy and mineralization

6.1 Garnet in the Tanvald Granite

Garnet is an uncommon accessory mineral in igneous rocks but is petrologically significant. The two-mica alkali-feldspar Tanvald Granite rimming the SW periphery of the large Krkonoše-Jizera Massif is S-type granite that contains magmatic garnet. The euhedral shape (icositetrahedron subordinately combined with cube – Fig. 6.1.2.) of orange coloured garnet crystals up to 0.6 mm in size indicates early crystallization from granite melt. EMP (Electron microprobe) analyses of the garnet proved its almandine character (Fig. 6.1.1) with prominent temperature-dependent zoning having almandine-rich cores and spessartine-rich rims with composition alm 0.75–0.61, spess 0.15–0.38, pyr 0.2–0.7, gross0.02–0.1, A low grossular component content indicates the shallow depth (< 4 Kbar) of the Tanvald Granite intrusion.

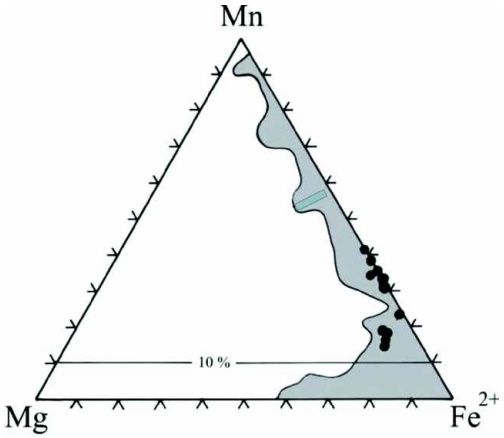

Figure 6.1.1 Diagram of the garnet composition from the Tanvald Granite in the ternary almandine – pyrope – spessartine series. Black dots are individual microprobe analyses. Fediuková et al. (2008).
Grey area is the field of the magmatic garnet (Miller and Stoddard, 1981).

REFERENCES

Fediuková, E. – Klomínský, J. – Schovánek, P. (2008): Spessartin-almandinové granáty z alkalicko- živcového tanvaldského granitu. – Zpr. Geol. Výzk. v r. 2007, 156–159.

Miller, C. F. – Stoddard, F. (1981): The role of manganese in the paragenesis of magmatic garnet: an example from the Old Woman-Piute Range, California. – J. Geol., 89, 233–246.

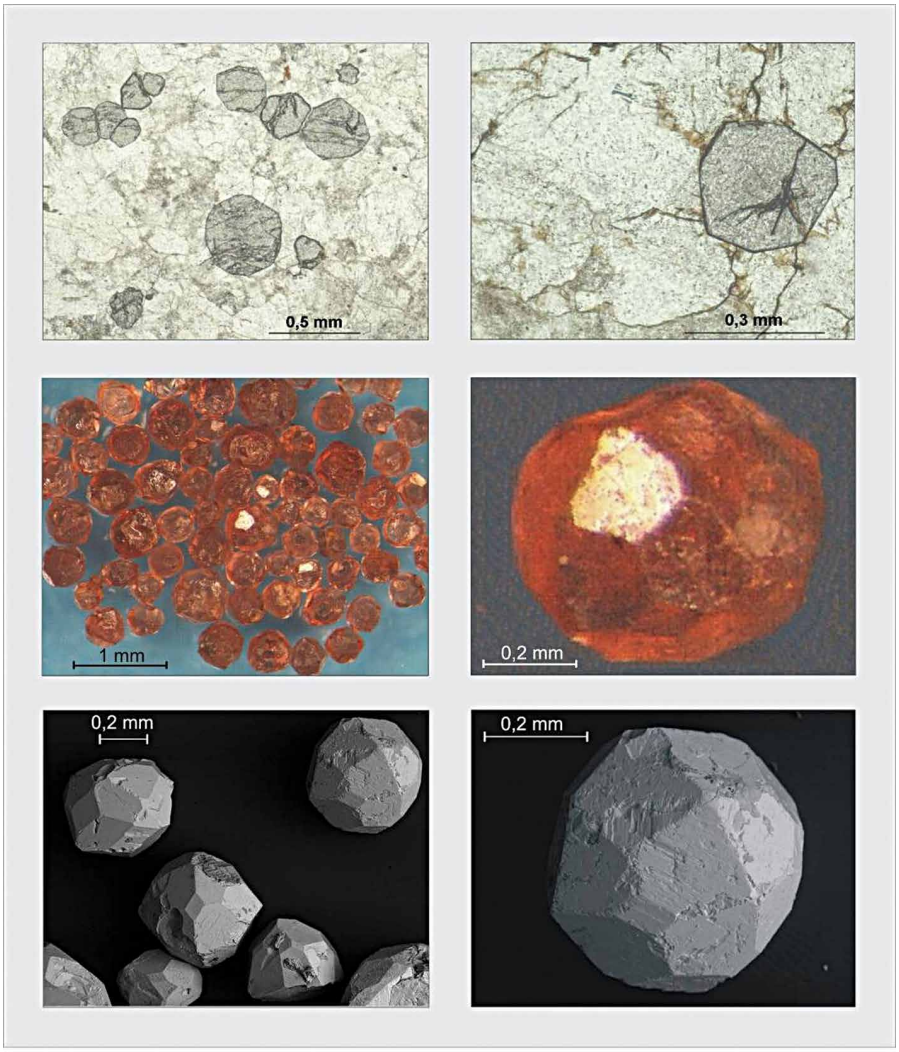

Figure 6.1.2. a – A group of euhedral garnet crystals in fine grained feldspar aggregate, thin section of the Tanvald Granite. b – Euhedral garnet 0.3 mm in size surrounded by plagioclase and K-feldspar, thin section of the Tanvald Granite. c – Euhedral shape of orange colour garnet crystals up to 0.6 mm in size (icositetrahedron subordinately combined with cube). d – Detail morphology of garnet crystal. e, f – electron microscope photographs of the garnet crystals. Fediuková et al. (2008).

6.2 Quartz-topaz greisens at periphery of the Krkonoše-Jizera Composite Massif

Topaz-bearing greisens are exotic rocks in the Western Sudetes domain which is mostly considered a part of the Saxothuringian zone of the Bohemian Massif. (Fig. 6.2.1.) The Western Sudetes comprise the Krkonoše-Jizera orthogneisses of Late Proterozoic up to Ordovician ages, Neoproterozoic to Lower Palaeozoic phyllites and the dominant Krkonoše-Jizera Composite Massif of Variscan age 320 Ma (Fig. 6.2.1.). Orthogneisses represented by biotite and two-mica strongly foliated rocks were probably the parent material of the locally intense metasomatized rocks, often comprising just quartz and topaz with white mica, tourmaline, traces of sulphides (molybdenite and arsenopyrite), wolframite and cassiterite (Karwowski 1973 and 1977). Similar mineral association is known from the interior and exocontact of the Krkonoše-Jizera Composite Massif (Fig. 6.2.1.).

Quartz-topaz greisen stratabound bodies are located on both sites of the Polish-Czech border (Fig. 6.2.1.). In Poland the quartz-topaz greisens occur between leucogranites and mica schists (rarely in association with hydrothermal kaolinisation) in a narrow zone in E-W direction. The zone is about 100 metres wide and more than 10 km long between Rebiszow and Gierałtówek settlements (Mlądz– Kamieň – Pobiedna zone, Karwowski 1973, 1977), parallel to well-known strata bound by Nové Město pod Smrkem – Giercyn – Krobica Variscan tin mineralisation (Fig. 6.2.1.). On Czech territory, similar greisen rocks have been located near Růžek and Vítkov

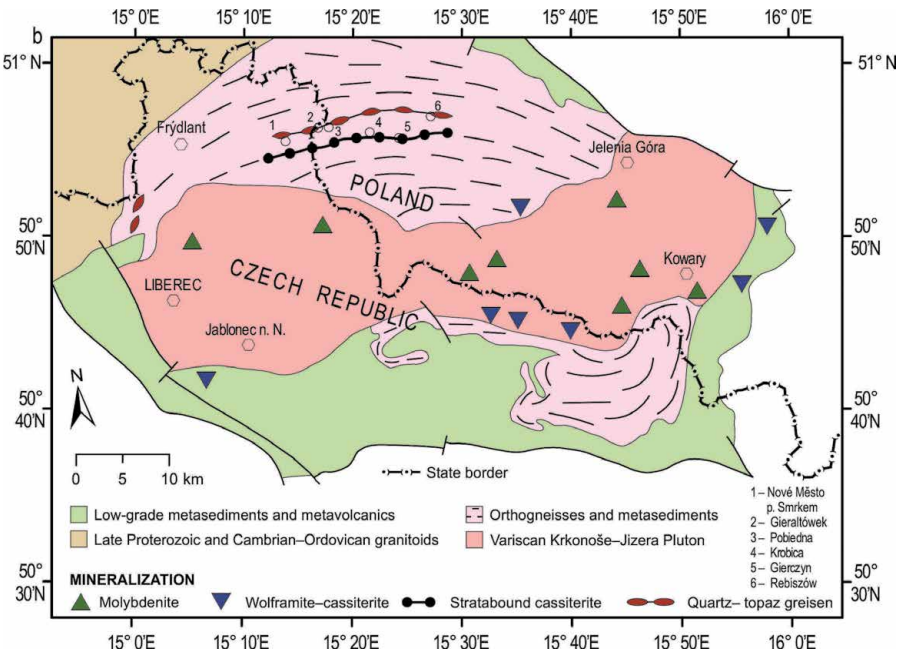

Figure 6.2.1. Simplified geological map of the Western Sudetes adapted after Chrt et al. (1968). Position of the Krkonoše-Jizera Composite Massif within the West Sudetes crystalline complexes and associated mineral deposits and occurences (Ba-F deposits are ommited).

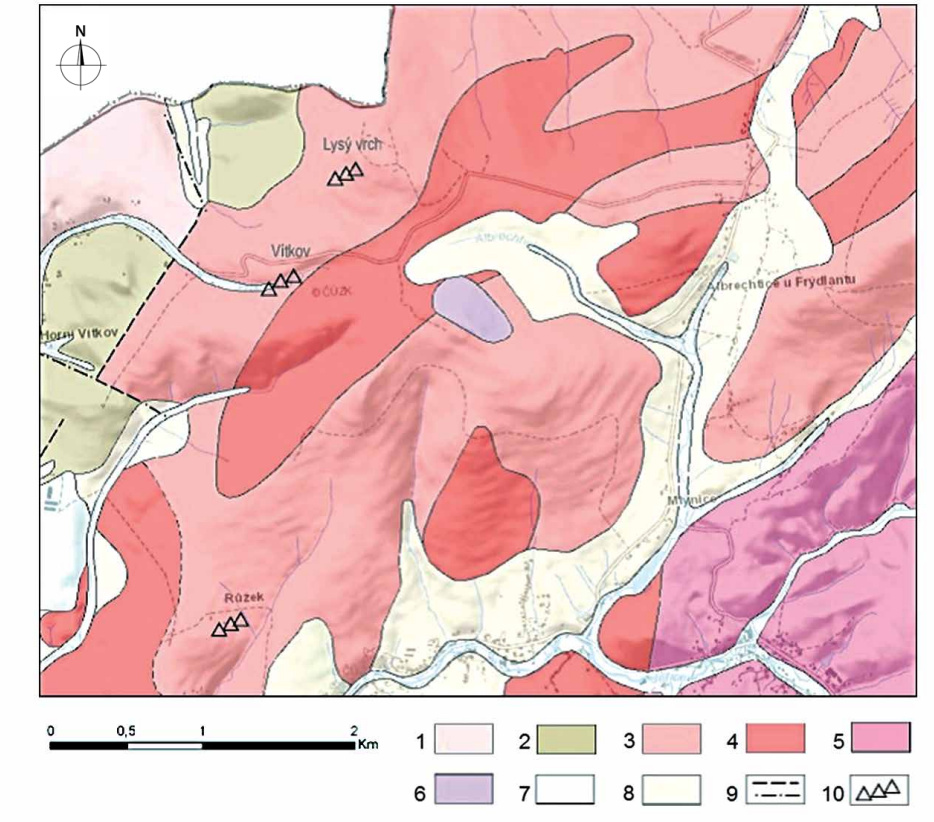

Figure 6.2.2. Localities of the quartz topaz greisen (Růžek, Vítkov, Lysý Vrch) in the Jizera orthogneisses west of Albrechtice nearby Frýdlant. Sidorínová and Dobeš (2015). 1 – granitoids of the Lužice Composite Batholith, 2 – metagreywacke and phylite of the Krkonoše-Jizera Crystalline, 3 – orthogneisses of the Krkonoše-Jizera Crystalline, 4 – metagranites of the Krkonoše-Jizera Crystalline, 5 – Granites of the KJCM, 6 – olivine nephelinite, 7 –alluvial sediments. 8 – deluvial sediments, 9 – faults, 10 – quartz-topaz greisen locality.

settlements (Watzernauer, 1940, Klomínský et al. 2003, Figs. 6.2.3 and 6.2.4). On both sites of the Polish-Czech border the only remnant outcrops are the detached greisen blocks that occur parallel to other geological structures (metamorphic foliation) of the Krkonoše-Jizera orthogneisses at a distance of 3 to 10 km from the northern margin of the Krkonoše-Jizera Composite Massif (Fig. 6.2.1.).

Two occurrences of topaz quartzolite (greisen) are located along the north trending zone north of Chrastava township in Northern Bohemia (Fig. 6.2.2.). The greisen consists of 65 vol. % quartz, 32 vol. % topaz, 2 vol. % mica and accessory alkali feldspar, and ilmenorutile. Dyke-like bodies of topaz quartzolite are indicators of high-temperature W – Sn mineralisation of the greisen type (~350 °C) which has up to now been dominant only in the Saxothuringican Zone (Krušné hory Mountains) only.

In the Vítkov locality (Fig. 6.2.4), dominantly wolframite (ferberite) accompanied accessorically by scheelite, fluorite pyrite, molybdenite, arsenopyrite, native bismuth,

Figure 6.2.3. Large block of the quartz topaz greisen in the Chrastava township park. Photo J. Klomínský.

ilmenorutile (with anomalous Nb and Ta content) and zircon were reported by Sidorínová and Dobeš (2015), Fig. 6.2.2.

At Vítkov, molybdenite sparsely occurs within tungsten mineralization which is hosted by topaz greisen in orthogneiss developed in the envelope of the Krkonoše-Jizera Composite Massif (Fig. 6.2.2.). Mineralogical study showed that sulphide assemblage started with precipitation of arsenopyrite, followed with molybdenite, tungstenite, and transitional Mo- and W-dominated disulfides and concluded by

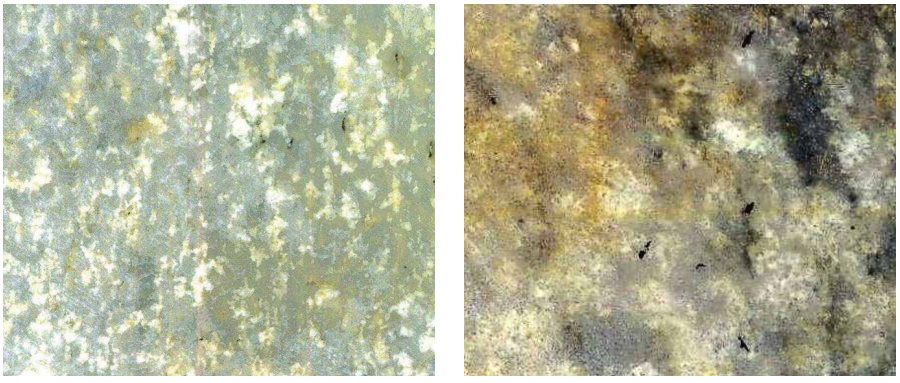

Figure 6.2.4. Two polished slabs of the quartz topaz greisens from Vítkov (left) and Růžek (right) localities (half size). Photo J. Klomínský. White field is topaz, light grey field is quartz, black needles are wolframite and dark clusters are dissemination of sulphides (pyrite and arsenopyrite).

pyrite. The textural relationship between molybdenite and tungstenite shows that tungstenite was formed during several stages related to molybdenite bending and fracturing (Fig. 6.2.5.).

The sulfidic mineral assemblage (from oldest to youngest) at Vítkov is thus as follows: arsenopyrite → molybdenite → tungstenite → W-Mo/Mo-W disulfides → pyrite.

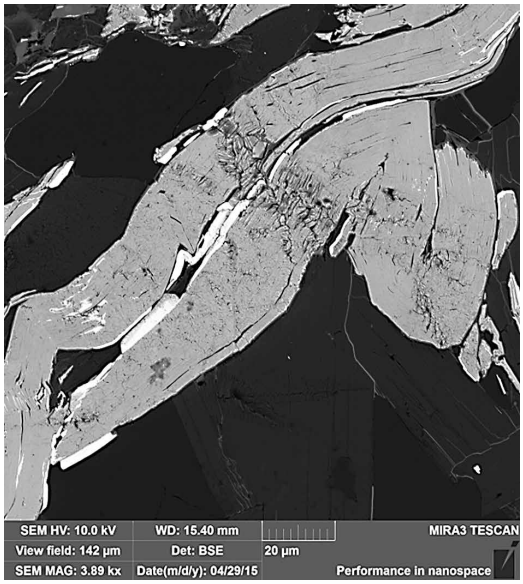

Figure 6.2.5. SEM photomicrographs of major sulfides from tungsten-bearing topaz greisen at Vítkov. Pašava et al. (2015). Folded micro-fillings of tungstenite (apparent kink) in inter-lamellar space in molybdenite which resulted from plastic deformation of molybdenite.

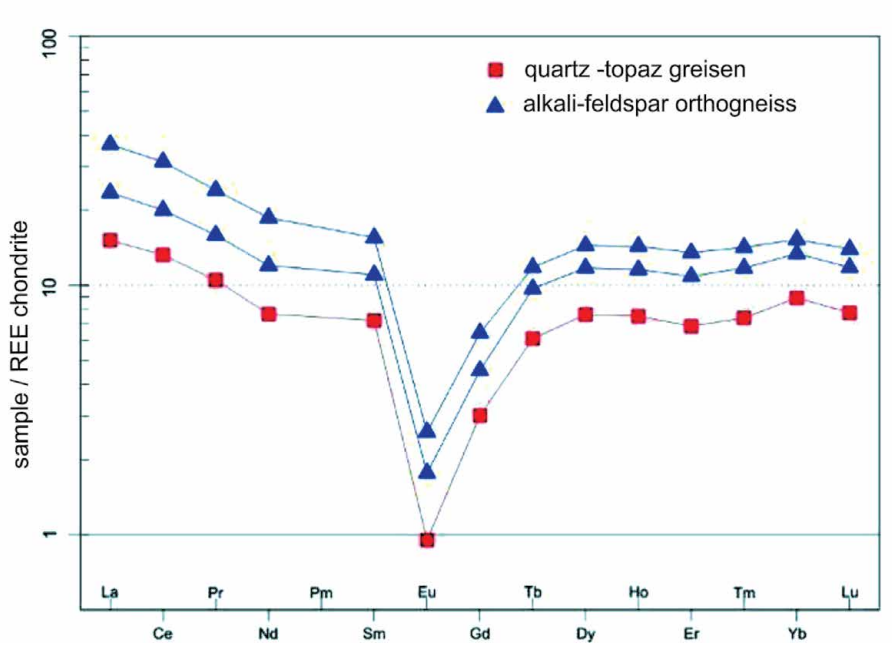

Figure 6.2.6. Correlation of the REE pattern of the topaz-quartz greisen and alkali-feldspar orthogneiss. (S. Vrána personal communication)

This is the first time that molybdenite associated with tungstenite and Mo-W and W-Mo disulfidic phases have been detected in tungsten-bearing topaz-quartz greisen in the Bohemian Massif (Pašava et al. 2015), Fig. 6.2.5.

Genetic affinity between the alkali-feldspar orthogneiss and quartz-topaz greisens is indicated by almost identical REE pattern (Fig. 6.2.6.).

REFERENCES

Chrt J. – Bolduan H. – Fedak J. – Holzer H. – Teuscher E. O. et al. (1968): Karte der postmagmatischen Mineralization der Böhmischen Masse. Zeitschrift für Angewandte Geologie Bd. 14, H.

Karwowski, Ł. (1973): Strefa grejzenowa Mlądz-Kamień-Pobiedna na Pogórzu Izerskim. Acta Geologica Polonica 23: 325–340.

Karwowski, Ł. (1977): Geochemiczne warunki greizenizacji na pogórzu izerskim (Dolny Śląsk). Archiwum mineralgiczne T. XXXIII, 2: 85–146.

Klomínský J. – Fediuk F. – Schovánek P. – Jarchovský T. – Táborský Z. (2003): Topazový kvarcolit (greisen) u Chrastavy v severních Čechách jako metalogenetický indikátor W-Sn mineralizace. Zprávy o geol. Výz. v Roce 2003. 112–114.

Pašava, J. – Veselovský, F. – Drábek, M. – Svojtka, M. – Pour, O. – Klomínský, J. – Škoda, R. – Ďurišová, J. – Ackerman, L. – Halodová, P. – Haluzová, E. (2015): Molybdenite-tungstenite association in the tungsten-bearing topaz greisen at Vítkov (Krkonoše-Jizera Crystalline complex, Bohemian Massif): indication of changes in physico-chemical conditions in mineralizing system. – Journal of Geosciences,

Sidorínová, T. – Dobeš, P. (2015): Wolframitová mineralizace z greisenu v krkonošsko-jizerském krystaliniku u Vítkova v Jizerských horách. Zprávy o geol. Výz. v roce 2014/I – ložiska, geogyzika. 179–183.

Watznauer, A. (1940): Metamorphe Greisen, ein Beitrag zur Frage kaledonischer Zinnerz-lagerstätten in den Sudeten. Firgenwald, 12, 3. Liberec.

6.3 Tungsten-tin mineralization in the exocontact of the Tanvald Massif

A new locality of wolframite-cassiterite mineralization has been discovered in an excavation near Jeřmanice, south of Liberec. This ore prospect has been never investigated in the past (Klomínský and Táborský 2003a). Contact metamorphosed Lower Palaeozoic phyllites are cut by a flat lying cluster of milky white quartz veins up to 30 cm thick close to the contact of the Tanvald Granite (Fig. 6.3.1.). The quartz vein stockwork contains abundant black wolframite (ferberite Fig. 6.3.3.) and less frequent dark brown cassiterite aggregates and crystals, up to 10 cm and 3 cm respectively. Phyllites are intensely impregnated by tourmaline along the margin of quartz veins (Figs. 6.3.2. and 6.3.4.). The roof of the granite intrusion is expected at a depth less than 100 m underneath the quartz vein stockwork. The approximate ore potential of the Jeřmanice prospect is estimated at 0.1 to 0.6 % W average content about 750 tonnes of tungsten (Klomínský and Táborský 2003b).

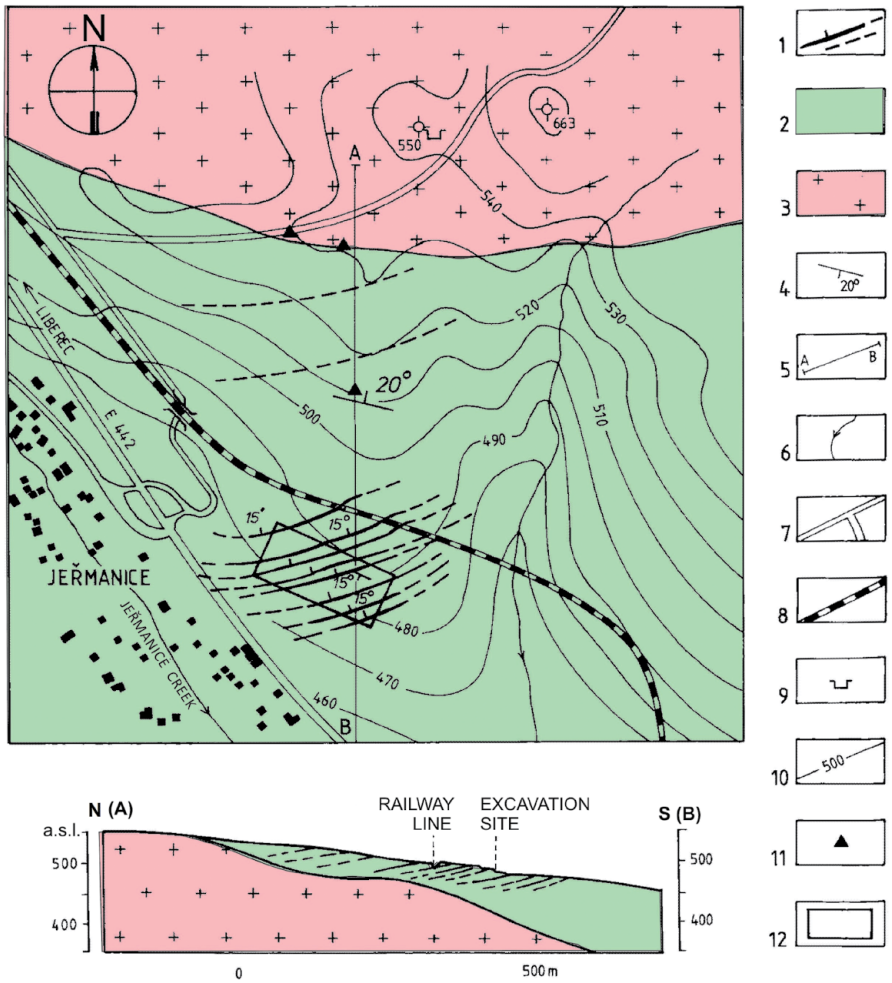

Figure 6.3.1. Map of the tungsten-tin prospect near Jeřmanice SE of Liberec City. Klomínský and Táborský (2003a).

1 – quartz veins with wolframite and cassiterite, 2 – chlorite-sericite contact metamorphosed phyllite, 3 – Tanvald Granite, 4 – metamorphic foliation, 5 – geologic profile line, 6 – Jeřmanice creek, 7 – main road, 8 – railway, 9 – abandoned sand pit, 10 – topographic contour line, 11 – stone dump, locality of quartz containing wolframite, 12 – excavation site.

Figure 6.3.2. Outcrop of the quartz vein with broad rims of intense tourmalinised phylites (black). Photo J. Klomínský.
Exposure in excavation near Jeřmanice (see the hammer for scale).

Figure 6.3.3. Clusters of wolframite crystals in quartz vein (natural size). Photo J. Klomínský.

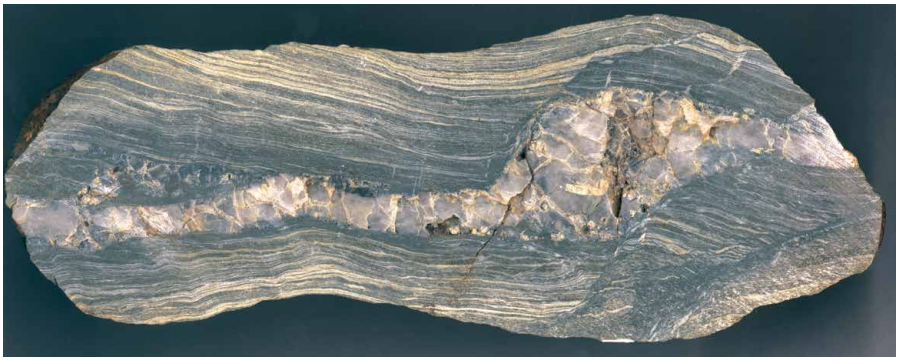

Figure 6.3.4. A slab of the quartz vein with broad rims of intense selectively tourmalinised phylites (dark grey). Half of original size. Photo J. Klomínský.

This wolframite prospect nearby Liberec is the first find of W-Sn quartz vein mineralization outside the Erzgebirge region where W-Sn deposits were intensively mined in the past (Dobeš et al. 2006).

REFERENCES

Dobeš, P. – Klomínský, J. – Táborský, Z. (2006): Fluidní inkluze v žilné Sn-W mineralizaci v exokontaktu tanvaldského granitu u Liberce v severních Čechách. In Zimák J: Mineralogie Českého masivu a Západních Karpat 2006, s. 11–12. – Univerzita Palackého v Olomouci. Olomouc. ISBN 80-244-1560-7.

Klomínský, J. – Táborský, Z. (2003a): Wolframitové zrudnění u jižního okraje tanvaldského granitu v severních Čechách. – Zprávy o geologických výzkumech v roce 2002, 169–170.

Klomínský, J. – Táborský, Z. (2003b): Nález křemenných žil s wolframitem a kasiteritem v exokontaktu tanvaldského granitu u Liberce v severních Čechách. – Uhlí-Rudy-Geologický průzkum 10, 8, 28–30.

6.4 Exotic hornfels from the contact aureole of the Tanvald Granite Massif – the raw material for Neolithic tools.

A prominent outcrop of contact metamorphosed metabasite, previously known only from fragments, loose stones and boulders, projects from the southern foreground of the granitic ridge between Tanvald and Liberec in Northern Bohemia. This rock is the source material for Neolithic stone artefacts used widely across Central Europe (Šrein et al. 2002, Přichystal 2002). The metabasite, having the character of an amphibole hornfels, was recently uncovered in a building excavation between the Jeřmanice and Rádlo townships 8 km SE of Liberec (Klomínský ae al. 2003). The character of the outcrop clearly shows that the rock is situated in the inner part of the contact aureole of the Tanvald alkali-feldspar granite and that its remarkable geotechnical properties are due to the effects of the contact metamorphism (Fig. 6.4.1.). A small thickness of

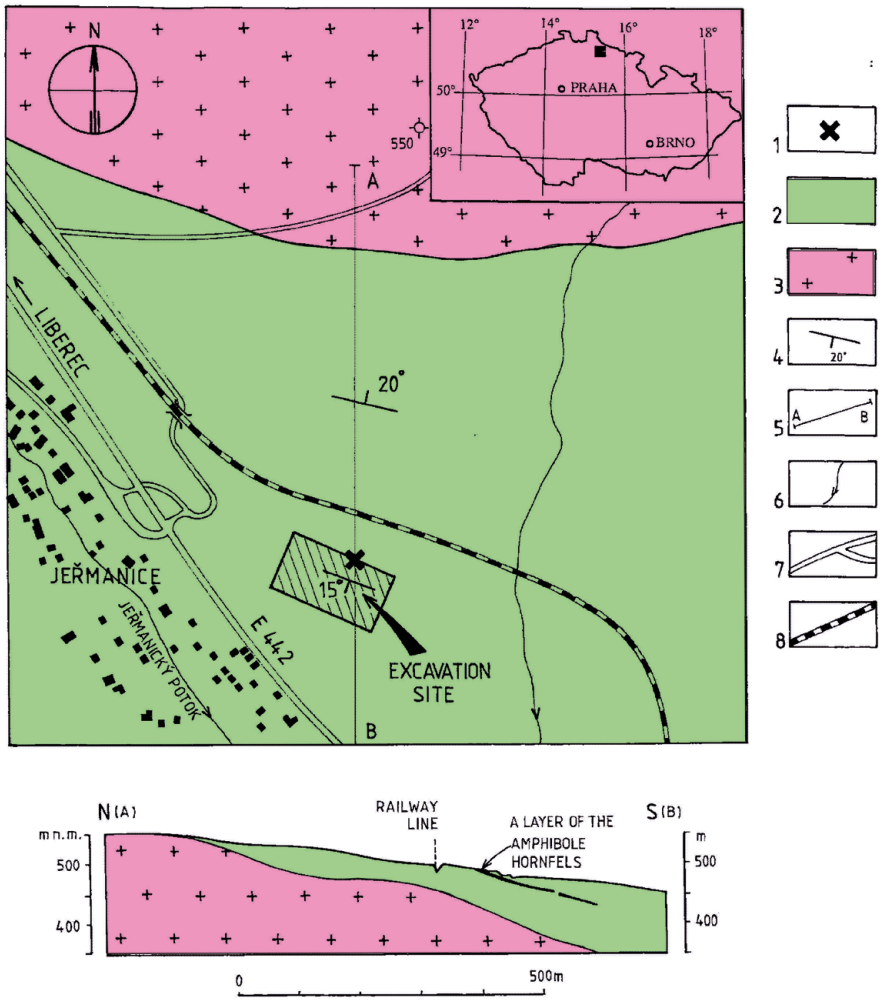

Figure 6.4.1. Locality map of the hornfels outcrop nearby Jeřmanice village. Klomínský et al. (2004).
1 – hornfels outcrop,
2 – chlorite-sericite contact metamorphosed phyllite,
3 – Tanvald Granite,
4 – metamorphic foliation,
5 – A-B geologic profile line,
6 – Jeřmanice creek,
7 – main road,
8 – railway.

some decimetres and large lateral extension (a segmented length of several km) of the "nephrite" layer obviously represents neither a dyke nor a lava sheet, rather a sill modified by tectonic deformation.

The replica of stone axe in Fig. 6.4.2. and the bowl replica in Fig. 6.4.3. are made of amphibole-plagioclase hornfels which shows radial, divergent, and felted (nephritic) texture that is responsible for exceptional tensile strength (Fig. 6.4.4.). The material is found as loose boulders and a few outcrops from lower slopes south of the granite ridge between Liberec, Jablonec nad Nisou and Tanvald. The rock occurs near the contact with the Tanvald alkali-feldspar granite and its remarkable mechanical resistance is due to effects of contact metamorphism. The hornfels, corresponding in chemical composition to tholeiitic basalt, forms thin layers (stratigraphic markers), originally a sill deformed together with hosting spotted phyllite. A protolith of the host rock is presumably of Silurian age (Klomínský et al. 2004).

Figure 6.4.2. Replica of stone axe of Neolithic age 20 cm long made from hornblende-plagioclase hornfels. Jeřmanice locality next to Liberec. Photo J. Klomínský.

Figure 6.4.3. A modern polished bowl 15 cm in diameter made from hornblende-plagioclase hornfels. Locality Jeřmanice next to Liberec. Photo J. Klomínský.

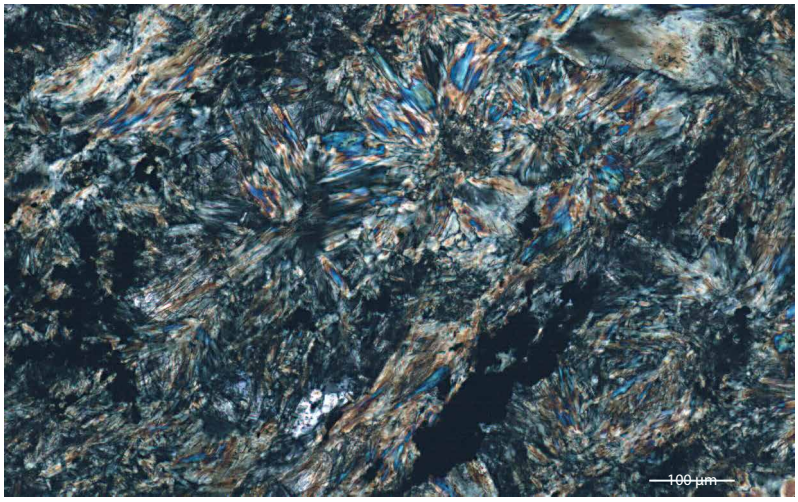

Figure 6.4.4. "Wisker" structure of hornblende-plagioclase hornfels showing radial, divergent, and felted (nephritic) texture that is responsible for exceptional tensile strength. Klomínský et al. (2004). Crossed nikols polarization, white bar 100 µm. The most dominant rock-forming mineral is magnesiohornblend, plagioclase, actinolite and ilmenite.

Polished stone tools produced from this type of hornfels have been found by archaeologists at many Neolithic sites in Europe, particularly in the Czech Republic, Germany and Poland, though the source of the raw material remained uncertain. As a result of increasing interdisciplinary research, a 21.2 ha site of large-scale production of stone implements from loose fragments of the hornfels was discovered in 2002 near Jistebsko SE of Jablonec nad Nisou. This well-preserved Neolithic shallow diggings is one of the oldest and largest of its type in the Czech Republic. Production there began in the earliest phase of the Neolithic Age (linear pottery culture – 5400 BC) and probably continued right up to the end of the later phase of the ornamented ware culture (4500 BC). The significance of this unique archeological locality extends well beyond the borders of the Czech Republic.

REFERENCES

Klomínský, J. – Fediuk, F. – Schovánek, P. (2003): Geologická pozice 'nefritu' v kontaktní obrubě tanvaldského granitu v severních Čechách. – Zprávy o geologických výzkumech v roce 2002, 26–28.

Klomínský, J. – Fediuk, F. – Schovánek, P. – Gabašová, A. (2004): The hornblende-plagioclase hornfels from the contact aureole of the Tanvald granite, northern Bohemia – the raw material for Neolithic tools. – Bulletin of Geosciences 79, 1, 63–70.

Přichystal, A. (2002): Objev neolitické těžby zelených břidlic na jižním okraji Jizerských hor (severní Čechy). – Kvartér, 8, 12–14. Brno.

Šrein, V. – Šreinová, B. – Šťastný, M. – Šída, P. – Prostředník, J. (2002): Neolitický těžební areál na katastru obce Jistebsko. – Archeologie ve středních Čechách. 6, 91–99. Praha.

6.5 Chemistry of allanite in relation to uranium release during alteration of the Jizera Granite

Changes in composition of metamict allanite (Fig. 6.5.1.) in biotite monzogranite (Jizera Granite) in the Bedřichov water-supply tunnel were studied using 65 microprobe analyses. The following compositional domains are recognised: I - domains with minimal change in allanite composition, II – domains with strongly lowered SiO_2, enriched in REE, with totals near 70 wt. %, probably carrying mainly REE fluorocarbonates bastnäsite or synchysite, III – domains rich in SiO_2, with decreased REE, Fe and Ca, probably enriched in aluminosilicates. Metamict and altered allanite studied contains < 0.06–0.18 wt. % UO_2 and 0.18–4.8 wt. % ThO_2. It is suggested that microcrystalline alteration domains in former allanite served for deposition of uranium released from other accessory minerals. Part of the uranium is mobilized by groundwater percolating through monzogranite and deposited in powdery coatings of schröckingerite on the walls of the Bedřichov water supply tunnel.

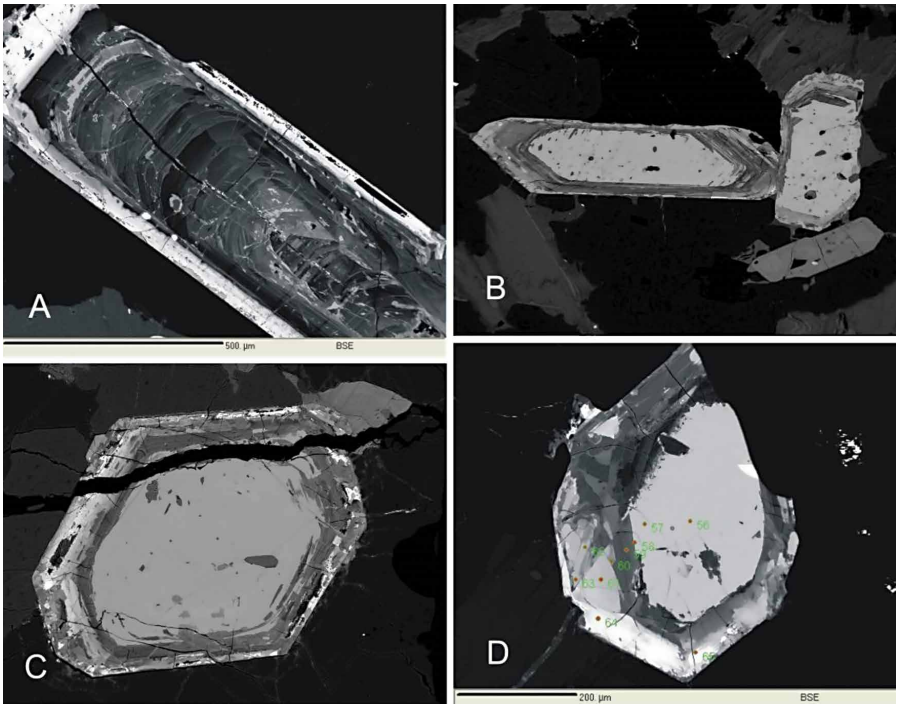

Figure 6.5.1. Allanite (Ce) crystals composite and alteration zonation in the Jizera Granite from Bedřichov water supply tunnel A. Vrána et al (2011). Back Scanned Elecrones (BSE) images. Bright pale crystal margins contain higher Fe and Th content.

REFERENCES

Vrána, S – Sulovský, P. – Schovánek., P. (2011): Změny chemismu allanitu-(Ce) vlivem alterace s ohledem na uvolňování uranu do horninového prostředí biotitického monzogranitu u Bedřichova ročník 45, 2012 (ZGV v roce 2011), str. 202–207.

6.6 Fracture carbonates in granites from Bedřichov water-supply tunnels

Open fractures in the Krkonoše-Jizera Composite Massif were healed in the early stage of massif consolidation by aplite dykes, and later by lamprophyre dykes and Cainozoic basalts (Klomínský et al. 2005, 2012). The youngest fillings are quartz-carbonate and carbonate veins, often with zoned or brecciated structure (Figs. 6.6.1. and 6.6.2.).

There is a significant variation in carbonate composition between individual sections of the tunnel (Klomínský and Woller 2010). Calcite is the predominating mineral in section A, while in section B carbonates of different compositions are present (Fig. 6.6.1). These differences partly correlate with the local granite type – i.e. Jizera Granite in section A and Liberec Granite in section B. Alternatively, the role of vertical zoning might be considered, with a more varied composition of minerals in a deeper level of the hydrothermal system (section B).

The analysis of carbonates from veinlets in section B of the tunnel show substantial differences in composition, corresponding to calcite $CaCO_3$, dolomite $CaMg(CO_3)_2$, ankerite $CaFe(CO_3)_2$, siderite $FeCO_3$ and rhodochrosite $MnCO_3$ (Fig. 6.6.3.) (Dobeš et al. 2013). Each of these compositionally distinct carbonates occupies a specific position in the succession of vein filling and indicates major variations in the composition and temperature of the palaeofluids from which these carbonates crystallized (Tab. 6.6.1.).

The vertical to subvertical veinlets are 0.5 mm to 15 cm wide. The hosting fractures are of extensional character (Klomínský et al. 2005). Quartz and calcite make up the main minerals, and minor components consist of chlorite, hematite, ankerite, fluorite, adularia and clay minerals. Monazite, rutile, xenotime, and synchysite – (Ce) $Ca(Ce,La)(CO_3)_2F$, a fluorocarbonate of REE, are accessory minerals (Fig. 6.6.2.). The veinlets form an orthogonal network with a prevailing NW-SE direction. These veins are 0.5–15 cm wide and carry mainly quartz and calcite. Veins trending NE-SW are largely thin, less than 1cm wide, and carry largely fine-grained minerals. The NW-SE fractures are the older of the two sets.

Origin of fracture-filling minerals in the Bedřichov water-supply tunnel sections A and B

The Liberec and Jizera Granites in the Bedřichov water-supply tunnel contain numerous veins, which can provide information on the character of fluid flow during early and late stages of postmagmatic evolution of the massif. The conditions under which fracture mineralization originated were studied using fluid inclusions and stable isotopes.

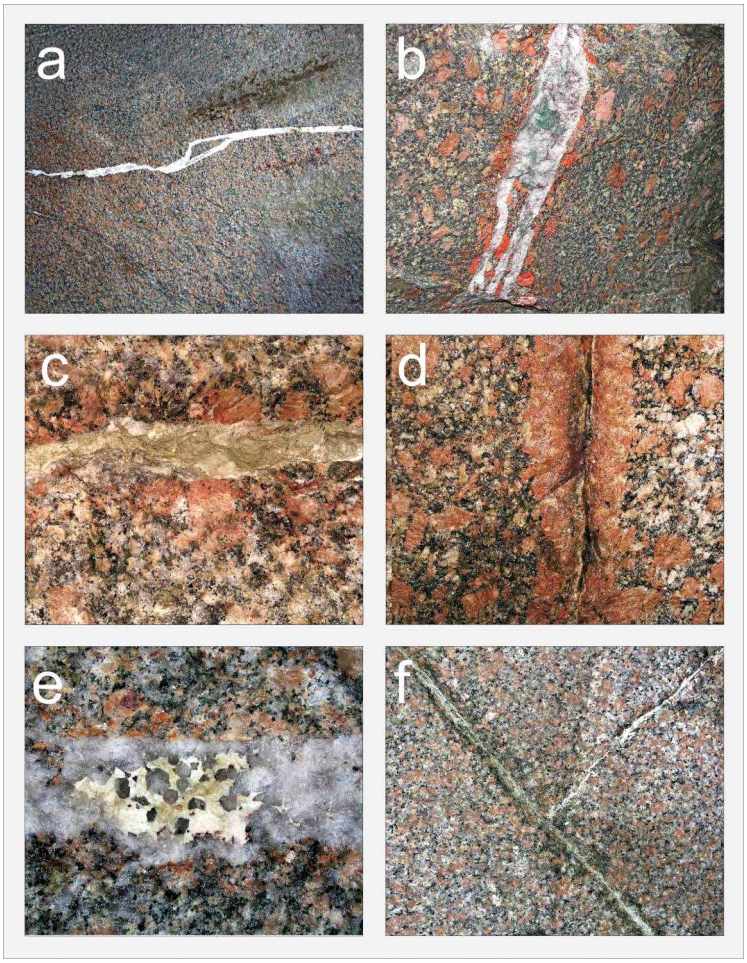

Figure 6.6.1. Examples of fracture filling in granites of the Bedřichov water-supply tunnels. Klomínský and Woller (2010). a – shear fracture 5 cm wide in the Liberec Granite (section B of the tunnel), filled with white calcite, b – quartz-carbonate (calcite) vein with chlorite and contrasting rims of hydrothermally altered Jizera Granite, 10 cm wide, (section A of the tunnel), c – tension fracture in the Jizera Granite (section A of the tunnel) with clay and carbonate fill, 2 cm wide, d – aplite dyke with central tension fracture filled with quartz and carbonate, 5 cm wide, e – detail of quartz vein with a vug partly filled by quartz crystals and younger calcite, 3 cm wide, f – contact of filled fractures of different age; the thicker vein is 1 cm wide.

Data from the fluid inclusion and stable isotope study indicates that pegmatite, quartz, and quartz-carbonate veins in the granitoids of the tunnel can be classified into three generations (Figs. 6.6.1. and 6.6.4.):

1. Pegmatite veins carrying NaCl-H_2O inclusions formed at temperatures up to 340 ºC and low salinity.
2. Epithermal veins formed at temperatures lower than 200 ºC. The veins tending NW-SE and NE-SW carry several types of water-rich inclusions with variable salinity and

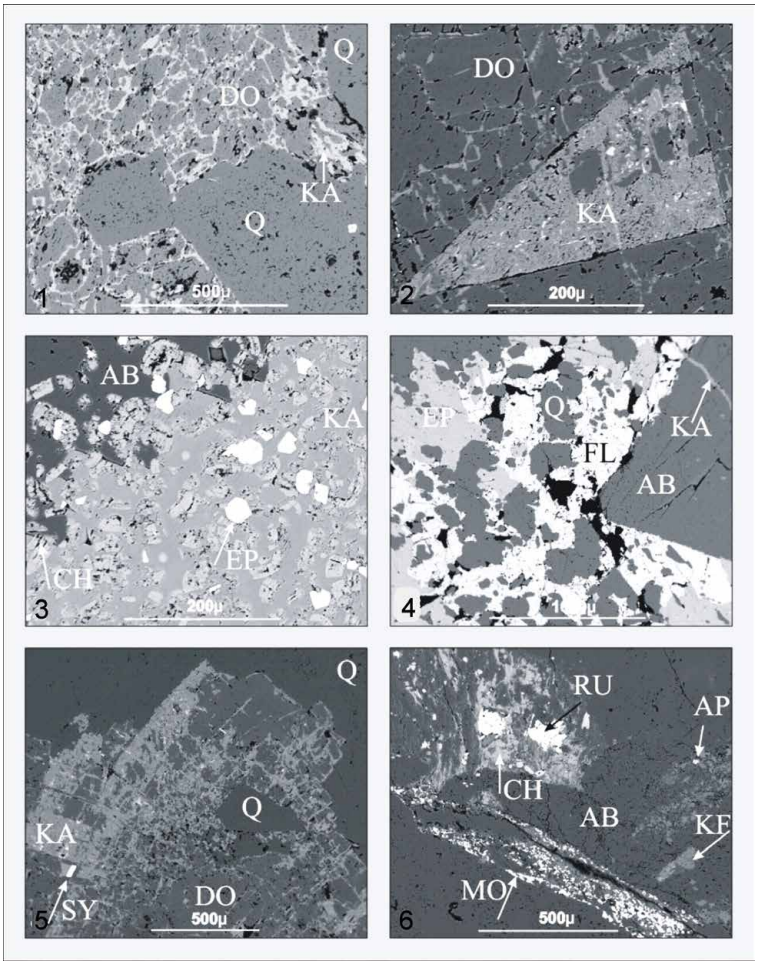

Figure 6.6.2. BSE images of individual minerals from hydrothermal veins of the Bedřichov water-supply tunnel. Klomínský and Woller (2010). KA – calcite, Q – quartz, AB – albite, CH – chlorite, EP – epidote, FL – fluorite, RU – rutile, KF – potassium feldspar, SY – synchysite, MO – monazite, DO – dolomite, AP – apatite.

water solution composition: LiCl vs. $CaCl_2$-NaCl vs. NaCl-KCl ± $MgCl_2$ ± $FeCl_2$. The isotope composition of carbon and oxygen in calcite from these veins is also variable and indicates a variety of solution sources, from water from a magmatic source and juvenile brines to water of meteoric origin (Fig. 6.6.5.).

3. Calcite filled fractures tending NE-SW, with indications of late tectonic displacement. Temperatures of the homogenization of the inclusions in the calcite reach 80–110ºC, and the salinity of the water solution is very low, up to 4 wt. % NaCl equivalent. These solutions most probably derived from meteoric waters.

Quartz and calcite in all studied veins contain only fluid inclusions with aqueous solutions. Inclusions carrying CO_2 and CH_4 gas were not identified. Phase transitions in inclusions were recorded using the following measured temperatures:

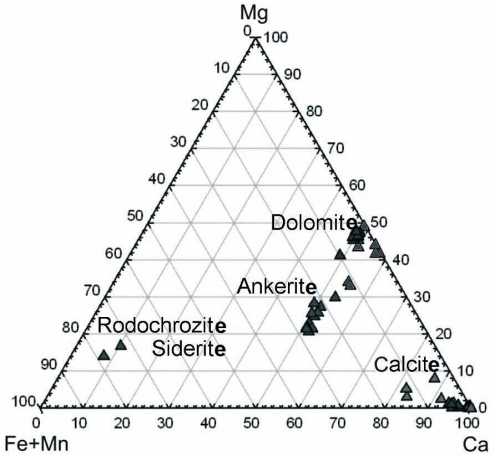

Figure 6.6.3. Chemical composition of carbonates in hydrothermal veins in the Bedřichov water-supply tunnel in the Fe + Mn – Mg – Ca diagrams. Klomínský et al. (2012).

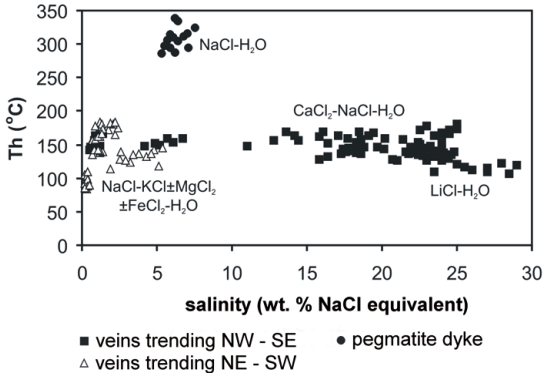

Figure 6.6.4. Homogenization temperature and salinity of solutions in fluid inclusions in minerals of quartz-carbonate veins and pegmatite dykes from A and B sections of the Bedřichov water-supply tunnel. Klomínský and Woller (2010).

Th – temperature of complete fluid inclusion homogenization,
Tm – temperature of thawing of the last ice crystal – determination of total salinity of fluid inclusion,
Te – eutectic temperature – determination of brine composition.

Coarse-grained quartz from pegmatite was found to contain inclusions of aqueous solution with a more or less constant ratio of liquid and gas phases, LVR = 0.6 to 0.7 (liquid and gas ratio). Homogenization temperatures vary in the range of 286 to 338 ºC, and salinity of the solution is low, from 5.3 to 7.5 wt. % of NaCl equivalent. The first ice thawing was observed at –22 ºC, which indicates a system of NaCl – H_2O solution.

Quartz-carbonate veins trending NW-SE contain primary and secondary inclusions with aqueous solutions. Many primary inclusions in quartz and calcite show a varying

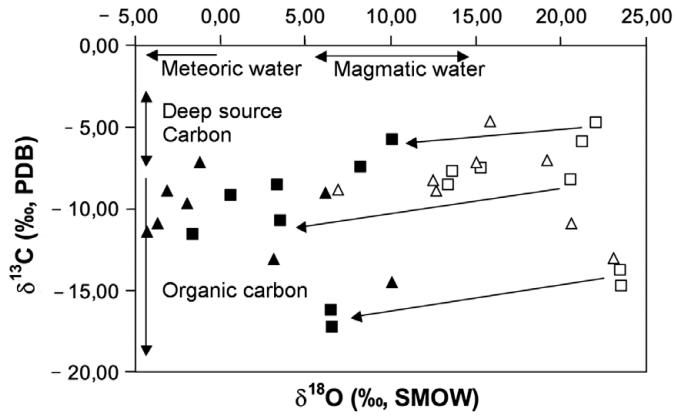

Figure 6.6.5. Isotope composition of carbon and oxygen in vein calcites from the A and B sections of the Bedřichov water-supply tunnel. Dobeš et al. (2017).

ratio of liquid and gas phase (LVR = L/L+V). This ratio is likely to reflect certain temperature-pressure conditions of the hydrothermal system at a time when the inclusions originated (homogeneous vs. heterogeneous environment, maturing time of inclusions), or it may be derived secondarily when the inclusions were closed due to processes such as the escape of liquid, diffusion, expansion and decrepitating and precipitation of phases (Barker and Goldstein 1990, Meunier 1989). In this case, a prolonged maturing of inclusions at relatively low temperature is likely to be responsible for irregular LVR. The Te measurements were not carried out in case of very varied LVR, but were undertaken when groups of inclusions showed more or less constant LVR.

Homogenization temperatures of fluid inclusions in calcites of the NW-SE veins are in the range between 107–147 ºC, and in quartz up to 184 °C (Fig. 6.6.4.). The inclusions in both minerals have variable salinity, from 0.4 to 29 mass % NaCl equiv. The eutectic temperatures of –50 to –56 ºC show a significant proportion of $CaCl_2$ in the solution. Homogenization temperatures of fluid inclusions in calcites of the NE-SW veins are in the range from 90 to 142 ºC, and in quartz up to 184 °C. All inclusions in both minerals have low salinity from 0.2 to 5.4 mass % NaCl equiv. Na-K-Mg-Fe chlorides are involved on the composition of the solution.

High-salinity fluid inclusions H_2O-LiCl (Te = –71.2 to –72ºC) with homogenization temperatures of 156 to 182ºC and salinity up to 29 wt. % were also identified in both sections of the Bedřichov water-supply tunnel.

The primary inclusions in quartz and calcite from veins trending NE-SW exhibit mostly an irregular liquid/gas ratio, while primary-secondary inclusions have LVR 0.9 to 0.95. Temperature values vary in the interval of 90–184ºC. All inclusions in this vein system are characteristic of low salinity ranging from 0.2 to 5.4 wt. % of NaCl equivalent. Eutectic temperature was observed only in one sample, Te = –32 ºC.

The youngest generation of fracture filling is represented by thin scaly calcite occurring in fractures with striations indicating late tectonic displacements (Klomínský et al. 2005). Homogenization temperature of H_2O-NaCl inclusions studied in this

calcite was found to be 80–110ºC; salinity of aqueous solution is very low, less than 4 wt. % of NaCl equivalent.

The oxygen isotopic composition of parental paleofluids shows that some of the calcites have δ ^{18}O from +6 to +10 ‰ (SMOW); magmatic water was likely to be their source solution (Fig. 6.6.5.). The other calcites have $\delta^{18}O$ slightly positive, +0.6 to +3.5 ‰ (SMOW). Brines circulating in the Jizera Granite at lower temperatures were apparently their source solutions. Calcites mainly from NE-SW veins have $\delta^{18}O$ negative values of their solutions to –5 ‰ (SMOW). This probably matches the late meteoric waters circulating in solidified and cooled granite.

A considerable variance of the isotopic composition of ^{13}C of calcite from all veins proves their multiple carbon sources. Some of them are likely to have carbon from a deep earth source; the others are probably influenced by organic carbon. The values for Sr content are mostly higher than 100 ppm and indicate the hydrothermal origin of calcites.

Fission track dating of apatites (AFTA) as indicators of the cooling history of the Jizera Granite in the Bedřichov water-supply tunnel

All Jizera Granite samples from the Bedřichov water supply tunnel (section A) show the same age-thermal evolution (Dobeš et al. 2017). Until the recent era, temperature

Table 6.6.1. Contents of trace elements in calcite veins from the Bedřichov water-supply tunnel A. Dobeš et al. (2017).

Location	Cr	Nb	Ni	Pb	Th	U	Y	Zr	Sr	Ba
(m) SW portal	ppm	ppm	ppm	ppm	ppm	ppm	ppm	ppm	ppm	ppm
NW-SE veins										
140	47.8	< 1.0	12.0	14.5	1.8	46.8	20.6	18.0	87.8	92.4
310.8	37.7	< 1.0	13.3	10.6	1.6	1.9	35.1	18.4	130.8	153.9
440	30.4	8.3	6.7	78.6	< 0.1	2.8	6.3	6.1	175.3	33.8
664	21.3	2.4	5.9	6.1	3.9	25.0	22.7	69.5	129.6	32.9
1296	4.9	< 1.0	5.5	4.7	1.5	0.9	37.2	14.2	133.8	5.0
NE-SW veins										
153	18.1	16.4	3.6	3.1	< 0.1	53.4	37.9	3.7	57.9	9.4
273.8	10.7	8.1	3.6	12.5	< 0.1	0.9	14.2	5.2	175.5	12.9
367	7.2	< 1.0	6.2	10.6	2.2	4.9	81.3	21.4	331.7	20.7
388.1	9.7	8.3	4.1	18.0	< 0.1	4.2	82.9	20.3	574.3	7.6

Explanations: An age is given in Ma with standard deviations (68%). ζ figure was 270 ± 2 y/cm^2 (J.Filip). n – number of the apatite grains. N_s a N_i – total reading of the spontaneous and induced tracks. ρ_s a ρ_i – density of the spontaneous and induced tracks (. 10^{6}cm^{-2}). χ^2 –Poisson test on level 95%. L – medium-length of the fission tracks. ρ_m – planar density of tracks in glass detector (CN5) 1.488 . 10^6 cm^{-2}.

Table 6.6.2. Fission track dating of apatite in Jizera Granite from Bedřichov water-supply tunnel.

Locality from SW portal	lithology	n	spont. tracks ρ_s	spont. tracks N_s	induc. tracks ρ_i	induc. tracks N_i	χ^2 test	age (Ma) ± σ	blocked tracks	L (μm)
tunnel A 248 m	Jizera Granite	20	1.27	1080	4.13	3400	yes	62.2 ± 10,0	109	12.6 ± 1,9
tunnel A 641 m	Jizera Granite	20	1.14	1260	3.37	3780	yes	67.2 ± 10,6	112	12.0 ± 2,0
tunnel A 1246 m	Jizera Granite	19	1.33	969	4.13	3059	yes	64.5 ± 10,8	112	11.7 ± 1.8
tunnel A 2161 m	Jizera Granite	20	0.98	1180	2.89	3420	yes	66.8 ± 11,2	101	12.4 ± 1.9

gradually declined, from 120 degrees C at the time the granite rose up from the zone of of full consolidation (around 70 Ma , Upper Cretaceous), at a rate of about 1.5 degrees C/Ma (Tab. 6.6.2.).

According to an apatite fission track study (Danišík et al. 2010), the Krkonoše-Jizera Composite Massif remained at a temperature under 190°C from Permian till Upper Cretaceous when it reached 120 °C (80 Ma). During this time fast uplift of the granite massif took place, and in the last 10 Ma its temperature rapidly dropped to under 50°C. According to AFT analysis the Jizera Granite was uplifted from the zone of total annealing (≥120 °C) in around 80 Ma, then its temperature slowly decreased to 80 °C, subsequently stagnated, and finally 10 Ma ago quickly dropped to the recent temperature (Fig. 6.6.6.).

Radiocarbon ^{14}C ages of the fracture calcites as timekeepers of the hydrothermal rest of the Jizera Granite in the Bedřichov water-supply tunnel A

For ^{14}C analysis, two calcites from NE-SW veins and one calcite from NW-SE vein were selected (Tab. 6.6.3.). The ratio of the physical ^{14}C half-time (5730 y) transformation and half-time ^{14}C (5568 y) transformation given by Stuiver-Polach convention is1029y (Stuiver and Polach 1977).

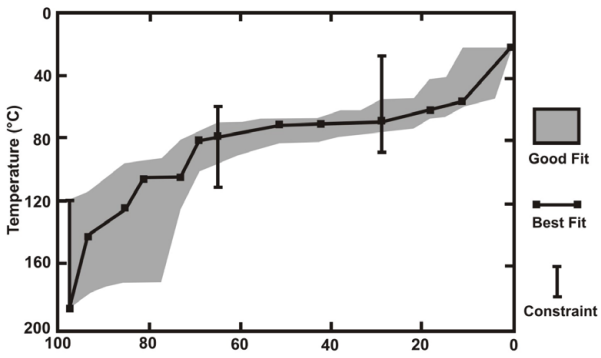

Figure 6.6.6. The time-cooling path of the Jizera Granite from the Bedřichov water-supply tunnel A according to apatite fission track analysis. Dobeš et al. (2017).

Table 6.6.3. Radiocarbon 14C dating of the vein calcites from the Bedřichov water-supply tunnel. Dobeš et al. (2017).

Sample locality from SW portal	Vein azimuth	Min. value conventional radiocarbon age in y BP	Min. calibrated age in y BP	P %
A-153,5 m	NE-SW	> 49,890	older than 51,000 y	95
A-388,1 m	NE-SW	> 49,891	older than 51,000 y	95
A-1296 m	NW-SE	> 45,246	older than 47,000 y	95

P – Total probability

^{14}C dating revealed that the hydrothermal calcites from the all fractures are older than 47 to 51,000 years BP.

REFERENCES

Barker, Ch. E. – Goldstein R. H. (1990): Fluid-inclusion technique for determining maximum temperature in calcite and its comparison to the vitrinite reflectance geothermometer. Geology, 18, 1003-1006.

Danišík, M. – Migoń, P. – Kuhlemann. J. – Evans, N. J. – Dunkl, I. – Frisch, W. (2010): Thermochronological constraints on the long-term erosional history of the Karkonosze Mts., Central Europe – Geomorphology 117 (2010) 78–89.

Dobeš, P. – Klomínský, J. –Jačková, I, – Veselovský, F. (2017): Puklinové kalcity jako indikátory paleohydrologie v granitech krkonošsko-jizerského plutonu (Česká republika). – Zprávy o geol výzk. Vol. 50, 2016. 195–201.

Klomínský, J. – Dobeš, P. – Škoda, R. – Jačková I. (2012): Žíly karbonátů v puklinách granitoidů bedřichovského vodárenského tunelu v Jizerských horách. – Zprávy o geologických výzkumech 45 v roce 2011, str. 173–176 .

Klomínský, J. – Woller, F. eds (2010): Geological studies in the Bedřichov water supply tunnel. – Technical report 02/2010. SÚRAO, ČGS Prague. 104 pp.

Klomínský, J. et al. (2005): Geologická a strukturní charakteristika granitoidů z vodárenských tunelů v Jizerských horách. Etapa 2004-2005. – MS Čes. geol. služba. Praha.gf

Meunier, J.D. (1989): Assessment of low-temperature fluid inclusions in calcite using microthermometry. – Economic Geology, 84: 167–170.

Stuiver, M. – Polach, H. (1977): Reporting of ^{14}C data. – Radiocarbon 19(3), 355–363.

6.7 Sekaninaite at the Liberec and Tanvald Granite contact

Sekaninaite (cordierite with iron content from 65 % to 68 % Fe^{+2}) has been detected in a leucogranite dyke in the Liberec Granite. The leucogranite dyke 80 cm wide crops out in the rock cutting at the contact between Liberec and Tanvald Granites next to the water reservoir in Nová Ves nad Nisou SE of Jablonec nad Nisou. Sekaninaite forms less frequent 5 to 20 cm dark brown zoned oval clusters with greenish grey rims (Fig. 6.7.1.).

Figure 6.7.1. Polished slab of the leucocratic biotite aplogranite with dark brown clusters of sekaninaite (actual size). Photo J. Klomínský.

REFERENCES

Fediuk, F. – Schovánek, P. – Klomínský, J. (2003): Sekaninait už i v severních Čechách (Sekaninaite now even in North Bohemia). – Bulletin miner.-petrolog. Odd. Národního Můzea (Praha), 11, 148–150.

6.8 Composition of the groundwaters in the Bedřichov water-supply tunnel

The hydrological and hydrochemical conditions in section A of the tunnel were studied during the period closely following tunnel construction (Němeček, 1982, 1984, Klomínský et al., 2010). Samples of groundwater were collected directly from debouches in selected fractures with mineral filling in the tunnel walls. Waters from the Bedřichov water-supply tunnel are weakly mineralised up to values of 250 mg/l TDS. Their chemical composition exhibits transitions from the Ca-HCO_3 type to the Ca-HCO_3-SO_4 type. Two samples differ from the average values and correspond to the Na-Ca-HCO_3 and Ca-Na-HCO_3 types. It is probable that these two samples were affected by the concrete casing of the tunnel. This suggestion is supported by the high pH value of 8.0 for the sample V6 collected in the part with concrete casing. The other samples, with 7.2 to 7.8 pH, are neutral to weakly alkaline. The generally low mineralization of waters indicates derivation from a near-surface zone with a quick circulation. The data in Fig. 6.8.1. and 6.8.2. indicate the existence of two different groups of TDS values. The first group has mineralization up to 140 mg/l; the second group has mineralization above 160 mg/l. The samples with higher mineralization have nearly uniform chemical composition of the Ca-HCO_3 type (Fig. 6.8.2.). The group with low mineralization has a variable chemical composition with a gradual transition to the Ca-HCO_3-SO_4 type. The magnitude of the SO_4 component probably

depends not only on the quantity of sulphides in granite in a certain part of the tunnel, but also on the extent of water interaction with rocks or presence and interaction of water in the oxidation zone. Interesting is the relationship between HCO_3 and SiO_2 ions. Waters with mineralization up to TDS < 140 mg/l have an HCO_3/SiO_2

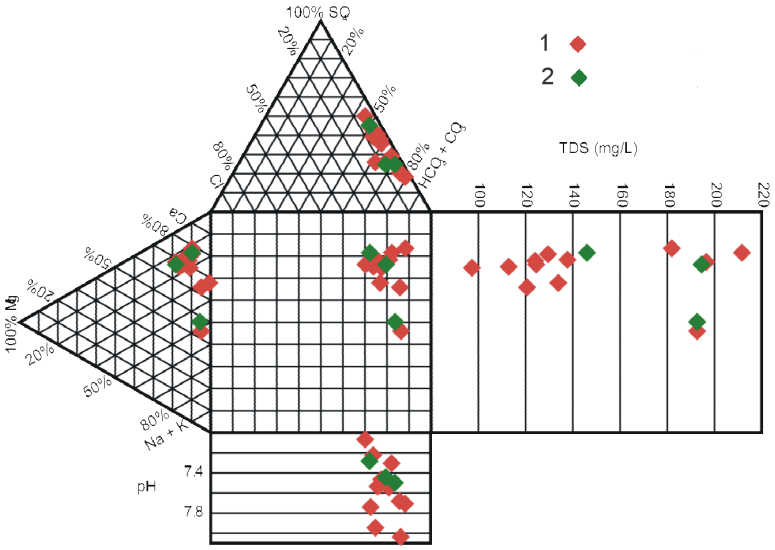

Figure 6.8.1. Durov diagram showing composition of the groundwater from the Bedřichov water-supply tunnel (sections A and B). (Explanation see in Fig. 6.8.2.). Klomínský and Woller (2010).

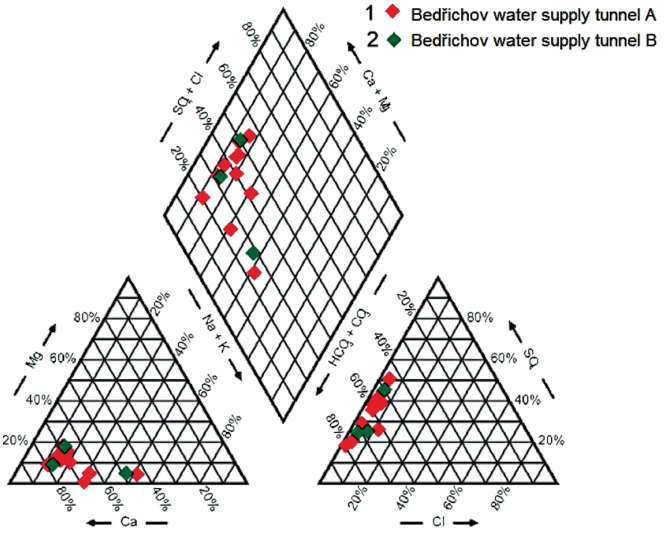

Figure 6.8.2. Piper diagram showing composition of the groundwater from the Bedřichov water-supply-tunnel (section A and B). Klomínský and Woller (2010).

ratio of between 1.96 and 2.36. The second group with TDS > 160 mg/l has a ratio between 3.0 and 5.35. The SO_4/SiO_2 ratio is in the range 0.97 to 1.65 in all samples. This low ratio shows that the SO_4 and SiO_2 contents are closely similar. The waters in the Bedřichov water-supply tunnel exhibit mixing of water from a shallow circulation and waters from a moderately deep circulation. No dependence on distance from the tunnel portal was observed in their composition.

Water samples collected in section A of the Bedřichov water-supply tunnel provide limited information on the origin and evolution of groundwater in the Krkonoše-Jizera Composite Massif. The natural hydrochemical system has been disturbed by tunnel construction, resulting in change in redox potential and in the partial pressure of gases, which have significant impact on water composition. This led to the occurrence of newly formed mineral schröckingerite. The formation and distribution of this mineral depends on penetration of O_2 and CO_2 contained in air along fractures and capillary discontinuities inside granite. This results in disturbance of equilibrium between rock and pore or fracture water and in dissolution mainly of Ca, Mg and U.

REFERENCES

Klomínský, J. – Woller, F. eds (2010): Geological studies in the Bedřichov water supply tunnel. Technical report 02/2010. SÚRAO, ČGS Prague. 104 pp.

Němeček, V. (1982): VD Josefův Důl – štola, zpráva o geologicko-průzkumných prací. Duben 1982, Stavební geologie n. p. Praha.

Němeček, V. (1984): VD Josefův Důl II – stavba, zpráva o geologicko-průzkumných prací. Prosinec 1984, Stavební geologie n. p. Praha.

6.9 Recent minerals and the processes of their precipitation on walls in the Bedřichov tunnel section A

The frequent occurrence of newly formed minerals in the form of thin coatings (Fig. 6.9.1.), powdery aggregates and tiny crystals was noted during the first stage of

Figure 6.9.1. White opal coatings on walls of the Jizera Granite in the Souš water-supply tunnel. Klomínský et al (2013).

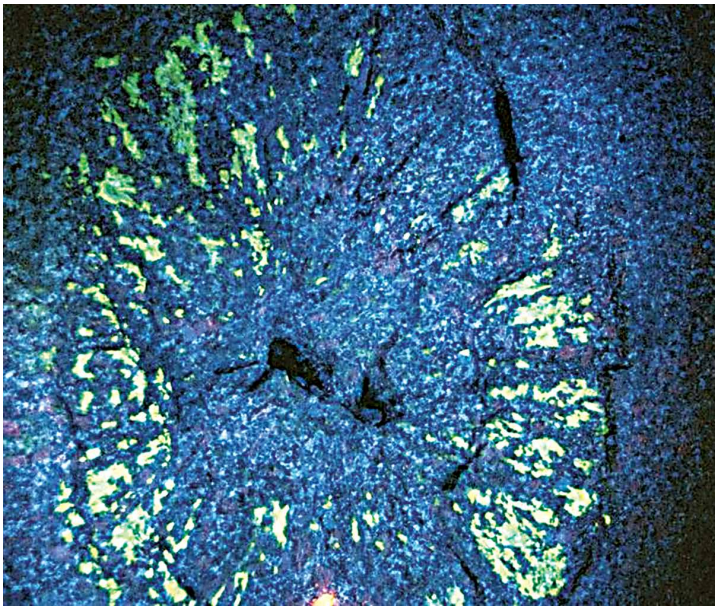

Figure 6.9.2. Recent U-bearing carbonate film on the surface of the Jizera Granite around the blast shatter cone in the Bedřichov tunnel section A. Klomínský et al. (2005) .

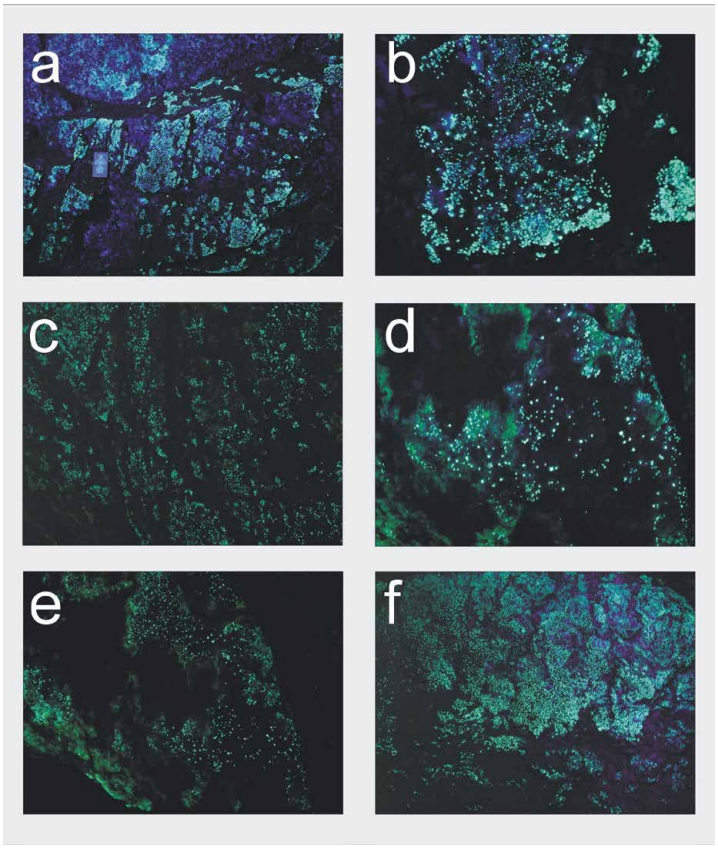

Figure 6.9.3. Coatings of recently formed minerals on the wall of section A excavated by blasting. Klomínský et al. (2013).
1, 3, 6 – coatings of opal, schröckingerite and calcite (surface dimensions 30 × 40 cm).
2, 4 – detail of opal, schröckingerite and calcite coatings with schröckingerite crystals (surface dimensions 10 × 15 cm).
5 – opal and calcite coatings with schröckingerite crystals (surface dimensions 30 × 40 cm).

investigation (Klomínský et al. 2005). Mineralogical study resulted in identification of opal and schröckingerite (Veselovský in Klomínský et al. 2005). These minerals show light green luminescence in short-wave ultraviolet light (Fig. 6.9.2.). The newly formed minerals occur mainly in the lower half of the tunnel profile, predominantly on new fracture planes in the blasted part of the tunnel. In section of the tunnel driven by drilling, the newly formed minerals occur on the surface of walls covered by dust in the lower part of the tunnel profile, on irregular surfaces of small craters originating from blasting and on small cuts in the walls of the drilled section of the tunnel (Fig. 6.9.2.).

Inconspicuous whitish films of U-bearing opal and calcite, showing a green luminescence in ultraviolet light, occur on the surface of fractures formed by blasting in the walls of section A of the Bedřichov water-supply tunnel (Fig. 6.9.3. and 6.9.5.). Mineral schröckingerite ($NaCa_3(UO_2)(CO_3)_3(SO_4)F \times 10\ H_2O$) often crystallizes on the surface of these films and can easily be mechanically removed (Fig. 6.9.4.). Once the wall is washed with water and brushed, the above secondary minerals continue to precipitate.

At 1350 m from the SW portal samples of the Jizera Granite were collected on the NW wall of the Bedřichov water-supply tunnel section A. These samples showed coatings and aggregates of minerals exhibiting yellow-green and green fluorescence. The coatings are composed of mineral phases among which schröckingerite, a radioactive uranium-containing sulphate-carbonate mineral, were identified. The water-soluble schröckingerite contains, according to stoichiometry, 28.33 wt. % of uranium. The formation and distribution of this mineral is governed by penetration of atmospheric O_2 and CO_2 along fractures and capillary discontinuities into granite, resulting in equilibrium disturbance between rock and pore- and fracture-contained water. This process leads to re-mobilization of elements via solution of Ca, Mg and U and transport of U and Fe. Uranyl carbonate is formed on the tunnel walls through the reaction of "fertile" pore water enriched with CO_2. The equilibrium between schröckingerite crystallization and solution is controlled mainly by variation in air humidity in the tunnel. Consequently, the occurrence or absence of schröckingerite depends on the intensity of tunnel ventilation.

A sample of 105 cm^2 total area, with coatings and aggregates showing yellow-green and green fluorescence, was dissolved in diluted HNO_3. The obtained solution contained 30.5 mg/l uranium. Additional calculation indicates that this sample contained 7.6 mg uranium, i.e., 723.8 mg U/m^2.

Coatings and aggregates of minerals with yellow-green and green fluorescence occur only on granite in the part of the tunnel excavated by blasting, typically on both walls up to a height of 1 meter from the floor. In this section of the tunnel, the granite is exposed for a total length of 500 m.

Taking into calculation the total length of both walls at 1000 m (2 × 500 m) and a band 1 m high from the tunnel floor, the total surface of 1000 m^2 contains 0.7 kg of uranium, i.e., with a content of 28.33 wt. % of uranium in schröckingerite total amount of the mineral is near 2.5 kg. The Jizera Granite in section A contains 8 ppm U and 25 ppm Th; zircon and allanite are the main carriers of these elements. The accessory minerals monazite, xenotime, and probably thorite, uraninite, rutile and apatite, are of lesser importance in terms of the total amount of uranium in the granite.

The allanite analyzed contains 0.06 – 0.18 wt % of UO_2; the thorium content of the allanite is relatively high at 0.18 – 4.8 wt. % of ThO_2.

Uranium in these minerals is in an immobile form of U^{IV} so that an increased redox potential of at least E^o (U^{VI}/U^{IV}) = 0.221 V is needed for its oxidation and transformation into mobile (UO_2^{2+}) uranyl complexes. Such conditions exist in the presence of atmospheric oxygen. Carbon dioxide necessary for formation of carbonates is present both in air and water. Solutions containing increased concentrations of the mobile uranyl-carbonate complexes indicate a neutral or slightly acid environment. Other elements, including K (or Na, Ca, and P), are released by decomposition (leaching) of some minerals in local granites, such as apatite and feldspars. Sulphate ions are likely to be derived from decomposed accessory sulphides (mainly pyrite) occurring in mineralized fractures or in granite as such. Alternatively, they could have been brought in by ascending aqueous solutions. Fluorine necessary for crystallization of schröckingerite is released from decomposed micas or apatite.

The sites with schröckingerite in the Bedřichov water-supply tunnel correspond with places with intense evaporation, e.g. places with abundant microfractures. These are sites in EDZ closely tied to holes drilled for blasting. The formation of schröckingerite proceeds rather quickly, depending on evaporation and drying of solutions via capillary elevation along tunnel walls.

On the surface of fractures formed by blasting and around excavations in the tunnel walls, inconspicuous white coatings were detected which give off light green luminescence in shortwave ultraviolet light and which persist even after cleaning the wall with water and a brush. The coatings are of opal with an admixture of a polymorph

Figure 6.9.4. Schröckingerite crystals (yellow-green) and coatings of uranium-bearing opal (white) on the surface of Jizera Granite in the blasted excavation section of the Bedřichov water-supply tunnel section A. Klomínský et al. 2013.

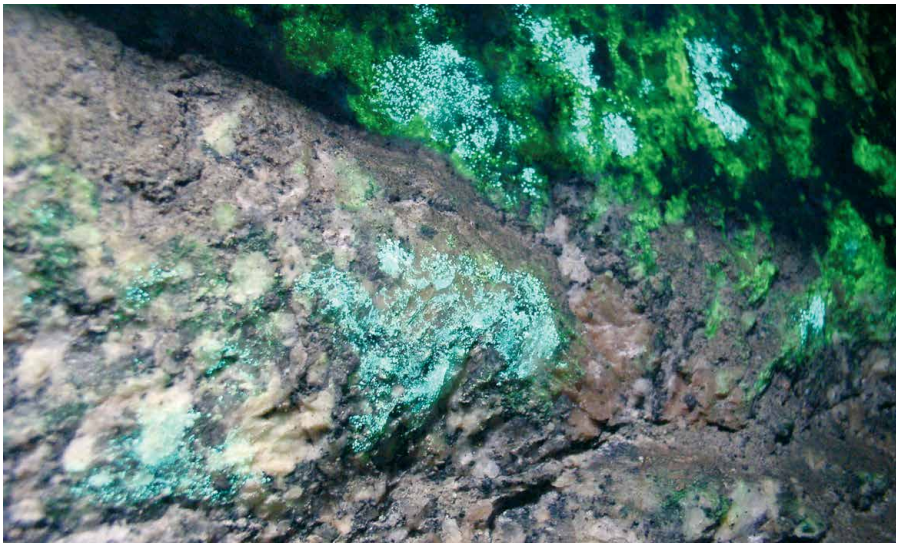

Figure 6.9.5. Schröckingerite crystals and coatings of uranium-bearing opal (white) on the surface of Jizera Granite in the blasted excavation section of the Bedřichov water-supply tunnel section A. Photo J. Klomínský.

of $CaCO_3$, most probably calcite (Fig. 6.9.4.). The luminescence effect is probably caused by a proven U admixture (maximum content near to 1 wt. %). The evolution and precipitation of newly formed uranium-bearing minerals on the tunnel walls was studied at 567 m from the portal. After washing the surface with water the coating re-generated itself after 24 months and the precipitation of these minerals continued.

Pseudocarst (technocarst) in the blasted section of the Bedřichov water-supply tunnel section A

In the blasted part of section A of the tunnel where the tunnel, walls are covered by concrete, white calcite has precipitated in the form of a number of stalactites and

Figure 6.9.6. Calcite stalagmites growing on the floor in blasted and concreted section of the Bedřichov water-supply tunnel section A. Photo J. Klomínský.
(Size of the largest stalagmite is about 30 cm.)

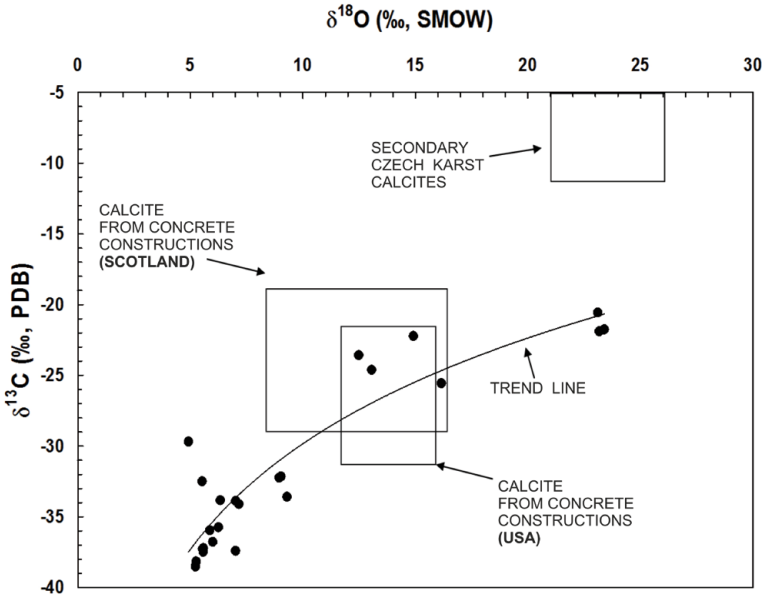

Figure 6.9.7. δ13C a δ18O isotopic composition of the secondary calcites from the Bedřichov water-supply tunnel section A (black dots) and from concrete structures in Scotland and USA (K. Žák in Klomínský et al. 2005). Klomínský et al. (2005).

stalagmites variegated in shape and size (Fig. 6.9.6.). They originate from reaction of atmospheric CO2 with the high pH solution of calcium hydroxide falling in drops from the concrete roof. δ13C a δ18O isotopic composition of the calcites is plotted in Fig. 6.9.7. The lowest isotopic values are from calcite stalactites and the highest ones come from stalagmites (K. Žák in Klomínský et al. 2005).

REFERENCES

Klomínský, J. – Veselovský, F. – Malec, J. (2013): Novotvořené minerály v bedřichovském vodárenském tunelu v Jizerských horách – příklad uvolňování uranu z jizerského granitu. – Zprávy o geologických výzkumech v roce 2012 neuveden, zima, 214–219. ISSN 0514-8057.

Klomínský, J. – Woller, F. eds (2010): Geological studies in the Bedřichov water supply tunnel. – Technical report 02/2010, 103 pp., Czech Geol. Survey, ISBN 978-80-7075-760-4 RAWRA.

Klomínský, J. ed. (2008): Studium puklinové sítě granitoidů ve vodárenském tunelu Bedřichov v Jizerských horách. Etapa 2006–2008. – Zavěrečná zpráva, 188 str. – MS Správa. úložišť radioaktivních . odpadů (SÚRAO). – Čes. geol. služba, Praha.

Klomínský, J. ed. (2005): Geologická a strukturní charakteristika granitoidů z vodárenských tunelů v Jizerských horách. Etapa 2004–2005. – MS Čes. geol. služba. Praha.

Klomínský, J. et al. (2003): Geologická a strukturní charakteristika granitoidů v tunelu v Bedřichově v Jizerských horách. – MS ČGS. Praha.

6.10 Migration of uranium and associated elements in the Bedřichov water-supply tunnel (section A)

The migration process of uranium was investigated by analysing groundwater trace elements and measuring flow rates in the Bedřichov water-supply tunnel (Klomínský 2017). Surface water percolating through Jizera Granite in the Krkonoše-Jizera Composite Massif along fractures up to depth of 150 m in the tunnel becomes enriched with number of mobile chemical elements and compounds generated by granite oxidation. The samples were taken from six different groundwater spring sites – three dripping ones (V1, V2/1, and V3), three with continual fluxes (V4/1, V5, V6) – and from one central drain collecting all outflows from the tunnel (V8), Fig. 6.10.1. Inflow to the groundwater sample sites was measured in ml/s (Tab. 6.10.1.). The groundwater samples were analysed for 72 chemical elements (Hokr et al. 2010).

Some inflows from individual water springs show a higher variability of uranium concentrations.

Higher uranium concentrations have been registered in water from springs in the central part of the the tunnel (V2 and V3), where the overlying granite thickness is maximal (Fig. 6.10.1.). For groundwater springs the water pathways are longer, along a 150 m fracture network, and water retentions are therefore longest. The longer

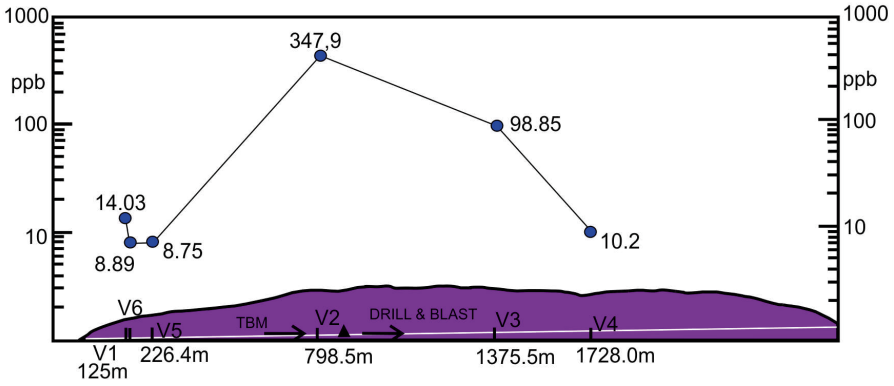

Figure 6.10.1. Uranium content in the groundwater springs in the Bedřichov water-supply tunnel section A. Klomínský (2017).

Table 6.10.1. Water springs (V) and total groundwater outflow from the Bedřichov water-supply tunnel (V8). Uranium content and amount of uranium leached from the Jizera Granite during one year and 30 years. Klomínský (2017).

Water spring	U content (ppb)	Groundwater outflow			Amount of realised Uranium	
		ml/s	m^3/year	m^3/30 years	g/year	g/30 years
V4/1	10.2	12,93	407,3	12219	4.1	123.0
V5	8.75	3,04	95,8	2874	1.0	30.0
V 6	8.89	11,85	373,2	11196	3.7	111.0
V8	16.70	1641	74.655	2239650	1.269	38.070

retention period results in a very high degree of mineralization. Balvín et al. (2012) estimated the transit time of the groundwater inflow in the Bedřichov water-supply tunnel, according to the ^{2}H and ^{18}O isotopes method, at 24.9 to 30.9 months.

The uranium content of groundwater samples, groundwater inflow and the cumulative flow rate during 1 year and 30 years of tunnel operation are summarized

Table 6.10.2. Chemical composition of the groundwater springs (V), total groundwater outflow (V8) from the Bedřichov water-supply tunnel (section A) and chemistry of the stream water from the Josefův Důl water reservoir. Klomínský (2017).

	Sample numbers	V1	V2-1	V4	V5	V-3	V-6	V-8	JDP
	Distance from SW tunnel A portal	125 m	798.5 m	1728.5 m	226.4 m	1375.5 m	142 m	SW portal of the tunnel A	Josefův Důl water reservoir
	Outflow ml/s	0.005	0.006	0.008	12.93	3.04	11.85	1641	
F	ppb	556	1970	730	610	1500	330	350	100
ALK	$CaCO_3$/l	50	44	38	42	73	32	35	3.3
Cl	ppm	4.0	1.6	1.5	1.3	1.8	3.6	1.6	0.9
SO4	ppm	15.7	13.5	23.6	17.8	25.1	15.7	15.4	10.6
Al	ppb	3	7	1	25	2	16	44	301
As	ppb	< 0.5	19.6	2	0.6	26.8	< 0.05	1.1	0.9
B	ppb	10	< 5	< 5	< 5	14	11	9	< 5
Ba	ppb	0.75	0.61	0.55	1.22	0.78	0.71	2.26	10.13
Ca	ppb	21740	20357	19262	23546	23785	16142	14614	3221
Cs	ppb	0.87	2.19	1.06	1.25	1.16	0.93	0.66	0.07
K	ppb	1028	212	811	790	217	949	1429	389
Li	ppb	4.50	13.80	13.70	7.90	20.60	4.90	8.80	1.50
Mg	ppb	3064	1186	2063	2174	246	2274	1653	790
Mn	ppb	0.21	0.36	0.06	0.14	0.14	0.06	0.32	48.46
Mo	ppb	0.7	16.0	0.7	1.1	11.8	0.2	0.7	< 0.1
Na	ppb	4562	11696	4325	4149	10637	3938	4213	1994
Rb	ppb	3.72	1.56	2.47	3.60	1.41	3.51	3.32	2.07
S	ppm	5	4	7	5	9	6	6	4
Si	ppb	7275	6798	8017	7200	5990	6684	6832	3831
Sr	ppb	35.14	87.23	35.45	51.60	98.49	31.03	54.31	22.85
Th	ppb	< 0.05	< 0.05	< 0.05	0.06	< 0.05	< 0.05	< 0.05	0.17
U	ppb	14.03	347.90	10.20	8.75	95.85	8.89	16.71	0.41
W	ppb	0.04	4.93	0.20	0.09	6.66	0.04	0.48	< 0.02
Zn	ppb	0.9	2.1	0.6	2.7	5.8	< 0.5	1.9	4.3

in Table 6.10.1. The total weight of uranium released from the Jizera Granite during 30 years of operation of the Bedřichov tunnel is estimated to be about 40 kilograms, including 2.5 kg of uranium bonded in schröckingerite on the tunnel walls (Klomínský et al. 2013). The migration of uranium and associated trace elements from the Jizera Granite in and out of the Bedřichov water-supply tunnel represents a continuous groundwater leaching process over the life of the tunnel.

The existence of the similar environment over whole area of the Krkonoše-Jizera Composite Massif is also indicated by uranium (0.41 ppb) and associated trace elements content in 22 600 000 m^3 water in the Josefův Důl water reservoir (Tab. 6.10.2.). An example of the migration speed and amount trace elements transported from the KJCM can explain their accumulation in the surrounding sedimentary basins.

REFERENCES

Balvín, A – Hokr, M. – Šanda, M. – Vitvar, T. – Rálek , P. (2012): Transit time estimation of tunnel inflow in fractured granites. Geophysical Research Abstracts Vol. 14, EGU2012-9809-6, 2012

Hokr, M. et al. (2010): Tunel Bedřichov – charakterizace granitoidů in situ. Závěrečná zpráva, 116 str., MS Spr. úlož. radioakt. odpadů. Praha. Techn. Univ. Liberec.

Klomínský, J. – Veselovský, F. – Malec, J. (2013): Novotvořené minerály v bedřichovském vodárenském tunelu v Jizerských horách – příklad uvolňování uranu z jizerského granitu. – Zprávy o geologických výzkumech v roce 2012, 214–219. ISSN 0514-8057

Klomínský, J. (2017): Migrace uranu a dalších stopových prvků v bedřichovském tunelu v Juzerských horách. – Geoscience Reseach Reports vol. 50, 2/2017. Zprávy o geologických výzkumech, 299–303. CGS Prague.

7. Urban geology of Liberec City

A model study by the Czech Geological Survey presented a broad spectrum of geological information about Liberec, a regional city in northern Bohemia, and provided data to the municipal government to assist reliable urban planning and sustainable development of building density. This study included data sets from geology, geophysics, natural resources, engineering geology, and industrial pollution in the town centre. All available information from various data sources has been linked in GIS format to the street plan at a scale 1 : 13 000, covering the town site of about 40 square kilometres (Fig. 7.1). An image analysis of the individual data layers and their mutual interferences gives some information about sources of groundwater, geothermal energy, and potential risks to the town and its residents (Fig. 7.2.).

Results of the urban geology model study of Liberec provide the following contributions applicable to other towns in the Czech Republic:

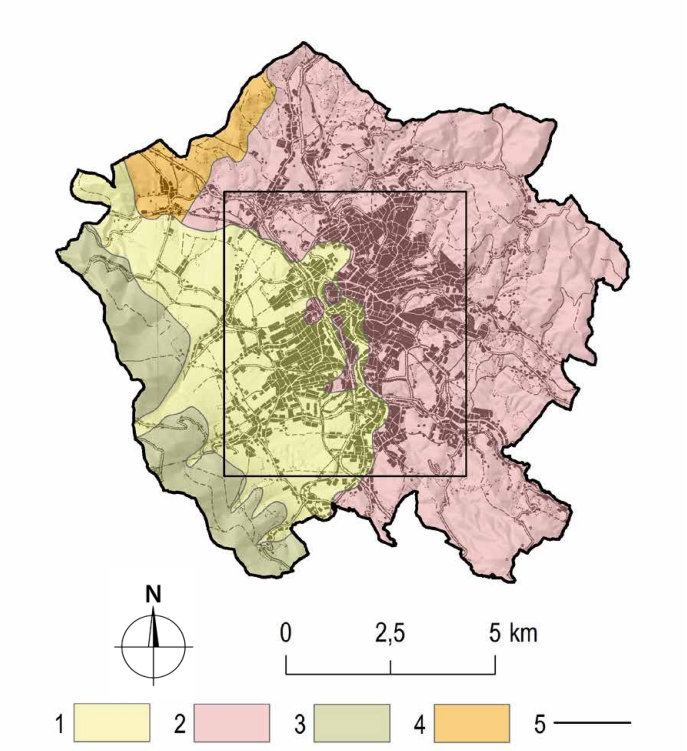

Figure 7.1. Simplified geology in the city of Liberec. Klomínský et al. (2016). 1 – Quaternary sediments, 2 – Krkonoše-Jizera Composite Massif, 3 – Ještěd Crystalline, 4 – Jizera Crystalline, 5 – Frame of the geological map 1 : 13,000.

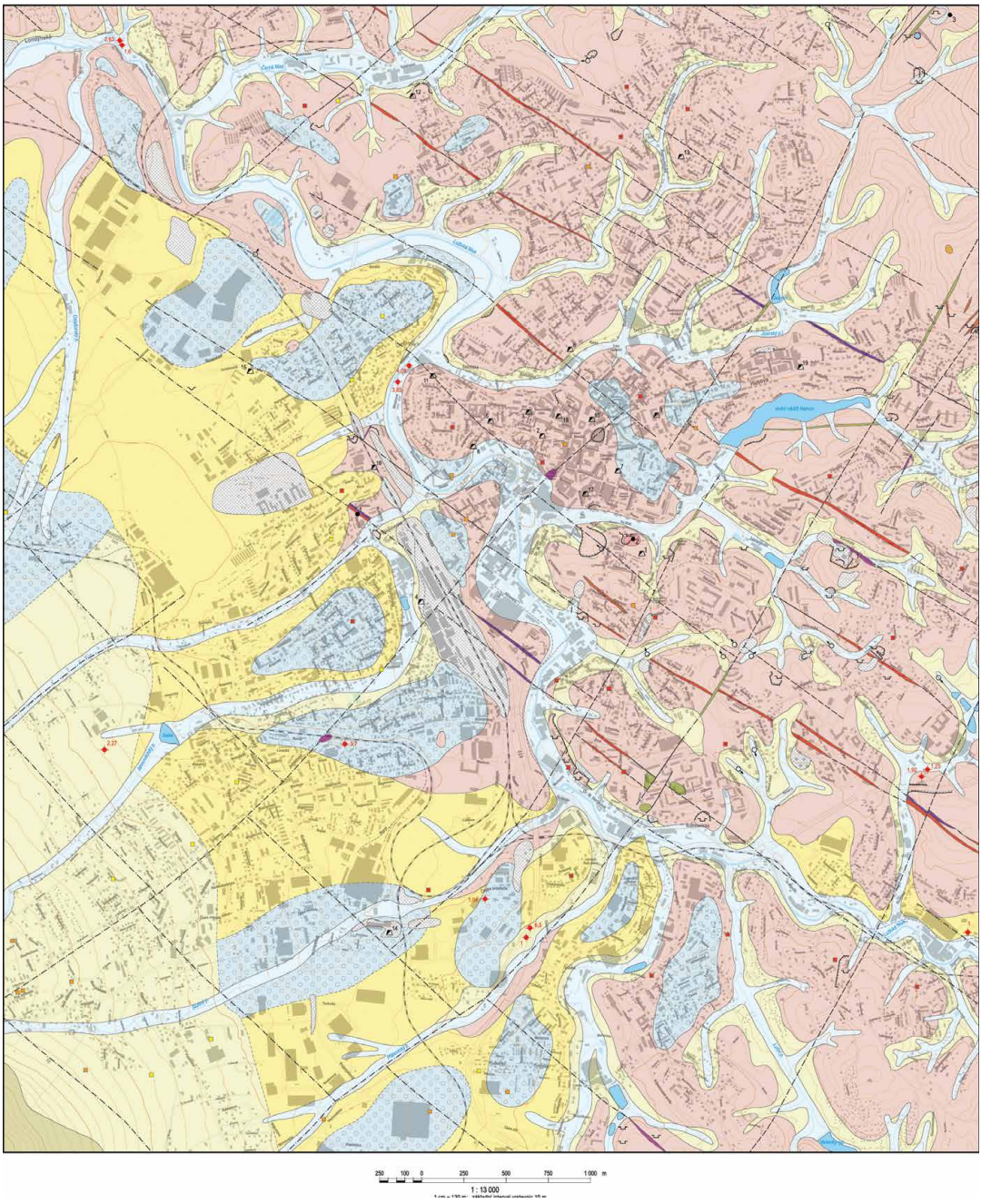

Figure 7.2. Geological map of the Liberec City centre (legend in Klomínský ed. 2016). Klomínský et al. (2016a).

– The ability to generate urban geological maps and spatial models for groundwater and geothermal energy exploitation, housing and planning of underground constructions.
– Geological information about identification of man-made infills, dangerous waste deposits and air pollutants.
– Better information for city dwellers and businesses about their environment, especially existing and anticipated geological risks in their towns.

The model study was includes spatial and attribute information on geological units and their lithology, the network of geological faults, the natural magnetic field, natural radioactivity, iron mining, coal mining, building stone, clay resources, groundwater and geothermal resources, engineering-geological ground classification, natural outcrops, antropogenous exposures, road cuts, the network of hydrogeological and geotechnical drill holes, underground objects and sewers, man-made deposits of industrial and municipal waste, paving and frontages of building in the Liberec conservation zone, natural seismicity, radon risk, radioactive fallout of caesium 137, soil cover contamination by industrial emissions, and the Lužice Nisa inundation area and its geological base in the town centre.

Figure 7.3. Model of the DMR G5 LIDAR surface morphology of the Liberec city centre. Klomínský et al (2016a).
(Vegetation cover is neglected.)

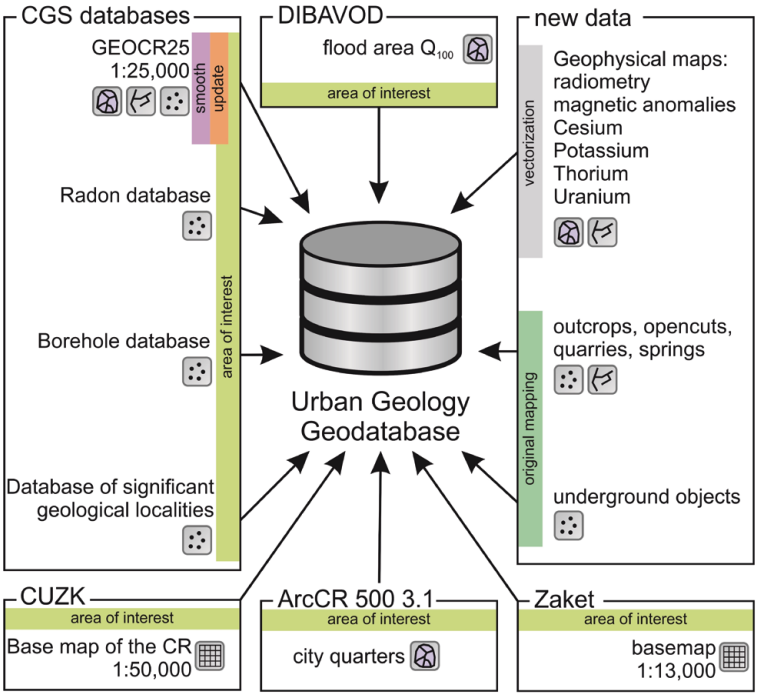

Figure 7.4. Scheme of data sources for the model study. Klomínský et al (2016).

Data on individual themes was obtained from existing Czech Geological Survey databases, and new geodata were created by detailed mapping. (Fig. 7.2.).

7.1 Spatial data layers

The Urban Geoportal for the Liberec City centre consists of the following 19 thematic map layers in GIS formats. By combining the individual thematic maps or groups of maps, it should be possible to create new maps showing hydrogeological and raw material resources in the town foundations as well as risk maps for engineering, soil pollution and land instability (Figs. 7.4. and 7.1.1.).

1. Geological map of Liberec City.
2. Rocky outcrops, road and railway cuttings, building excavations.
3. Underground constructions (cellars, adits, sewerage network).
4. Mining objects (portals of adits, shafts, undermined areas).
5. Geological barriers in the flooding model of the Lužice Nisa river.
6. Man-made deposits,excavations and waste dumps.
7. Groundwater springs, water wells, hydrogeological drillings (Fig. 7.1.3.).
8. Geomorphology and geological fault network and its rock and mineral filling (Fig. 7.3.).
9. Landslide and rock fall sites and areas.
10. Dimension and building stone quarries and sand pits.
11. Quaternary cover lithology and thickness.

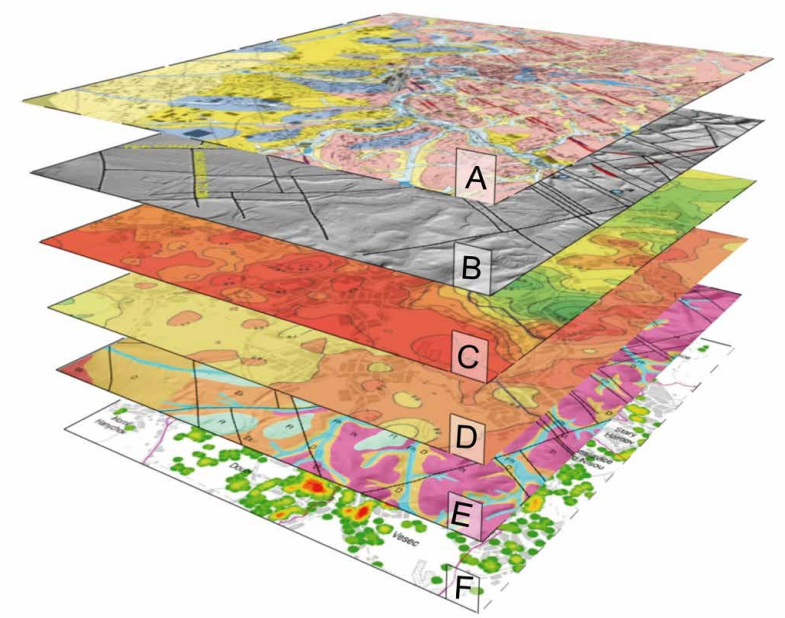

Figure 7.1.1. Model of the thematic layers for the Liberec City centre in oblique parallel projection. Klomínský et al (2016a).

A – geology, B – geomorphology and tectonics, C – airborne magnetic field, D – airborne radiometry of uranium, E – engineering-geological domains, F – density of the borehole networks.

12. Key geological localities and protected natural objects.
12. Natural radioactivity field (U, Th and K content, Fig. 7.1.2.).
13. Radon risks.
14. Airborne magnetic field map.
15. Polygons of mineral resources.
16. Drill holes networks, including parameters, density and uses (Fig. 7.1.3.).
17. Shallow geothermal field, geothermal sources in the sedimentary cover and bedrock.
18. Building and dimension stones in historical buildings and street paving.
19. Geochemistry of the soil cover.
20. Engineering-geological domains.

REFERENCES

Klomínský, J. – Petyniak, O. – Dudíková, B. – Štor, T. – Rous, I. – Šrek, – Dostalík, M. – Krupička, J. – Malík, J. – Bělohradský, V. – Burda, J. – Dvořák, I – Sedláček, J. (2016): Urban geology of Liberec – model study of spatial information for sustainable development of cities in the Czech Republic. Geoscience Reseach Reports vol. 49, 2016, 165–170. CGS Prague.

Klomínský, J. ed. (2016a): Modelová územní studie urbanistické geologie města Liberce. Závěrečná zpráva interního projektu ČGS. MS ČGS 153 pp.

Klomínský, J. ed. (2016): Liberec – Urbanistická geologie města s mapou 1 : 13 000. ČGS Praha.

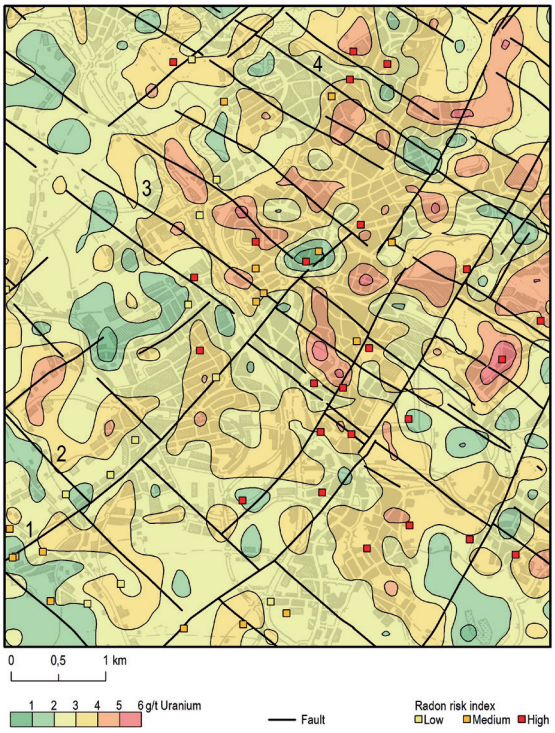

Figure 7.1.2. Airborne radiometric map of natural uranium concentration (Gnojek et al. 2005) with points of the radon risk index (Barnet et al. 2005).
Faults:
1 – Devil's Walls tectonic zone,
2 – Šimonovice-Machnín fault,
3 – Vratislavice fault,
4 – Harcov fault.

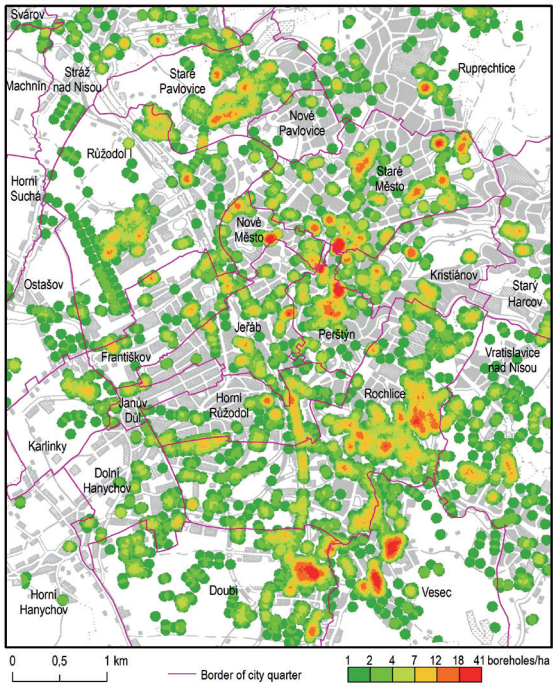

Figure 7.1.3. Hydrogeological and geotechnical visualisation of borehole density per 1 hectare (100 × 100 m).

8. Conclusions

Studies of the Krkonoše-Jizera Composite Massif, situated on the boundary of Poland and the Czech Republic and with a complicated political history, serve as an inspirational example of effective and fruitful international co-operation in the field of geological research. German, Polish, Czech, French, English, Austrian, Hungarian, Slovenian and even Mongolian earth scientists have contributed to understanding of this remarkable granitic body, which became world famous as the cradle for the granittectonics branch of geological science. Czech geologists are proud that their share of this effort has not been overlooked. Their recent contributions can be summarized as follows:

– modern geological maps 1 : 25 000,
– substantial extension and refinement of chemical rock data and their interpretation,
– a new concept of the division of rock-types, developed in the field as well as throuth laboratory based research, and the mutual relations of rock-types,
– geological evaluation of subsurface water-supply tunnels,
– potential information to enable valorisation of raw materials and enhance environmental policy and landscape protection.

Studies undertaken along the 6 km length of the Bedřichov water-supply tunnel, which penetrates both the Jizera and Liberec Granites of the Krkonoše-Jizera Composite Massif, have substantially enhanced geological understanding of the area. Magmatic structures in granites are represented by mostly planar schlieren, magmatic folds and gravity-dependent structures. The two most prominent sets of joints (in terms of joint abundance) display an orientation of 22–55/70–90° SE and 120–150/75–90° NE. The sum of the micro- displacement velocities inside the granite massif in 2004–2008 amounted to 0.22 mm/yr along the NE-SW faults and 0.16 mm/yr along the NW-SE faults. The character of the displacement corresponds to the compression stress model in an approximately N-S direction with north-verging over-thrusting. The coatings of supergene radioactive minerals on the Bedřichov water-supply tunnel walls are products of recent water-rock interaction along fractures originated in the Jizera Granite during the tunnel's excavation.

Tectonic melange from Harzov fault as the final impression of this work. Photo J. Klomínský.

Josef Klomínský (ed.) with contributions from F. Fediuk – P. Schovánek – T. Jarchovský (2018): The Krkonoše-Jizera Composite Massif – never ending granite stories. 145 pp.

The team members (in alphabetic order): Vladimír Bělohradský, Zita Bukovská, Jiří Burda, Petr Dobeš, Martin Dostalík, Igor Dvořák, Barbora Dudíková, Ferry Fediuk, Eva Fediuková, Tomáš Jarchovský, Josef Klomínský, Pavel Kopecký, Bohuslav Košťák, Veronika Kopačková, Jiří Krupička, Jiří Málek, Jan Malec, Jan Molík, Štěpánka Mrázová, Otmar Petyniak, Ivan Rous, Pavel Schovánek, Josef Stemberk, Tamara Sidorinová, Karel Šalanský, Tomáš Štor, Jakub Šrek, Zdeněk Táborský, Miroslav Toužimský, Stanislav Vrána, Kryštof Verner, František Veselovský, František Woller, Jiří Žák, Karel Žák, Tomáš Žitný.

Acknowledgments: This research was financially supported by institutional projects of the Czech Geological Survey. We thank Catherine Kraina for constructive comments and English correction of this book. We are indebted to Miroslav Toužimský, Jan Sedláček, Martin Dostalík, Oleg Man, Michaela Zemková and Pavla Müllerová for technical asistance.

The content of this book was not checked by a reviewer of the Publishing Department of the Czech Geological Survey.

Corresponding author: Josef Klomínský. Czech Geological Survey, Klárov 131/3, Praha 1, Czech Republic. Fax (+420) 257 531 376. E-mail address: josef.klominsky@geology.cz (J. Klomínský)**.**

THE KRKONOŠE-JIZERA COMPOSITE MASSIF

NEVER ENDING GRANITE STORIES

Josef Klomínský

With contributions and assistance from
F. Fediuk – P. Schovánek –T. Jarchovský

Cover and graphic design Oleg Man
Published by the Czech Geological Survey
Prague 2018

First edition, 145 pages
Printed in the Czech Republic
03/9 446-401-18

ISBN 978-80-7075-929-5

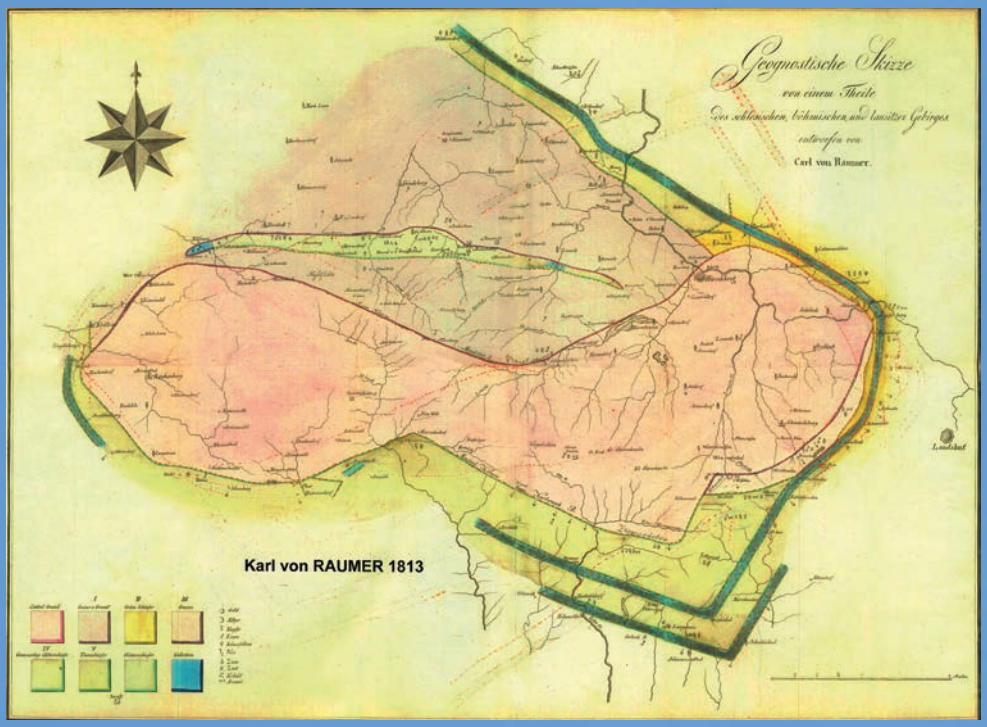

First geognostic draft of the Krkonoše-Jizera Composite Massif according to Karl von Reumer (1813): Die Granite des Riesengebirges and die sie umgebenden Gebirgsfamilien. Berlin, 92 p.

Czech Geological Survey
www.geology.cz

ISBN 978-80-7075-929-5